



October 2010

## QuO Va Dis? Quarterly Ocean Validation Display #2

Validation bulletin for July-August-September (JAS) 2010

Edition:

Charles Desportes, Marie Dré villon, Charly Rég nier  
(MERCATOR OCEAN/Production Dep./Products Quality)

Contributions :

Olivier Le Galloudec, Jean-Michel Lellouche, Bruno Levier, Gilles Garric  
(MERCATOR OCEAN/ Production Dep./R&D)  
Eric Greiner (CLS)

Credits for validation methodology and tools:

Eric Greiner, Mounir Benkiran, Nathalie Verbrugge, Hélène Etienne (CLS)  
Charly Rég nier, Fabrice Hernandez, Laurence Crosnier (MERCATOR OCEAN)  
Nicolas Ferry, Gilles Garric , Jean-Michel Lellouche (MERCATOR OCEAN)  
Jean-Marc Molines (CNRS), Sébastien Theeten (Ifremer)  
Nicolas Pene (AKKA), Silvana Buarque (Météo-France)

Information on input data:

Christine Boone, Stéphanie Guinehut, Gaél Nicolas (CLS/ARMOR team)

Contact:

qualif@mercator-ocean.fr

Abstract

*This bulletin gives an estimate of the accuracy of MERCATOR OCEAN's analyses and forecast for the season of **July-August-September 2010**. It also provides a summary of useful information on the context of the production for this period. Diagnostics will be displayed for the global  $\frac{1}{4}^\circ$  (PSY3) and the Atlantic and Mediterranean zoom at  $1/12^\circ$  (PSY2) monitoring and forecasting systems currently producing daily 3D temperature salinity and current products. A special focus is made on the major improvements brought by the new versions of these systems, which products will be available by the end of this year. The water masses characteristics are more realistic in these systems, in addition to a general improvement of*

*the physics due to the use of Incremental Analysis Update (IAU). The performance with respect to observations is clearly better for most variables and regions in both the new versions of PSY3 and PSY2. Nevertheless the performance of the new version of PSY2 is not satisfactory in the Mediterranean Sea in the first 150m and a fresh bias is under investigation. Finally we present a preliminary intercomparison of a few physical processes viewed by the operational systems and by the IBI system at 1/36° horizontal resolution.*

## Table of contents

I	Status and evolutions of the systems .....	7
II	Summary of the availability and quality control of the input data.....	10
II.1.	Observations available for data assimilation .....	10
II.1.1.	In situ observations of T/S profiles.....	10
II.1.2.	Sea Surface Temperature.....	11
II.1.3.	Sea Level Anomalies .....	12
II.2.	Observations available for validation.....	12
III	Information on the large scale climatic conditions.....	12
IV	Accuracy of the products .....	15
IV.1.	Data assimilation performance .....	15
IV.1.1.	Sea surface height .....	15
IV.1.2.	Sea surface temperature.....	19
IV.1.3.	Temperature and salinity profiles.....	25
IV.2.	Accuracy of the daily average products with respect to observations.....	29
IV.2.1.	T/S profiles observations.....	29
IV.2.2.	Drifting buoys velocity measurements .....	37
IV.2.3.	Sea ice concentration .....	39
V	Forecast error statistics.....	41
V.1.	Forecast accuracy: comparisons with observations when and where available .....	41
V.2.	Forecast verification: comparison with analysis everywhere.....	43
VI	Monitoring of ocean and sea ice physics .....	47
VI.1.	Global mean SST and SSS .....	47
VI.2.	Mediterranean outflow .....	48
VI.3.	Surface EKE.....	49
VI.4.	Sea Ice extent and area .....	49
VI.5.	High frequency behaviour at moorings.....	50
VII	Process study: A warm coastal current in the Bay of Biscay.....	54
VIII	Annex A .....	58
VIII.1.	Maps of regions for data assimilation statistics.....	58
VIII.1.1.	Tropical and North Atlantic.....	58
VIII.1.2.	Mediterranean Sea.....	59
VIII.1.3.	Global ocean.....	60

## Table of figures

Figure 1: geographical distribution of validated and undersampled T (upper panel), S (lower panel) profiles in 1°×1° boxes, for July-August-September 2010, by courtesy of ARMOR team (CLS).....	11
Figure 2: SST monthly anomalies (°C) at the global scale from the 1/4° ocean monitoring and forecasting system PSY3V2R2 with respect to Levitus (2005) climatology. Upper panel April anomaly, middle panel May anomaly, lower panel June anomaly. ....	14
Figure 3: Arctic sea ice extent from the NSIDC: <a href="http://nsidc.org/data/seaice_index/images/daily_images/N_stddev_timeseries.png">http://nsidc.org/data/seaice_index/images/daily_images/N_stddev_timeseries.png</a> .....	14
Figure 4: Comparison of SLA data assimilation scores (left: average misfit in cm, right: RMS misfit in cm) in JAS 2010 and between all available Mercator Ocean systems in the Tropical and North Atlantic. The scores are averaged for all available satellite along track data (Jason 1, Jason 2 and Envisat). For each region from bottom to top, the bars refer respectively to PSY3V2, PSY2V3, PSY3V3, PSY2V4, PSY4V1. The geographical location of regions is displayed in annex A. ....	15
Figure 5: Synthetic map of regional SLA RMS misfit (upper panel) and of regional ratio of RMS misfit over RMS of SLA data (lower panel) in the Atlantic Ocean and Mediterranean Sea for the new system PSY2V4 in JAS 2010. The scores are averaged for all available satellite along track data (Jason 1, Jason 2 and Envisat). ....	16
Figure 6: Comparison of SLA data assimilation scores (left: average misfit in cm, right: RMS misfit in cm) in JAS 2010 and between both PSY2 systems in the Mediterranean Sea. For each region from bottom to top: PSY2V3, and new version PSY2V4. The scores are averaged for all available satellite along track data (Jason 1, Jason 2 and Envisat). The geographical location of regions is displayed in annex A. ....	17
Figure 7: Comparison of SLA data assimilation scores (left: average misfit in cm, right: RMS misfit in cm) in JAS 2010 and between all available Mercator Ocean systems in all basins but the Atlantic and Mediterranean. For each region from bottom to top: PSY3V2, PSY3V3, and PSY4V1. The geographical location of regions is displayed in annex A. ....	18
Figure 8 : Synthesis of regional RMS misfit (upper panel), and ratio between RMS misfit and RMS of data (lower panel) in the Global Ocean (except the Mediterranean). ....	19
Figure 9: Comparison of SST data assimilation scores (left: average misfit in °C, right: RMS misfit in °C) in JAS 2010 and between all available Mercator Ocean systems in the Tropical and North Atlantic. Upper panel: RTG-SST data assimilation scores, lower panel: in situ SST data assimilation scores. For each region from bottom to top: PSY3V2, PSY2V3, PSY3V3, PSY2V4, PSY4V1. ....	20
Figure 10: Comparison of SST data assimilation scores (left: average misfit in °C, right: RMS misfit in °C) in JAS 2010 and between both PSY2 systems in the Mediterranean Sea. Upper panel: RTG-SST data assimilation scores, lower panel: in situ SST data assimilation scores. For each region from bottom to top: PSY2V3, and new version PSY2V4.....	22
Figure 11: Comparison of SST data assimilation scores (left: average misfit in °C, right: RMS misfit in °C) in JAS 2010 and between all available Mercator Ocean systems in all basins but the Atlantic and Mediterranean. Upper panel: RTG-SST data assimilation scores, lower panel: in situ SST data assimilation scores. For each region from bottom to top: PSY3V2, PSY3V3, and PSY4V1. ....	23
Figure 12 Average JAS 2010 regional SST (°C) data assimilation scores of RMS of misfit for RTG-SST (upper panel) and in situ observations (lower panel) for PSY3V3 at the global scale.....	24
Figure 13: mean JAS 2010 temperature profiles (°C) of average of innovation (left column) and RMS of innovation (right column) on the global PSY3V2 (upper panel) PSY3V3 (middle panel) and PSY4V1 (lower panel). ....	26
Figure 14: mean JAS 2010 salinity profiles (psu) of average of innovation (left column) and RMS of innovation (right column) on the global PSY3V2 (upper panel) PSY3V3 (middle panel) and PSY4V1 (lower panel). ....	27
Figure 15 : mean JAS 2010 temperature profiles (°C) of average of innovation (left column) and RMS of innovation (right column) on the whole domain of PSY2V3 (upper panel) and PSY2V4 (lower panel).....	28

Figure 16: mean JAS 2010 salinity profiles (psu) of average of innovation (left column) and RMS of innovation (right column) on the global PSY3V2 (upper panel) and PSY3V3 (lower panel).....	29
Figure 17: RMS temperature (°C) difference (model-observation) between all available T/S observations from the Coriolis database and the daily average PSY3V2 (upper panel) and PSY3V3 (lower panel) products (here the nowcast run) colocalised with the observations. The size of the pixel is proportional to the number of observations used to compute the RMS in 2°x2° boxes. ....	30
Figure 18: RMS salinity (psu) difference (model-observation) between all available T/S observations from the Coriolis database and the daily average PSY3V2 (upper panel) and PSY3V3 (lower panel) products colocalised with the observations. The size of the pixel is proportional to the number of observations used to compute the RMS in 2°x2° boxes. ....	31
Figure 19: stability of the temperature (upper panel) and salinity (lower panel) RMS errors over the 2007-2010 period for PSY3V2R2 (red line), PSY3V3R1 (black line), Levitus WOA05 climatology (blue line) and Ifremer ARIVO climatology (green line).....	32
Figure 20: Upper panel: RMS temperature (left column) and salinity (right column) difference (model-observation) between all available T/S observations from the Coriolis database and the daily average PSY2V3 products colocalised with the observations. Lower panel: same with PSY2V4. ....	33
Figure 21: Water masses (Theta, S) diagrams in the Bay of Biscay (upper panel), Gulf of Lyon (middle panel) and Western Tropical Atlantic (lower panel), comparison between PSY2V3 (left column) and PSY2V4 (right column). PSY2 (yellow dots), Levitus WOA05 climatology (red dots), in situ observations (blue dots).....	35
Figure 22 : Water masses (Theta, S) diagrams in the Eastern Tropical Pacific for PSY2V3 and PSY2V4 (upper panel), PSY3V2 and PSY3V3 (middle panel) and in situ observations (lower panel) only in the Western (right panel) and Eastern (left panel) tropical Atlantic. PSY2 (yellow dots), Levitus WOA05 climatology (red dots), in situ observations (blue dots). ....	36
Figure 23: Water masses (Theta, S) diagrams in South Africa (upper panel) and Kuroshio (lower panel) in PSY3V2 and PSY3V3.....	37
Figure 24: PSY3 analyses of velocity (m/s) collocated with drifting buoys velocity measurements. Upper left panel: difference model - observation of velocity module. Upper right panel: ratio model/observation per latitude. Lower panel: distribution of the velocity vector direction errors (degrees) for PSY3V2R2 (left panel) and PSY3V3R1 (right panel) .....	38
Figure 25: sea ice cover fraction (%) mean (left) and RMS (right) difference between CERSAT observations and PSY3V2 (upper panel) and PSY3V3 (lower panel) in regional boxes in the Arctic Ocean.....	40
Figure 26: Comparison of the sea ice cover fraction mean for JAS 2010 between PSY3V2 (upper panel) and PSY3V3 (lower panel), for each panel the model is on the left the mean of Cersat dataset in the middle and the difference on the right. ....	40
Figure 27: Upper panel: In the North Atlantic region for PSY2V3, time series of forecast (FRCST) accuracy at 3 (green line) and 6 (red line) days range, together with analysis (ANA in blue and HDCST in black), and climatology (TMLEV Levitus (2005) in cyan and in orange TMARV Arivo from Ifremer). Accuracy as measured by a RMS difference with respect to all available temperature (°C) observations from the CORIOLIS database. Lower panel: accuracy comparison of the analysis of PSY2V3 (red line) and PSY2V4 (black line) compared to WOA05 (blue line) and ARIVO (green line) climatologies. Left column: 0-50m layer, right column: 0-500m layer.....	41
Figure 28: same as Figure 27 for the Mediterranean Sea in the PSY2V3 system (upper panel) and comparison with the new system PSY2V4 (lower panel), in the 0-500m layer. On the left temperature (°C) and on the right salinity (psu) .....	42
Figure 29: same as Figure 27 for temperature only in the 0-500m layer, the PSY3 system and the South Atlantic Ocean (upper left panel), the Tropical Atlantic (upper right panel), the Tropical Pacific (lower left panel) and the Indian Ocean (lower right panel). ....	43
Figure 30: comparison of the sea surface height (m) forecast – hindcast RMS differences for the 1 week (upper panels) and 2 weeks (lower panels) ranges for the PSY3V2R2 system.....	44
Figure 31: comparison of the sea surface height (m) forecast – hindcast RMS differences for the 1 week (upper panels) and 2 weeks (lower panels) ranges, for the PSY2V3R1 system.....	45
Figure 32: comparison of the temperature (°C) forecast – hindcast RMS differences for the 1 <sup>st</sup> week at surface (upper panels) and 110 m (lower panels), for the PSY2V3R1 system.....	46
Figure 33: daily SST (°C) and salinity (psu) global mean for a one year period ending in JAS 2010, for PSY3 (in black) and RTG-SST observations (in red). Upper panel: PSY3V2R2, lower panel: PSY3V3R1. ....	47

*Quo Va Dis ? Quarterly Ocean Validation Display #2, JAS 2010*

Figure 34: Comparisons between mean salinity (upper panel) and temperature (lower panel) profiles in PSY2V3 (left), PSY2V4 (right) and in the Levitus WOA05 and ARIVO climatologies. ....	48
Figure 35: surface eddy kinetic energy EKE ( $\text{m}^2/\text{s}^2$ ) for PSY3V2R2 (left panel) and PSY3V3R1 (right panel) for JAS 2010. ....	49
Figure 36: Sea ice area (left panel, $10^3 \text{ km}^2$ ) and extent (right panel, $10^3 \text{ km}^2$ ) in PSY3V2 (black line), PSY3V3 (blue line) and SSM/I observations (red line) for a one year period ending in JAS 2010, in the Arctic (upper panel) and Antarctic (lower panel). ....	50
Figure 37: 2m wind velocity (upper panel, m/s), and 0-500 zonal velocity (in m/s, middle panel PSY2V4 and lower panel PSY2V3) 2-hourly time series at BATS near $64.18^\circ\text{W}$ and $31.67^\circ\text{N}$ . ....	51
Figure 38: 0-500m temperature ( $^\circ\text{C}$ , left column) and salinity (psu, right column) time series for the JAS 2010 period at $23^\circ\text{W}$ and $21^\circ\text{N}$ for PSY2V3 (upper panel), at the PIRATA mooring (middle panel) and in PSY2V4 (lower panel). ....	52
Figure 39: 0-500m temperature ( $^\circ\text{C}$ , left column) and salinity (psu, right column) time series for the JAS 2010 period at $23^\circ\text{W}$ and $3^\circ\text{N}$ for PSY2V3 (upper panel), at the nearest PIRATA mooring (at $4^\circ\text{N}$ , middle panel) and in PSY2V4 (lower panel). ....	53
Figure 40: Sea Surface Temperature ( $^\circ\text{C}$ ) from MODIS on $15^{\text{th}}$ September (upper left panel), IBI (upper right, hourly average of 2010/15/09 at 00h), PSY2V3 (lower left, daily average of 2010/14/09) and PSY2V4 (right panel, daily average of 2010/14/09). ....	54
Figure 41: Current velocity (m/s, daily average) near $1.5^\circ\text{W}$ , $44.6^\circ\text{N}$ from 2010/10/08 to 2010/16/09 for IBI (upper panel), PSY2V3 (middle) and PSY2V4 (lower panel). ....	55
Figure 42: Bottom temperature ( $^\circ\text{C}$ , daily average) near $1.5^\circ\text{W}$ , $44.6^\circ\text{N}$ from 2010/10/08 to 2010/16/09 for IBI (black curve), PSY2V3 (red) and PSY2V4 (blue). ....	55
Figure 43: temperature ( $^\circ\text{C}$ ) and current at 47 m depth for IBI (upper panel), PSY2V3 (middle) and PSY2V4 (lower) for 2010/08/09 (left column) and 2010/04/09 (right column). ....	57

## I Status and evolutions of the systems

New versions of the PSY3 and PSY2 (see Table 1 and Table 2) systems are currently in “transition to operations” at MERCATOR OCEAN. These systems will provide the version 1 products of the MyOcean global monitoring and forecasting system. The new products will replace the current version by mid-December 2010 (and will be made available for users starting mid-November).

The scientific evolution of the systems includes:

- NEMO version 3.1, ORCA grid, 50 levels 1 to 450m spacing, non tidal free surface, ECMWF 3-hourly forcing (bulk), LIM2-EVP Sea ice
- Multivariate data assimilation (Kalman Filter SEEK kernel) of *in situ* T and S, along track SLA (+MDT CNES/CLS09), SST, with incremental analysis update (IAU) of T, S, U, V and SSH centred on the 4<sup>th</sup> day of the 7-day assimilation window. The assimilation cycle consists of a first 7-day simulation called **guess or forecast**, at the end of which the analysis takes place. The IAU correction is then computed and the model is re-run on the same week, progressively adding the correction. The increment is distributed in time with a Gaussian shape which is centred on the 4<sup>th</sup> day. This second run is called **analyzed or analysis** run. The main improvements in comparison with the previous system concern the IAU, the adaptive scheme (tuning of the ratio between the variances of the background and the errors of the observations), the extension of the state vector and the introduction of pseudo-observations (innovations equal to zero). Their main objective is to overcome the deficiencies of the background errors, in particular for extrapolated variables. We apply this kind of parameterization on the barotropic height, the variables under the ice, on coastal salinity (runoffs), at the equator on the velocities and on open boundaries (for the zoom at 1/12°).
- In addition to the assimilation scheme, a method of bias correction has been developed. This method is based on a variational approach which takes into account cumulative innovations on recent period (typically 3 months) in order to estimate a large scale bias. Additionally, the bias correction provides information on the observations that significantly differ from the model estimate. This information will be sent to data centres, and synthesised in future QuO Va Dis bulletins.
- The Atlantic and Mediterranean configuration PSY2V4R1 is nested in the global solution of PSY3V3R1 with open boundary conditions.
- Real time (OGDR) along track Aviso data will be assimilated (IGDR near real time are used in the current version) with an expected positive impact on the forecast quality.

The system is started in October 2006 from a 3D climatology of temperature and salinity (Levitus 2005). After a short 3-month spin up of the model and data assimilation, the

performance of the system has been evaluated on the 2007-2009 period (MyOcean internal calibration report, which results are synthesised in this QuO Va Dis).

<b>PSY2: Atlantic and Mediterranean at 1/12°</b>			
System name	Model	Assimilation	status
PSY2V3R1	NATL12 LIM2 NEMO 1.09 (Tropical, North Atlantic and Mediterranean Sea, 1/12° horizontal resolution, 50 vertical levels) Daily atmospheric forcing, bulk CLIO.	Assimilating RTG-SST, SLA from Jason 1, Jason 2 and Envisat, in situ profile from CORIOLIS with SAM2 (SEEK Kernel)	Operated weekly, with daily updates of atmospheric forcing
PSY2V4R1	NATL12 LIM2 EVP <b>NEMO 3.1</b> (Tropical, North Atlantic and Mediterranean Sea, 1/12° horizontal resolution, 50 vertical levels) <b>3-hourly atmospheric forcing,</b> bulk CORE.	Assimilating RTG-SST, SLA from Jason 1, Jason 2 and Envisat, in situ profile from CORIOLIS with SAM2 (SEEK Kernel) <b>+ IAU and bias correction</b>	In transition to weekly operation (15/12/2010) , with daily updates of atmospheric forcing

**Table 1: synthetic description of the PSY2 system, in yellow the main improvements included in the new version**

<b>PSY3: global at 1/4°</b>			
System name	Model	Assimilation	status
PSY3V2R2	ORCA025 LIM2 NEMO 1.09 (Global, 1/4° horizontal resolution, 50 vertical levels) Daily atmospheric forcing, bulk CLIO	Assimilating RTG-SST, SLA from Jason 1, Jason 2 and Envisat, in situ profile from CORIOLIS with SAM2 (SEEK Kernel)	Operated weekly
PSY3V3R1	ORCA025 LIM2 EVP <b>NEMO 3.1</b> (Global, 1/4° horizontal resolution, 50 vertical levels) <b>3-hourly atmospheric forcing,</b> bulk CORE	Assimilating RTG-SST, SLA from Jason 1, Jason 2 and Envisat, in situ profile from CORIOLIS with SAM2 (SEEK Kernel) <b>+ IAU and bias correction</b>	In transition to weekly operation (15/12/2010) , with daily updates of atmospheric forcing

**Table 2: synthetic description of the PSY3 system. In yellow the main improvements included in the new version**

<b>PSY4: global at 1/12°</b>			
System name	Model	Assimilation	status
PSY4V1R3	ORCA12 LIM2 NEMO 1.09 (Global, 1/12° horizontal resolution, 50 vertical levels) Daily atmospheric forcing, bulk CLIO	Assimilating RTG-SST, SLA from Jason 1, Jason 2 and Envisat, in situ profile from CORIOLIS with SAM2 (SEEK Kernel) + IAU	Operated weekly, available to users by the end of 2010

**Table 3: synthetic description of the PSY4 system**

During the JAS season, two major scientific updates were made on the new systems PSY3V3R1 and PSY2V4R1 after the validation was made on the 2007-2009 period.

- The mean dynamic topography has been updated in closed seas (correction of the long term bias in the CNES/CLS09 MDT) and shifted in Mediterranean Sea.
- The diurnal cycle of SST has been taken into account in the observation operator (innovation is computed at night).

No major technical problem was encountered with PSY3V2R2 and PSY2V3R1 during the JAS quarter.

The PSY4 system is back to weekly operation after the correction of a technical problem in June. PSY4 data should be available for users by the end of 2010.

<b>IBI: regional at 1/36°</b>			
System name	Model	Assimilation	status
IBI (temporary)	NEATL36 NEMO 2.3 (North East Atlantic and West Mediterranean Sea, 1/36° horizontal resolution, 50 vertical levels) 3-hourly atmospheric forcing, bulk CORE.	None. Restarted every week with initial conditions from PSY2V3R1	In transition to weekly operation.

**Table 4: synthetic description of the IBI system**

## **II Summary of the availability and quality control of the input data**

### ***II.1. Observations available for data assimilation***

#### **II.1.1. In situ observations of T/S profiles**

PSY2V3 and V4: between 300 and 750 temperature profiles and between 300 and 500 salinity profiles are assimilated per analysis.

PSY3V2: between 2000 and 3850 temperature profiles and between 2000 and 3050 salinity profiles are assimilated per analysis.

PSY3V3: between 2000 and 4250 temperature profiles and between 2000 and 3380 salinity profiles are assimilated per analysis.

PSY4: between 2000 and 3850 temperature profiles and between 2000 and 3050 salinity profiles are assimilated per analysis.

The maximum number of observations occurs in August. July and September are less observed, especially in salinity.

In the following we remind the quality check procedure that is performed by the ARMOR team prior to data assimilation in the PSY systems (from "Rapport trimestriel de suivi des observations T/S – Juillet/Septembre 2010").

The temperature and salinity profiles provided by Coriolis are first validated (quality check, about 3% of the profiles are rejected) and then undersampled, to meet assimilation's needs and keep, at the most, one profile per 0.1° box every 24 hours. This way, about 60 000 temperature profiles and 60 000 salinity profiles (Figure 1) have been delivered to Mercator for assimilation during the last three months. That is about 4600 temperature profiles and 4600 salinity profiles available for assimilation per week. Among these, about 38 % come from Argo profilers, 12 % are moorings from TAO and PIRATA, 38 % are in the tesac format and about 6 % in the bathy format. This distribution is quite stable from a period to another. Among all global Mercator Ocean systems, PSY3V3 (the most recent version of the global systems) takes the best advantage of all available profiles. This is a tuning of the number of observations allowed for a given local analysis which will be updated in future versions of PSY4.

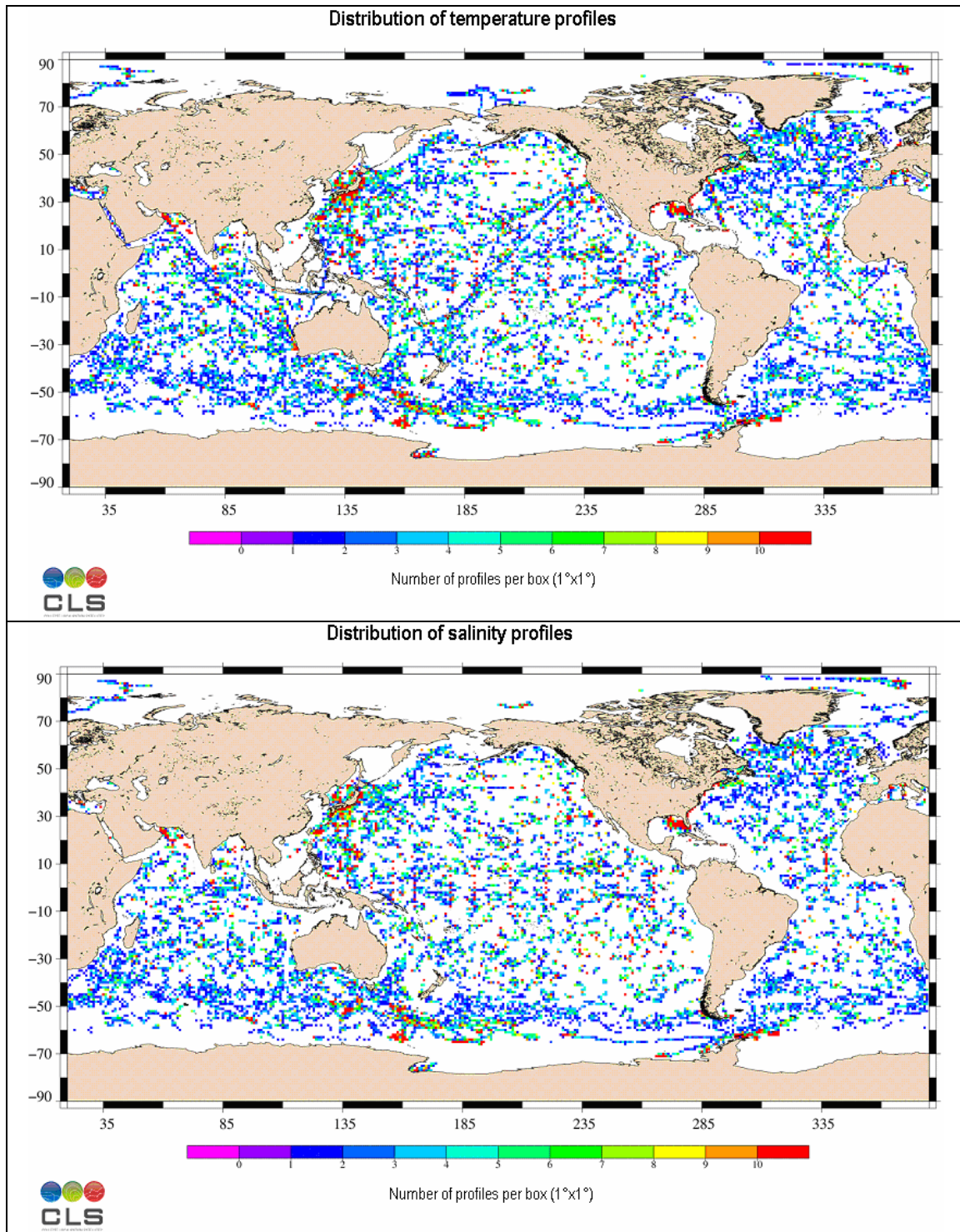


Figure 1: geographical distribution of validated and undersampled T (upper panel), S (lower panel) profiles in  $1^\circ \times 1^\circ$  boxes, for July-August-September 2010, by courtesy of ARMOR team (CLS).

### II.1.2. Sea Surface Temperature

PSY2 : 29000 to 31000 observations are assimilated per analysis

PSY3 : 165000 to 170000 observations are assimilated per analysis

PSY4 : 175000 to 180000 observations are assimilated per analysis

Due to a pre-processing error RTG-SST observations were not assimilated in PSY3V3 in September. This month was reprocessed in October in order to assimilate these observations, and data assimilation scores shown in the following were updated. The other diagnostics were not updated due to a lack of time. However, the scores shown that the performance of the system over the JAS season was not significantly degraded.

### **II.1.3. Sea Level Anomalies**

For PSY2: the order of magnitude is 15000 observations per satellite and per analysis, which gives a total of 45000 observations per analysis.

PSY3 and PSY4: For each satellite the number of data assimilated per analysis in the global systems is of the order of 90000, giving a total of the order of 250000-300000 observations per cycle. PSY4 assimilates more data o(300000) than PSY3 o(250000)

There was a drop in the number of Jason 1 data assimilated in the analyses of July 21<sup>st</sup> and July 28<sup>th</sup> (approximately divided by 3 on the 21<sup>st</sup>).

Due to a pre-processing error no Jason 1 data were assimilated in PSY3V3R1 between December 2<sup>nd</sup>, 2009 and August 4<sup>th</sup>, 2010 and in PSY2V4R1 between December 2<sup>nd</sup>, 2009 and March 3<sup>rd</sup>, 2010.

## **II.2. Observations available for validation**

Both observational data and statistical combinations of observations are used for the real time validation of the products. Most of them were available in real time during the season:

- T/S profiles
- OSTIA SST (with one problem on July 21<sup>st</sup>)
- Arctic sea ice concentration
- Surcouf surface currents
- Armor-3D 3D temperature and salinity fields.

SST Odyssey SST maps (temporarily stopped) and Arctic sea ice drift products were not available during this season, and the delivery of drifters data was delayed several times.

## **III Information on the large scale climatic conditions**

Mercator Ocean participates in the monthly seasonal forecast expertise at Météo-France. This chapter summarizes the state of the ocean and atmosphere during the JAS 2010 season, as discussed in the “Bulletin Climatique Global” of Météo-France.

This season was characterized by the strengthening of La Niña atmospheric and oceanic conditions. In the ocean (see surface temperatures in Figure 2), the Eastern Tropical Pacific Ocean gets cooler, with negative temperature anomalies at depth. The eastern Pacific is anomalously cold through all the season. The equatorial currents of the Pacific are anomalously strong (<http://www.cpc.ncep.noaa.gov/products/CDB/Tropics/figa1.7.shtml> ).

*Quo Va Dis ? Quarterly Ocean Validation Display #2, JAS 2010*

A strong African monsoon together with warm subtropical Atlantic SSTs results in an active hurricane season in the Atlantic. In contrast, La Niña leads to below average hurricane activity in the Pacific.

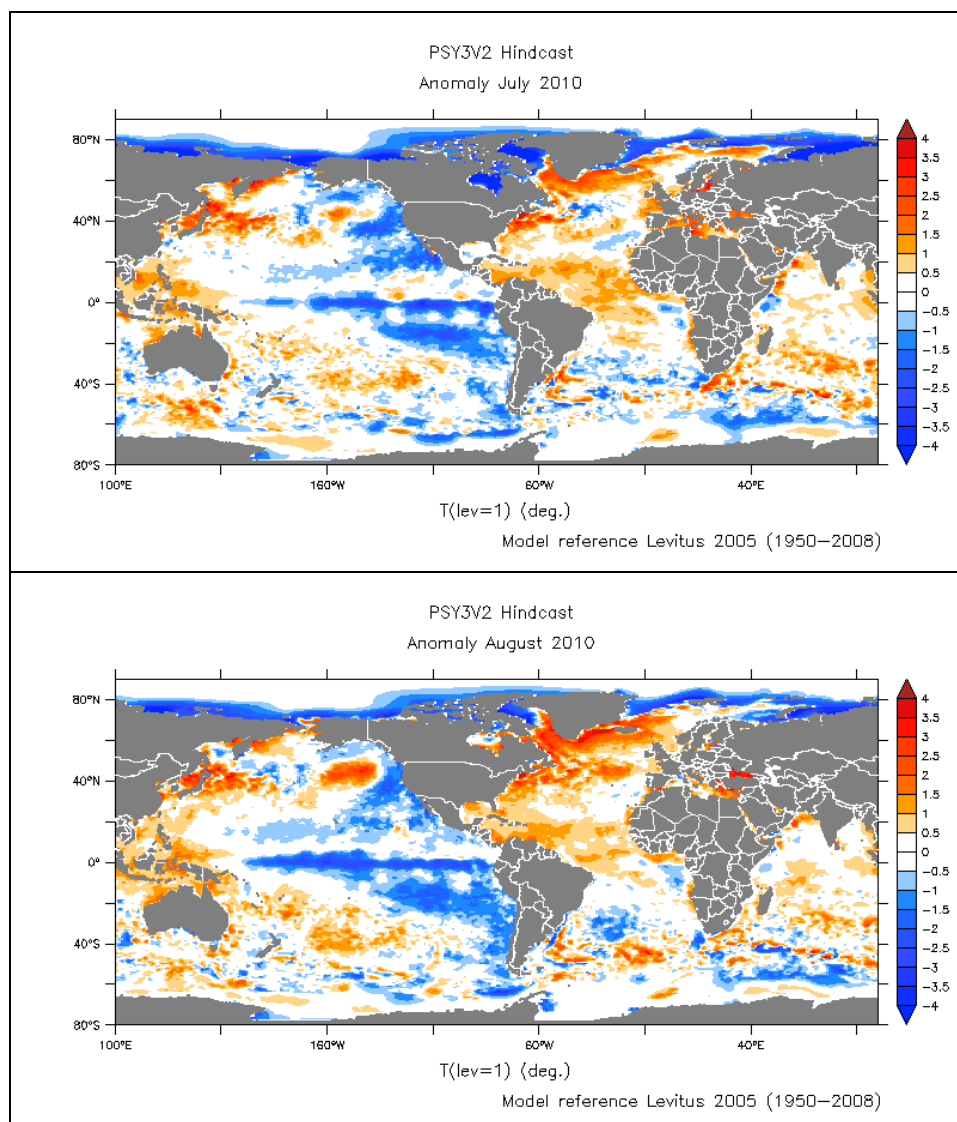
A strong Indian monsoon was observed, as well as stronger than normal western monsoon current in the Indian Basin

(<http://www.cpc.ncep.noaa.gov/products/CDB/Tropics/figa1.8.shtml>).

Precipitations were above average over Indonesia, the Caribbean Sea and Gulf of Mexico, the Eastern Tropical Atlantic and were below average in the eastern Tropical Pacific.

The Tropical Atlantic and the North Atlantic Sub-polar gyre surface temperatures were anomalously warm over the whole season. This signal is also clear in the heat content over the first 300m of the ocean (not shown). The North Atlantic oscillation is still negative, but the negative anomaly in the centre of the North Atlantic basin tends to disappear (probably due to the dominant Atlantic Ridge or East Atlantic mode positive phases).

The Mediterranean Sea is anomalously warm in the eastern parts.



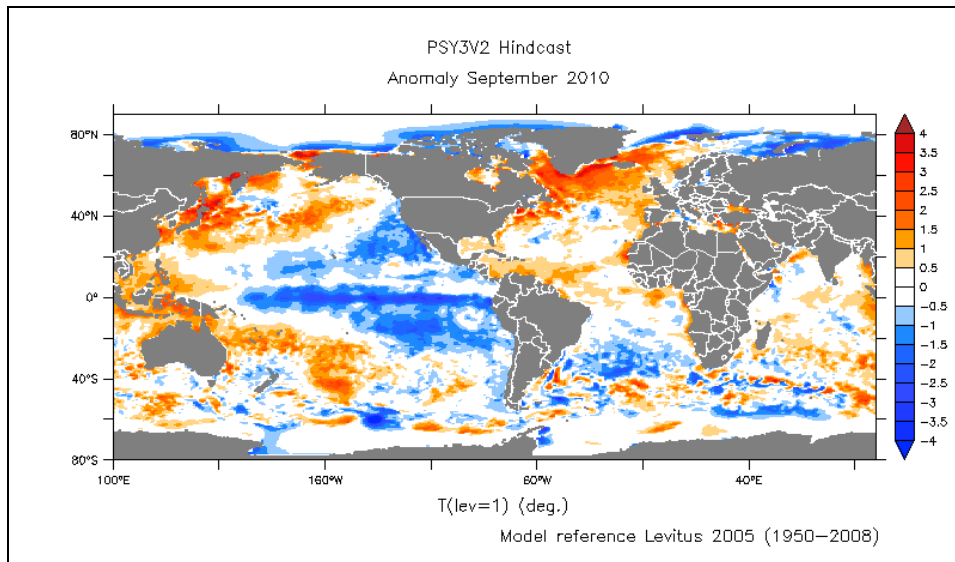


Figure 2: SST monthly anomalies (°C) at the global scale from the 1/4° ocean monitoring and forecasting system PSY3V2R2 with respect to Levitus (2005) climatology. Upper panel July anomaly, middle panel August anomaly, lower panel September anomaly.

This season also sees the minimum extent of arctic Sea Ice (in September) as can be seen in Figure 3.

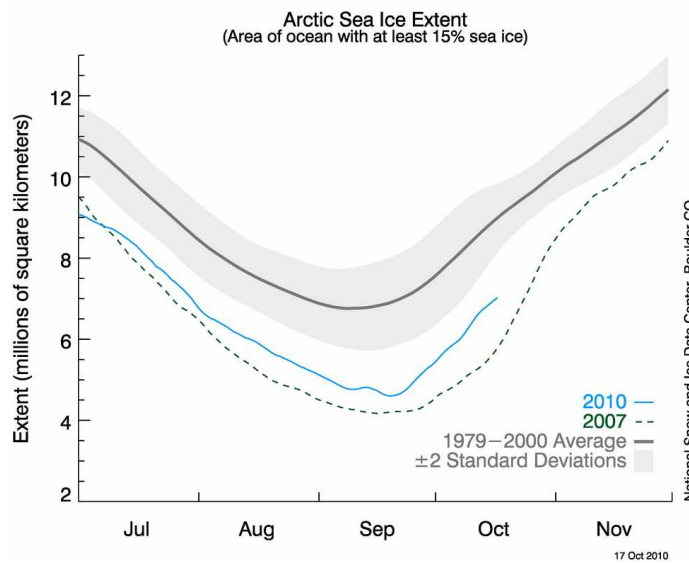


Figure 3: Arctic sea ice extent from the NSIDC:  
[http://nsidc.org/data/seaiice\\_index/images/daily\\_images/N\\_stddev\\_timeseries.png](http://nsidc.org/data/seaiice_index/images/daily_images/N_stddev_timeseries.png)

## IV Accuracy of the products

### IV.1. Data assimilation performance

#### IV.1.1. Sea surface height

##### IV.1.1.1. North Atlantic Ocean for all systems

The Tropical and North Atlantic Ocean Sea SLA assimilation scores for all systems are displayed in Figure 4. The most recent systems' performance (PSY4V1, PSY3V3, PSY2V4) is very similar to the current ones, except for slight improvements in the small Florida Strait region and in the Gulf of Guinea for instance. The biases generally decrease in the new systems, while the RMS errors increase in the regions of high mesoscale variability like the Gulf Stream. The RMS error (order of magnitude 5-8 cm) is generally lower than the intrinsic variability of the observations which indicates a good performance of the system in the region, provided that the scores of the other assimilated observations are also good (see the ratio Figure 5 and Mercator Quarterly Newsletter #9).

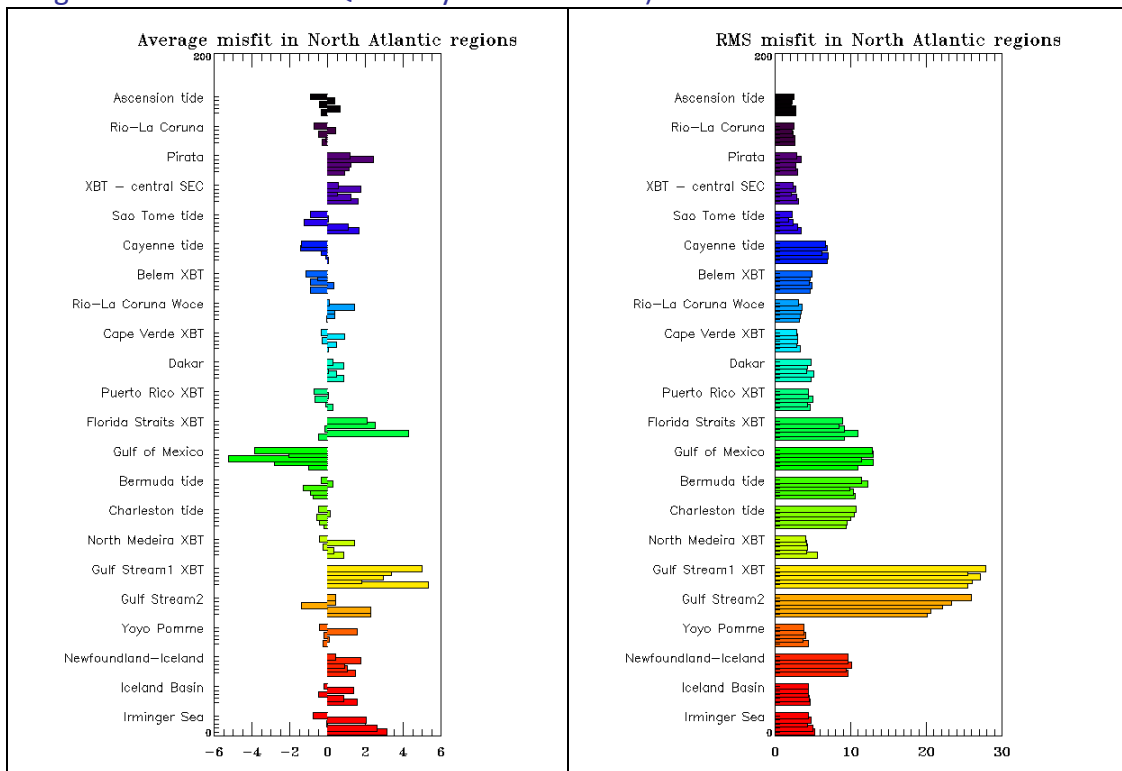


Figure 4: Comparison of SLA data assimilation scores (left: average misfit in cm, right: RMS misfit in cm) in JAS 2010 and between all available Mercator Ocean systems in the Tropical and North Atlantic. The scores are averaged for all available satellite along track data (Jason 1, Jason 2 and Envisat). For each region from bottom to top, the bars refer respectively to PSY3V2, PSY2V3, PSY3V3, PSY2V4, PSY4V1. The geographical location of regions is displayed in annex A.

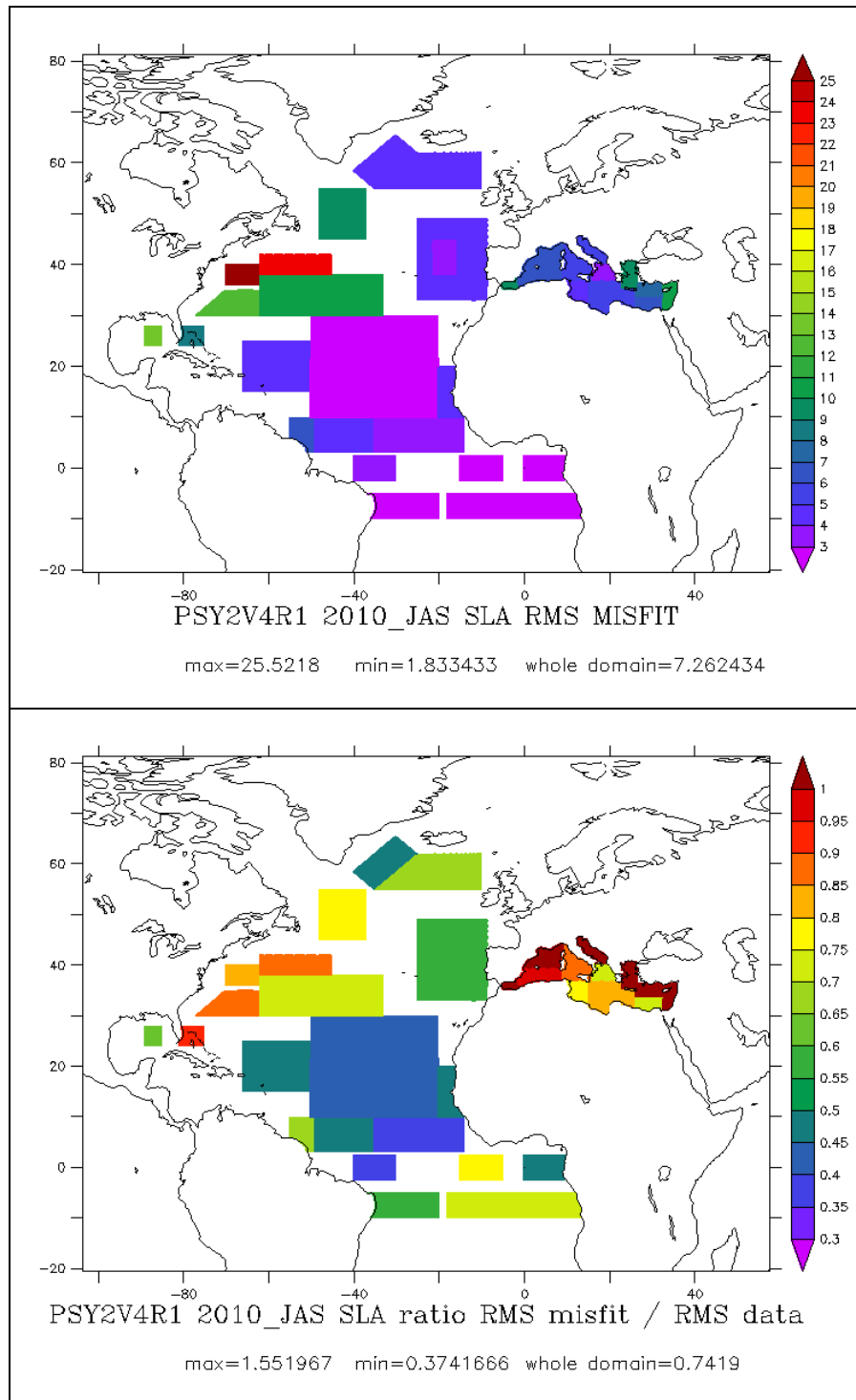


Figure 5: Synthetic map of regional SLA RMS misfit (cm, upper panel) and of regional ratio of RMS misfit over RMS of SLA data (lower panel) in the Atlantic Ocean and Mediterranean Sea for the new system PSY2V4 in JAS 2010. The scores are averaged for all available satellite along track data (Jason 1, Jason 2 and Envisat).

#### IV.1.1.2. Mediterranean Sea in PSY2 (1/12°)

The bias is reduced in PSY2V4 as can be seen in Figure 6, except in the Aegean Sea and western Mediterranean Sea (regions Alboran, Lyon, Algerian). The RMS misfit of PSY2V3 and PSY2V4 have very similar levels, with regional differences. The RMS increases where the bias increases, while it decreases slightly elsewhere. The PSY2V4 mean SSH has been shifted starting in August in the Mediterranean in order to reduce biases, thus these scores might evolve positively during the next quarter.

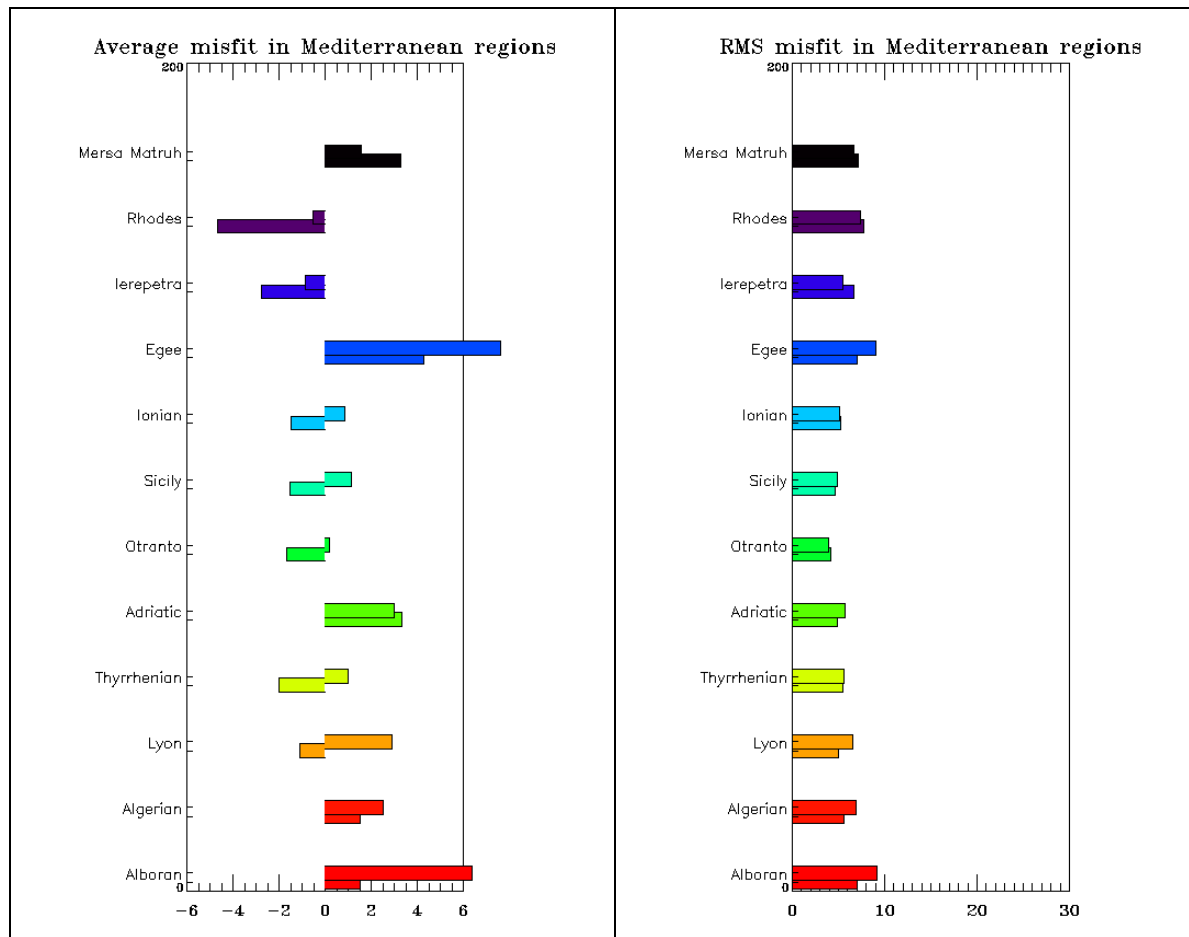


Figure 6: Comparison of SLA data assimilation scores (left: average misfit in cm, right: RMS misfit in cm) in JAS 2010 and between both PSY2 systems in the Mediterranean Sea. For each region from bottom to top: PSY2V3, and new version PSY2V4. The scores are averaged for all available satellite along track data (Jason 1, Jason 2 and Envisat). The geographical location of regions is displayed in annex A.

#### IV.1.1.3. Performance at global scale in PSY3 (1/4°) and PSY4 (1/12°)

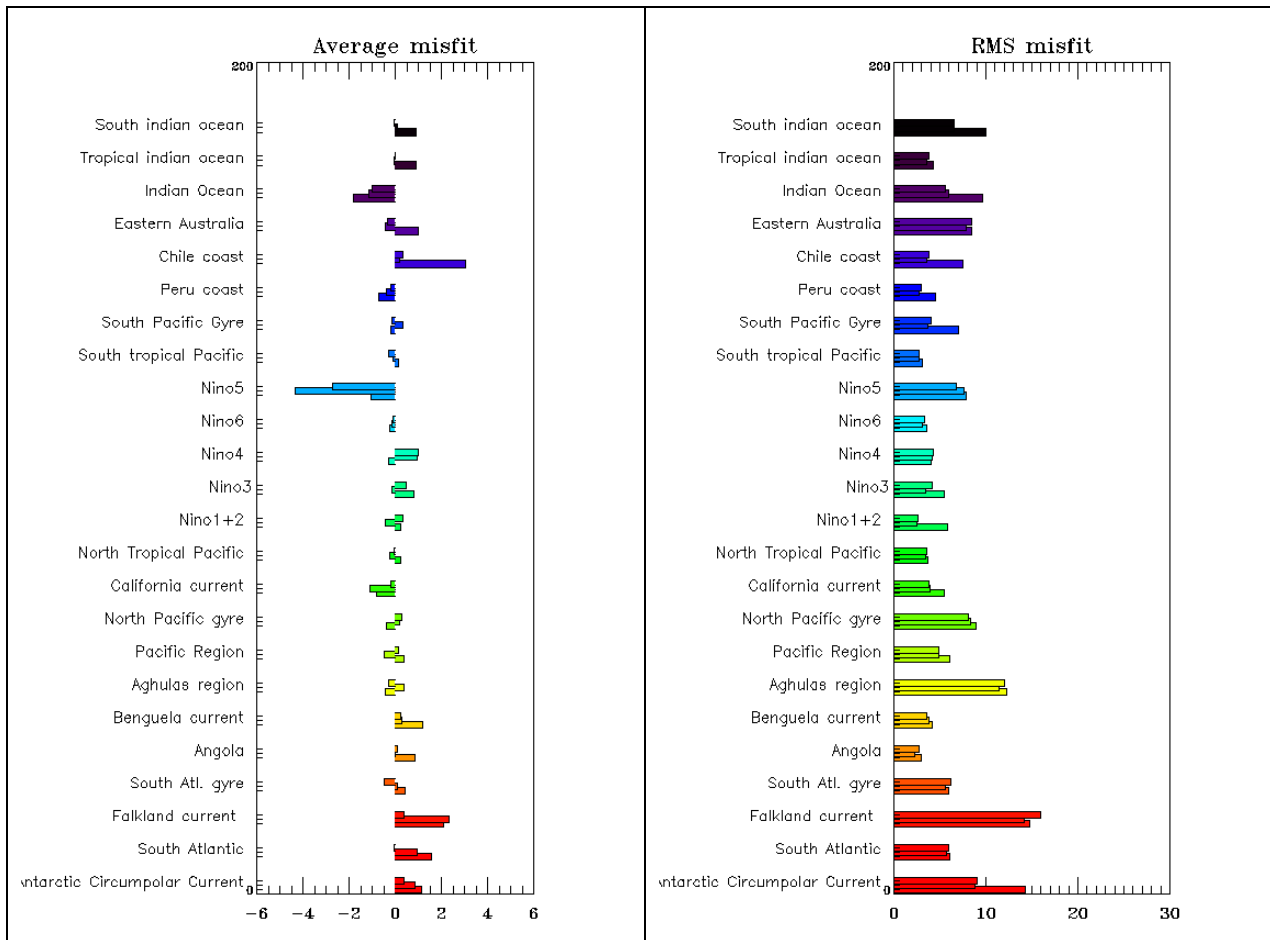
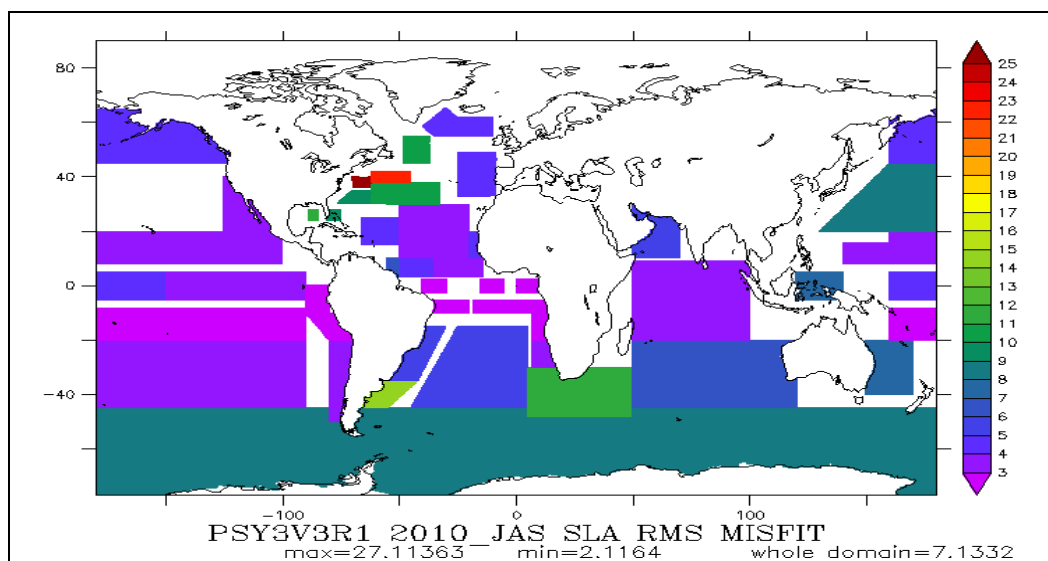
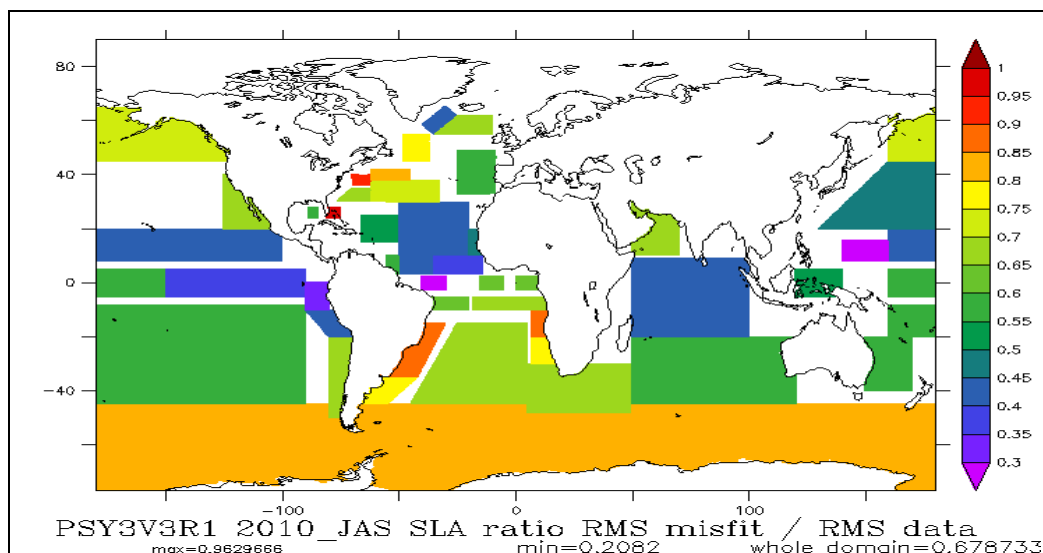


Figure 7: Comparison of SLA data assimilation scores (left: average misfit in cm, right: RMS misfit in cm) in JAS 2010 and between all available Mercator Ocean systems in all basins but the Atlantic and Mediterranean. For each region from bottom to top: PSY3V2, PSY3V3, and PSY4V1. The geographical location of regions is displayed in annex A.





**Figure 8 : Synthesis of regional RMS misfit (cm, upper panel), and ratio between RMS misfit and RMS of data (lower panel) in the Global Ocean (except the Mediterranean).**

As can be seen on Figure 7 both new systems PSY3V3 and PSY4V1 perform significantly better than PSY3V2 in terms of SLA assimilation, especially in the southern oceans. Either the bias or the RMS error is reduced.

The RMS error has been increasing regularly in the Antarctic Ocean in PSY3V2R2 since April, which is not the case in the new systems. This problem is under investigation and might be due to aliasing phenomena in the observation operator of PSY3V2.

The ratio between RMS misfit and RMS of SLA data shown on Figure 8 reach the lowest values ever obtained with the PSY3 system.

#### IV.1.2. Sea surface temperature

##### IV.1.2.1. North and Tropical Atlantic Ocean in all systems

In the Atlantic the new systems SST RMS error is significantly lower than in the current systems' as illustrated on Figure 9. Over all systems, PSY2V4 is the closest to RTG-SST satellite observations in terms of RMS. PSY4V1 which has IAU and daily average atmospheric forcings (instead of IAU and 3-hourly forcings for PSY2V4 and PSY3V3) is the less biased of all system. There is a cold bias in PSY3V3 north of 30°N of about 0.5°C. The calibration of the system over the 2007-2009 period shows that this bias is seasonal and is maximum during boreal summer (JAS season). This will be especially looked after, and corrections have already been made starting in August that should improve the results on the long term. The observation operator now considers only night-time SSTs to compare with RTG-SST. PSY2V4 does not exhibit the same bias as PSY3V3 in the northern seas (Irminger Sea, Iceland Basin), moreover it is close to in situ observations in these regions.

Quo Va Dis ? Quarterly Ocean Validation Display #2, JAS 2010

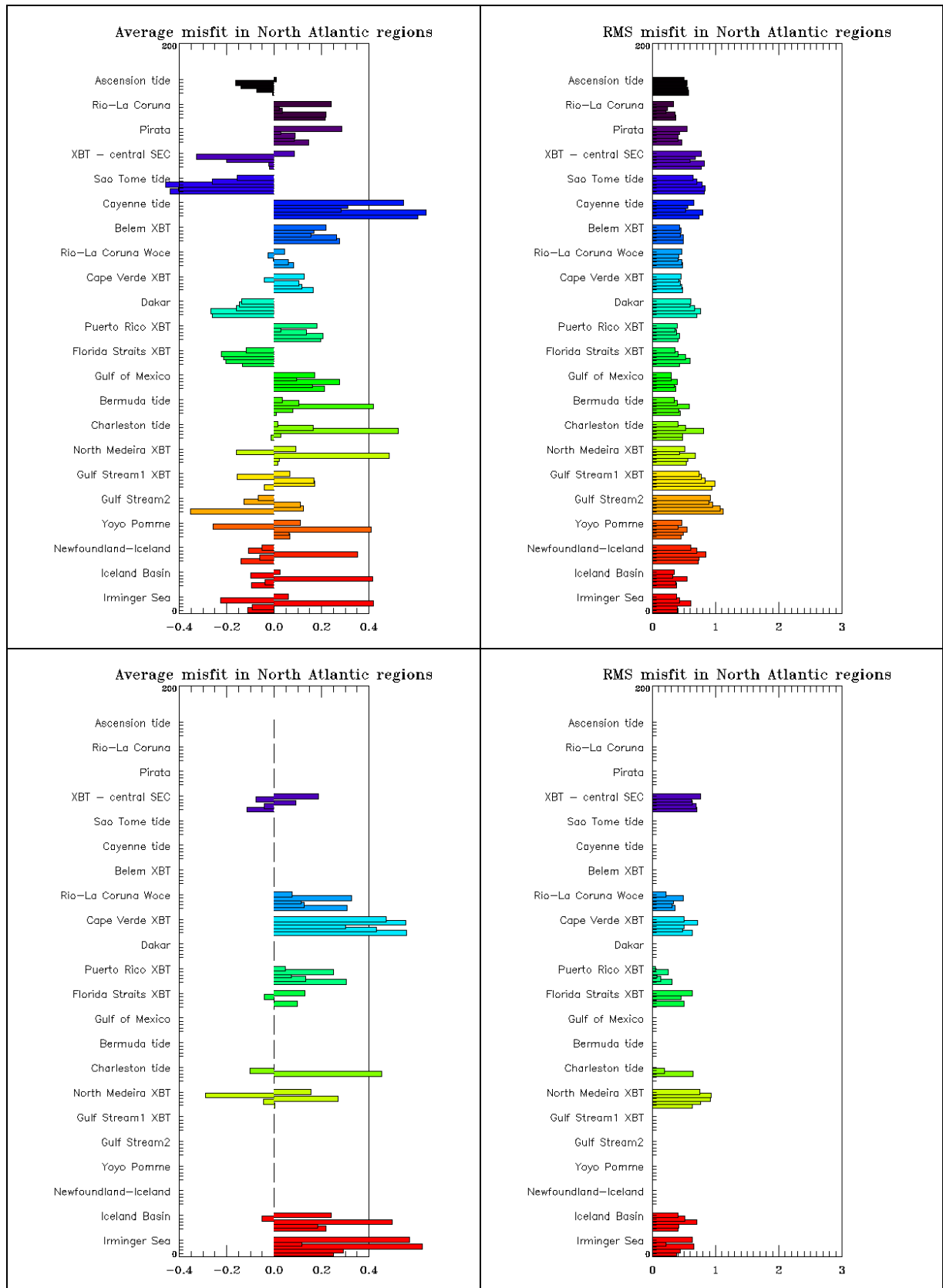
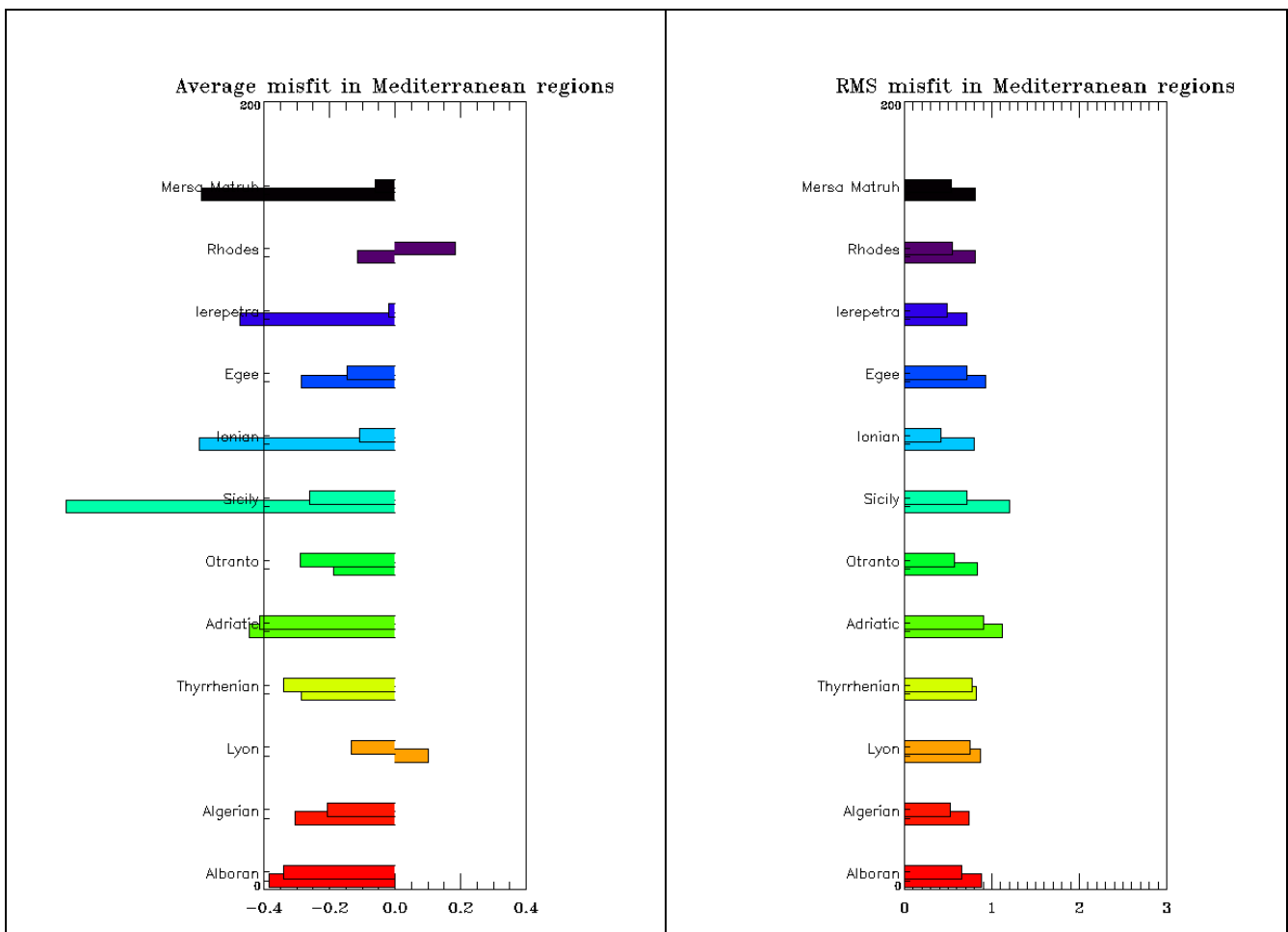


Figure 9: Comparison of SST data assimilation scores (left: average misfit in °C, right: RMS misfit in °C) in JAS 2010 and between all available Mercator Ocean systems in the Tropical and North Atlantic. Upper panel: RTG-SST data assimilation scores, lower panel: in situ SST data assimilation scores. For each region from bottom to top: PSY3V2, PSY2V3, PSY3V3, PSY2V4, PSY4V1.

#### IV.1.2.2. Mediterranean Sea by PSY2 (1/12°)

The SST RMS errors with respect to RTG-SST in the Mediterranean Sea are clearly reduced in PSY2V4 in all regions (Figure 10). Southern regions exhibit major bias reduction like Ionian and Sicily. This reduction of RMS errors is not as clear with respect to in situ data, in particular again in the western and northern parts of the Mediterranean (Alboran, Algerian and Lyon regions). The effect of the change of the observation operator cannot be quantified yet.



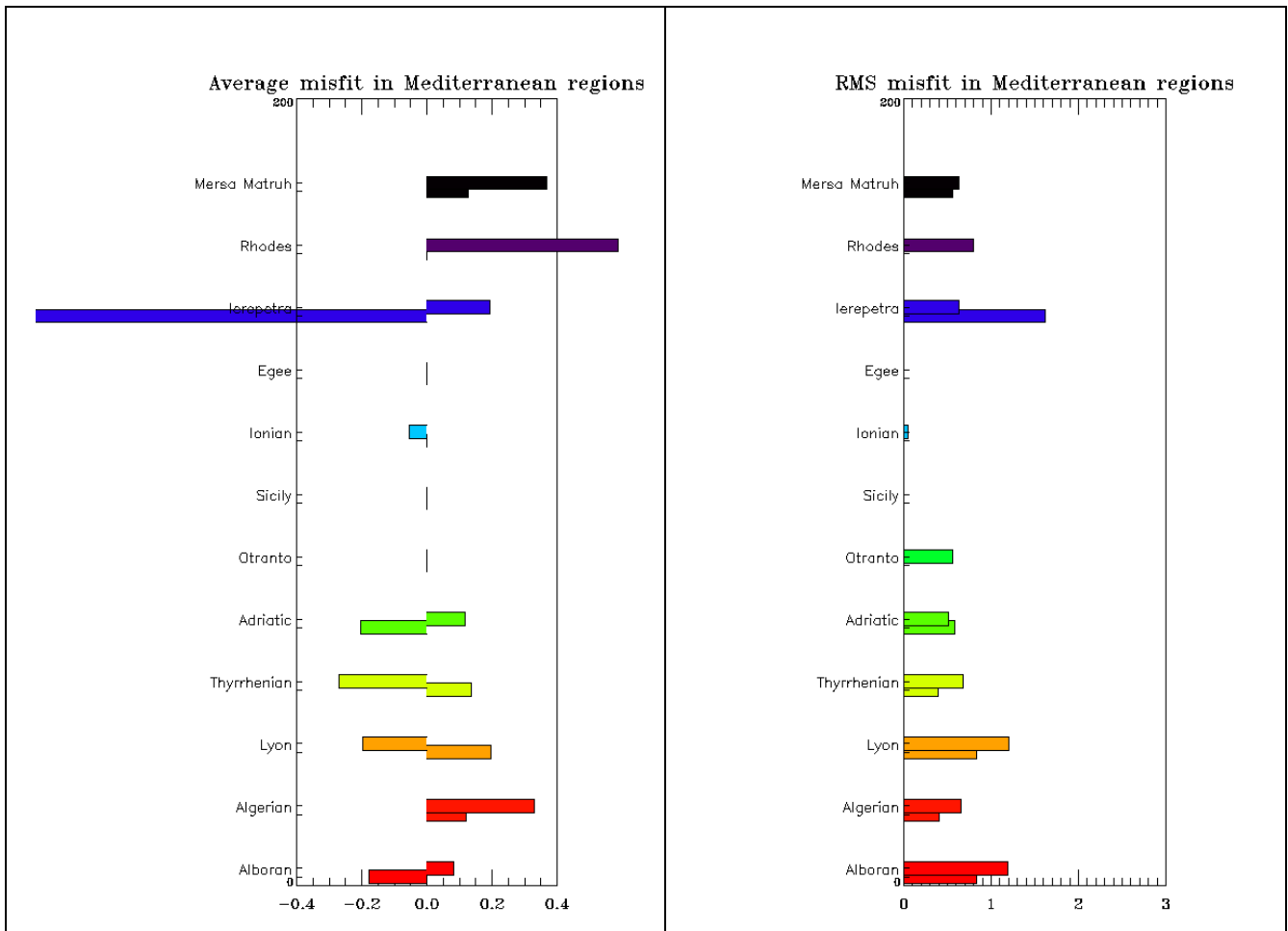


Figure 10: Comparison of SST data assimilation scores (left: average misfit in °C, right: RMS misfit in °C) in JAS 2010 and between both PSY2 systems in the Mediterranean Sea. Upper panel: RTG-SST data assimilation scores, lower panel: in situ SST data assimilation scores. For each region from bottom to top: PSY2V3, and new version PSY2V4.

IV.1.2.3. Performance at global scale in PSY3 (1/4°) and PSY4 (1/12°)

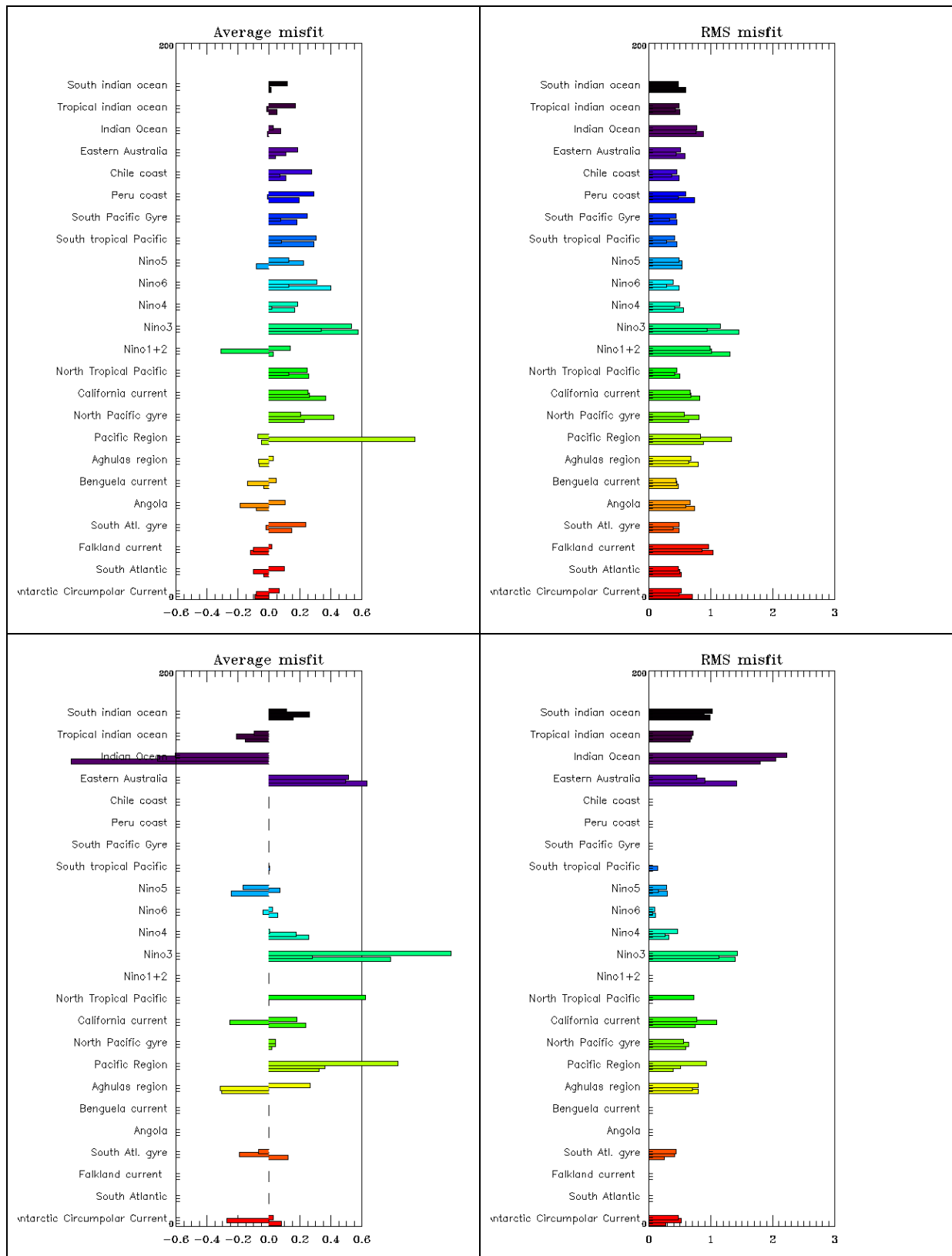
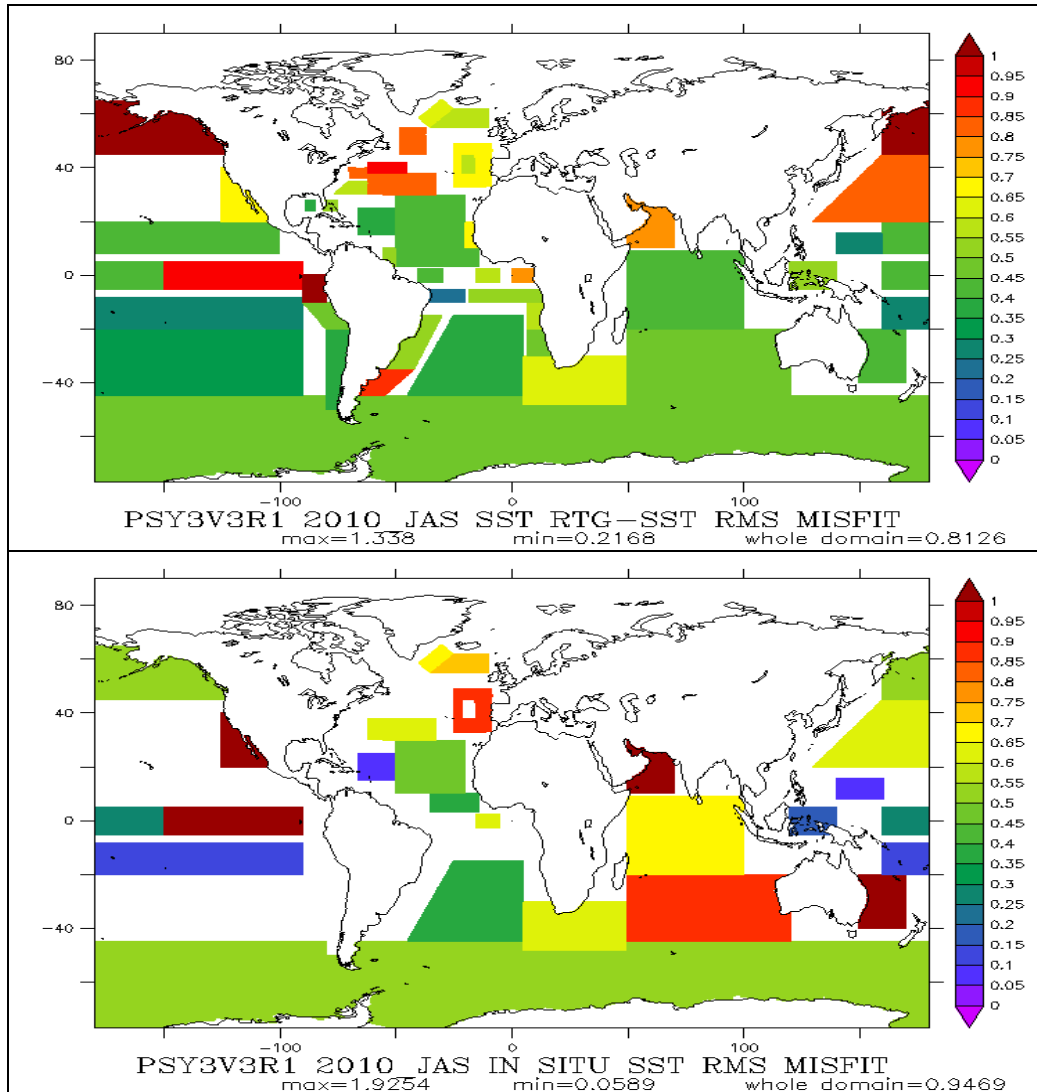


Figure 11: Comparison of SST data assimilation scores (left: average misfit in °C, right: RMS misfit in °C) in JAS 2010 and between all available Mercator Ocean systems in all basins but the Atlantic and Mediterranean. Upper panel: RTG-SST data assimilation scores, lower panel: in situ SST data assimilation scores. For each region from bottom to top: PSY3V2, PSY3V3, and PSY4V1.



**Figure 12 Average JAS 2010 regional SST ( $^{\circ}\text{C}$ ) data assimilation scores of RMS of misfit for RTG-SST (upper panel) and in situ observations (lower panel) for PSY3V3 at the global scale.**

As in the North Atlantic a bias seems to develop in the North Pacific in PSY3V3 (Figure 11). Nevertheless the RMS error stays in the expected range (Figure 12). The Antarctic Ocean and Southern Oceans in general are closer to the observations in PSY3V3 than in PSY3V2. The bias and RMS error is significantly reduced in PSY3V3 in the Niño regions 3, 4 and 6, with respect to RTG-SST as well as with respect to in situ data. Peru and Chile regions, as well as the East Australia region are also closer to the observations in PSY3V3 than in PSY3V2. In general PSY3V3 performs better than PSY4V1, however the higher resolution of PSY4 can contradictorily lead to poorer forecast scores (with few observations leading to few innovations).

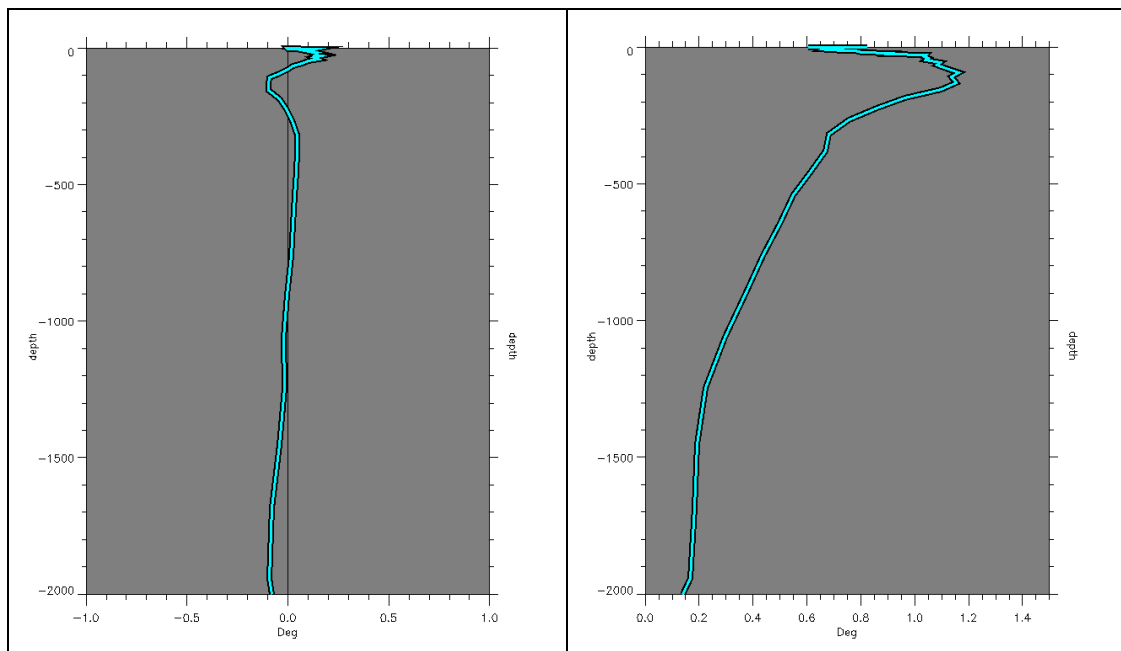
NB: the number of in situ SST data in the statistics has not been considered here, but in situ statistics in the smallest regions should be considered with caution.

### IV.1.3. Temperature and salinity profiles

#### IV.1.3.1. Performance at global scale of PSY3 (1/4°) and PSY4 (1/12°)

As can be seen in Figure 13 PSY3V2 is generally too cold over 100 m, and too warm (0.3 °C) between 100 and 200 m. A warm bias can be seen at depth. PSY4V1 is too cold (0.2 °C) over the 0-500m water column, and too warm under 1500m. The warm bias at depth is equivalent to PSY3V2. In both systems the RMS error reaches 1.2°C near 100m at the average thermocline position. Under 1000m the RMS error is lower in PSY4V1 (0.1 °C) than in PSY3V2 (0.15 °C).

The latest system PSY3V3 displays the best performance as the bias at depth disappears. A cold bias of 0.2°C is still visible in the surface layer, as well as a warm bias of 0.1 °C near 100m and a cold bias of 0.1°C or less between 100 and 500m. The RMS error is reduced by at least 0.1°C on the whole water column, and is lower than in PSY4V1 in the 0-200m layer.



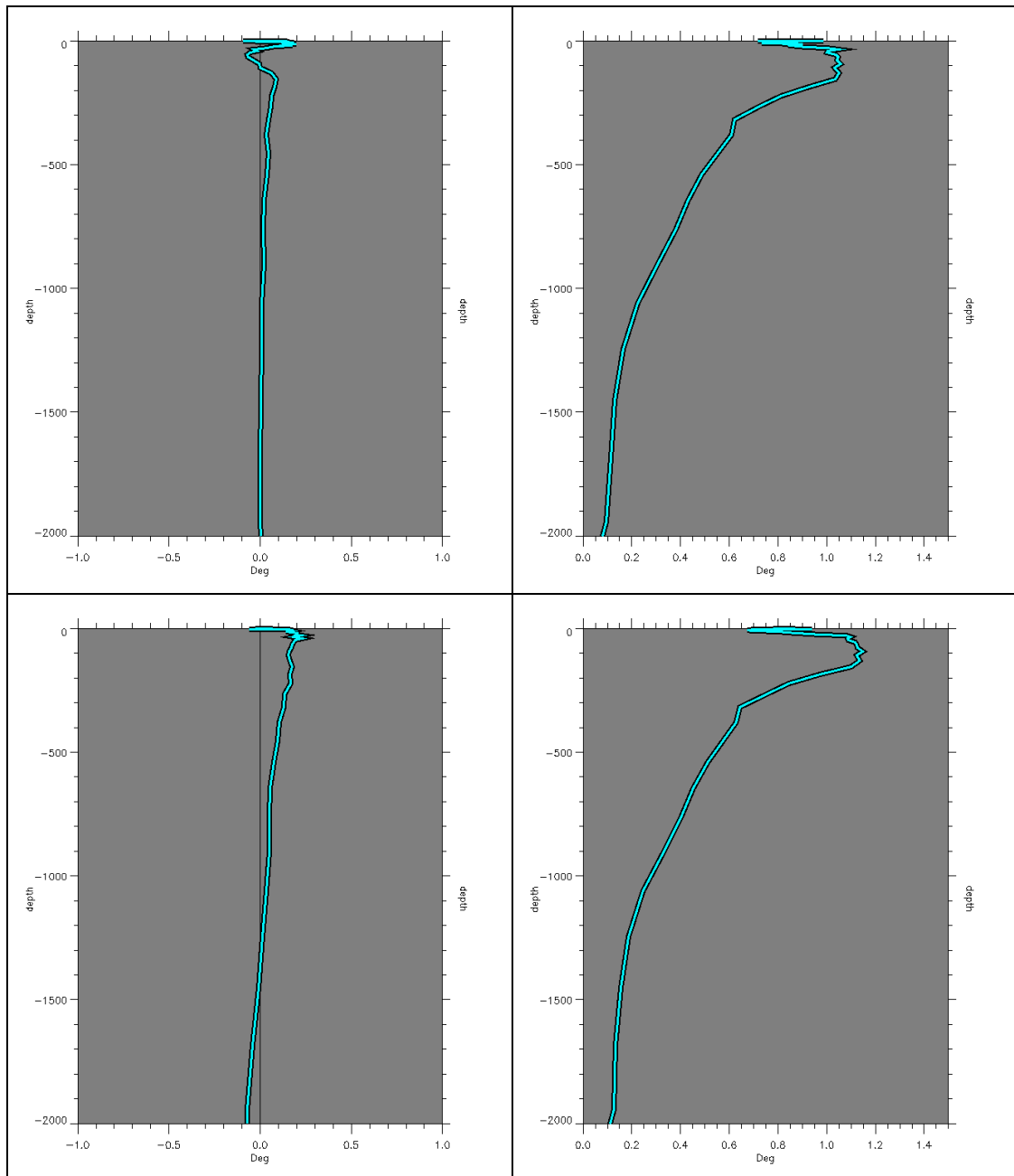


**Figure 13: mean JAS 2010 temperature profiles (°C) of average of innovation (left column) and RMS of innovation (right column) on the global PSY3V2 (upper panel) PSY3V3 (middle panel) and PSY4V1 (lower panel).**

The three systems display a salty bias near 100m and fresh bias near the surface (Figure 14). The fresh bias visible in PSY3V2 below 1000m disappears in PSY3V3 and PSY4V1, with consequently a division by 2 of the RMS error from 0.05 psu in PSY3V2 to 0.025 in PSY4V1 and PSY3V3. The bias at 100m is reduced in the most recent system PSY3V3 compared to PSY4V1, thus PSY4 water masses still can be improved in future versions.

Quo Va Dis ? Quarterly Ocean Validation Display #2, JAS 2010

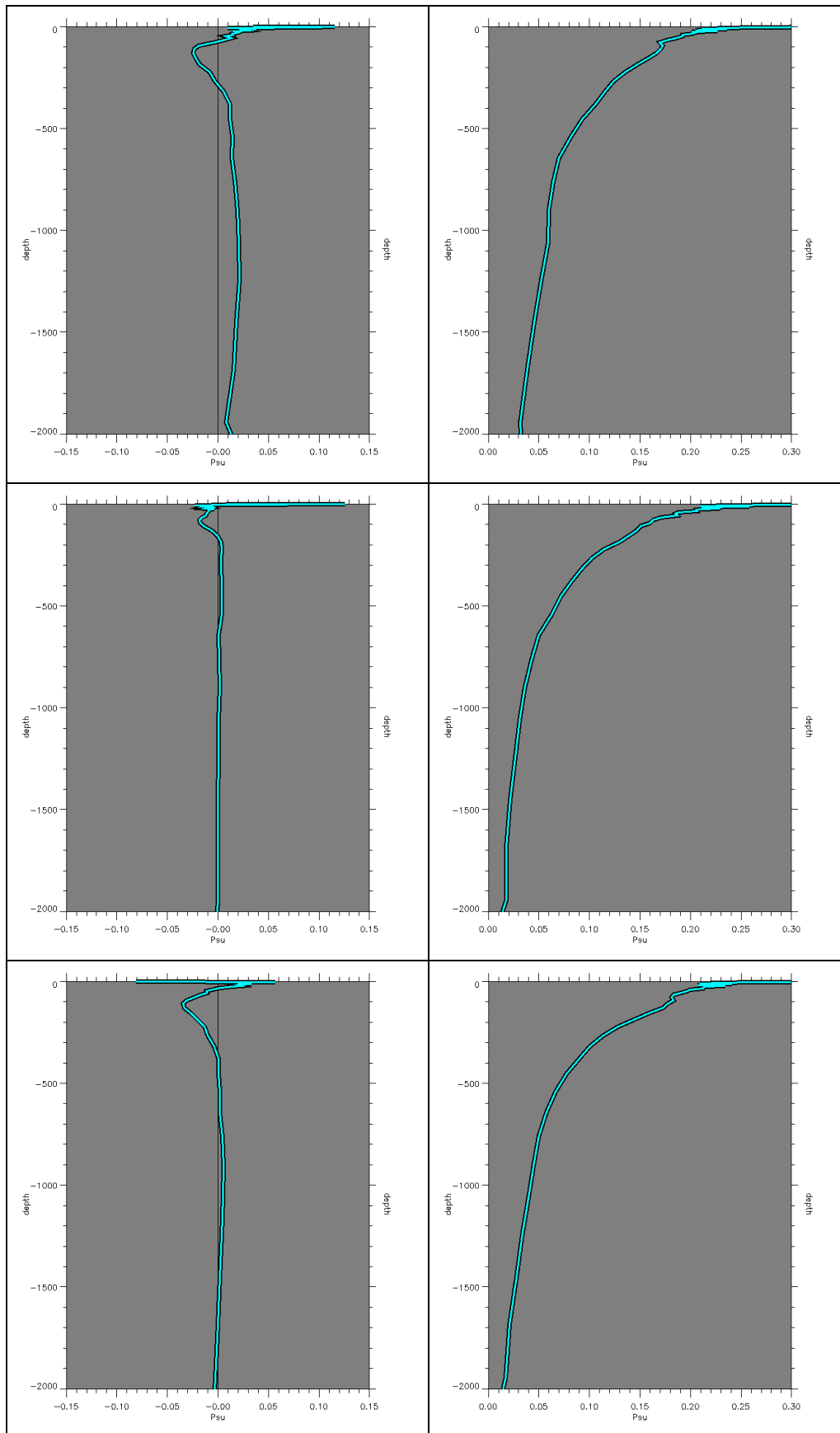


Figure 14: mean JAS 2010 salinity profiles (psu) of average of innovation (left column) and RMS of innovation (right column) on the global PSY3V2 (upper panel) PSY3V3 (middle panel) and PSY4V1 (lower panel).

### IV.1.3.2. Tropical and North Atlantic Ocean, Mediterranean Sea by PSY2 (1/12°)

Due to a smaller sample PSY2 temperature and salinity biases are amplified with respect to the global domain averages of PSY3 and PSY4. A salty and cold bias structure appeared in PSY2V3 near 1000-1500m due to the ill positioned Mediterranean outflow in the Atlantic. This bias is strongly reduced in the new systems and especially in PSY2V4 as can be seen in Figure 15 and Figure 16 (see also Figure 34).

The RMS error in the 0-200m layer is not reduced in the new PSY2V4 with respect to PSY2V3. This is due to a warm and fresh bias mainly in the 0-100m layer which occurs in the Mediterranean as will be shown in the following. We expect this bias to decrease in the future after the modifications that have been made in August (shift of the MSSH/MDT).

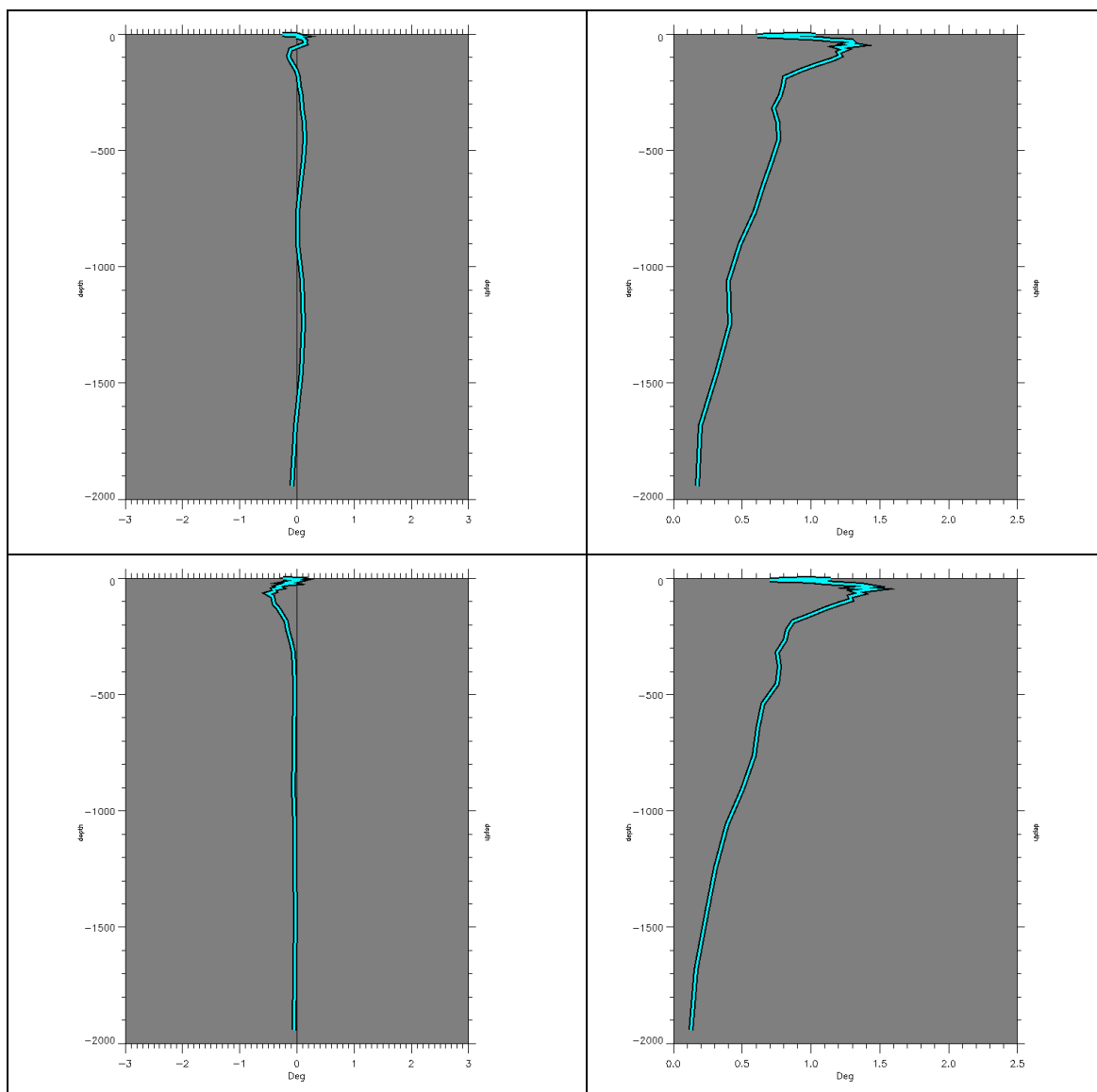


Figure 15 : mean JAS 2010 temperature profiles (°C) of average of innovation (left column) and RMS of innovation (right column) on the whole domain of PSY2V3 (upper panel) and PSY2V4 (lower panel).

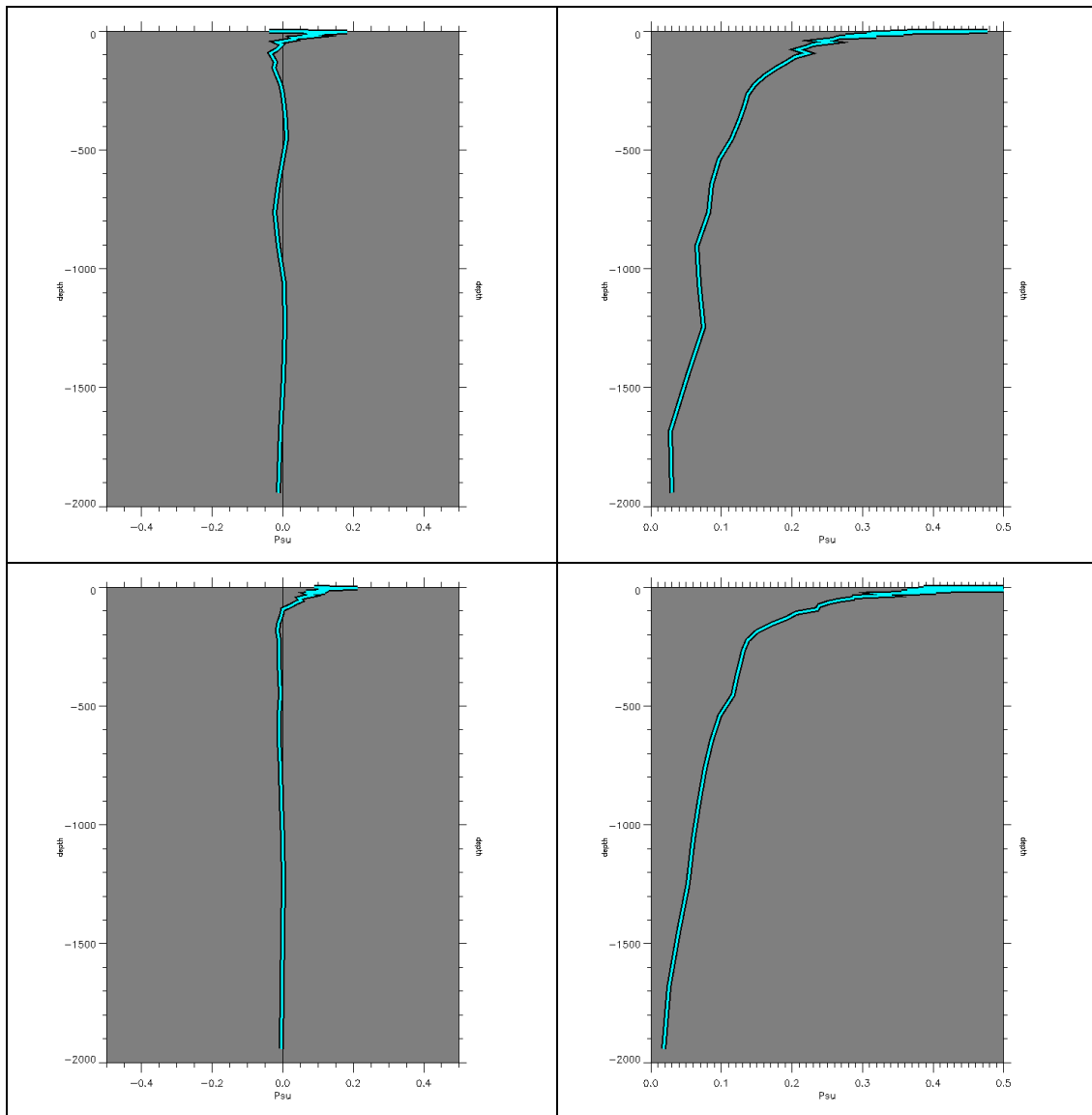


Figure 16: mean JAS 2010 salinity profiles (psu) of average of innovation (left column) and RMS of innovation (right column) on the global PSY3V2 (upper panel) and PSY3V3 (lower panel).

## IV.2. Accuracy of the daily average products with respect to observations

### IV.2.1. T/S profiles observations

#### IV.2.1.1. Global statistics

As can be seen in Figure 17, temperature errors in the 0-500m layer stand between 0.5 and 1°C in most regions of the globe in both PSY3V2 and PSY3V3. Regions of high mesoscale activity and regions of Sea Ice melting experience higher values (up to 3°C). PSY3V3 is clearly closer to the observations in the tropical oceans. The signal is very clear in the Pacific where PSY3V3 will describe the Niña signal with more accuracy. A bias in the Southern Indian ocean basin present in PSY3V2 (and probably linked with the bias in SLA) disappears in PSY3V3. We note that for a given region a minimum of 90 measurements is used to compute the

statistics for this three months period. The salinity RMS errors are usually less than 0.2 psu but can reach high values in regions of high runoff (Amazon, Sea Ice limit) or precipitations (SPCZ), and in regions of high mesoscale variability. The salinity error is globally reduced in PSY3V3 with respect to PSY3V2.

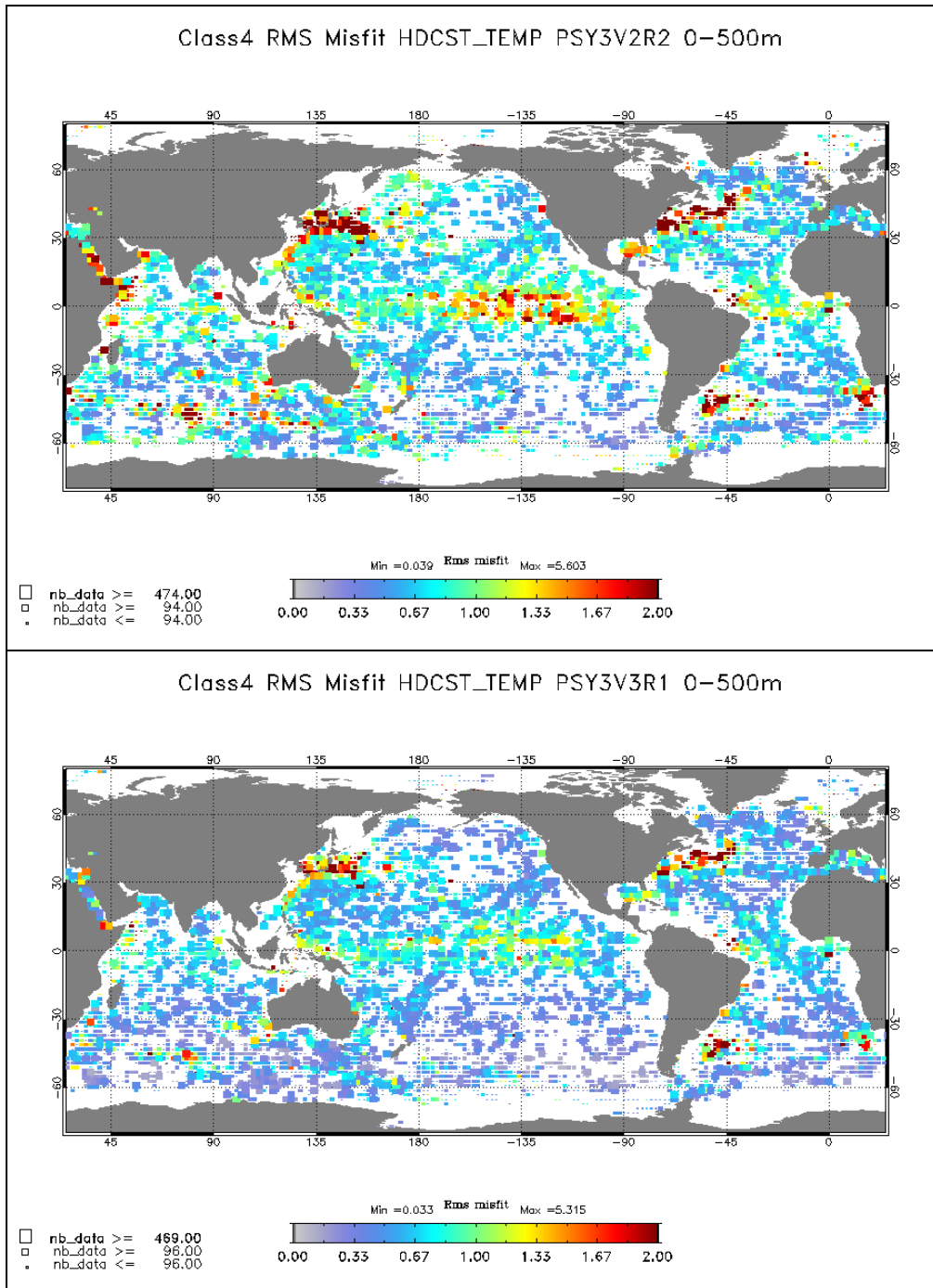


Figure 17: RMS temperature (°C) difference (model-observation) between all available T/S observations from the Coriolis database and the daily average PSY3V2 (upper panel) and PSY3V3 (lower panel) products (here the nowcast run) colocalised with the observations. The size of the pixel is proportional to the number of observations used to compute the RMS in 2°x2° boxes.

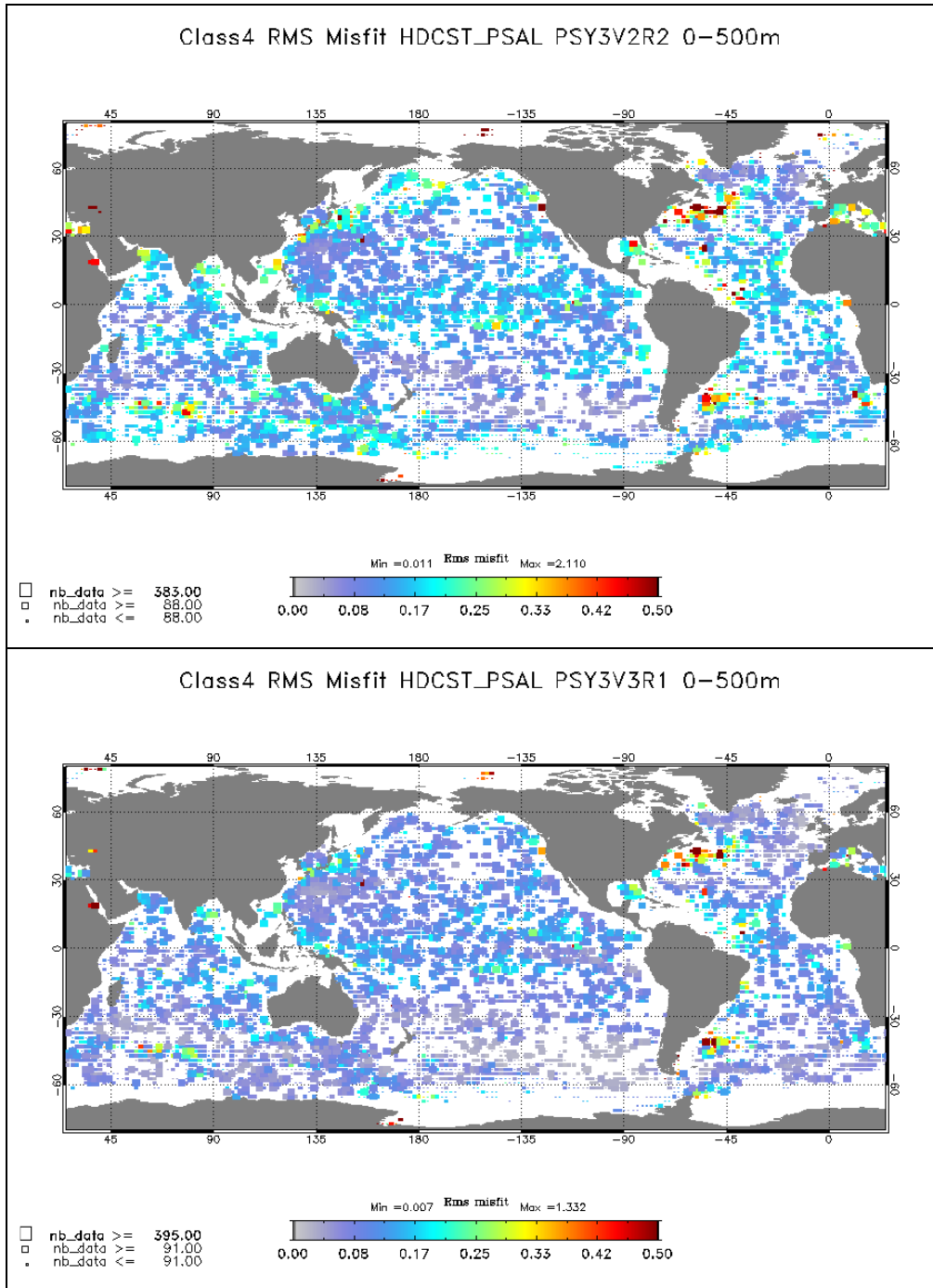


Figure 18: RMS salinity (psu) difference (model-observation) between all available T/S observations from the Coriolis database and the daily average PSY3V2 (upper panel) and PSY3V3 (lower panel) products colocalised with the observations. The size of the pixel is proportional to the number of observations used to compute the RMS in 2°x2° boxes.

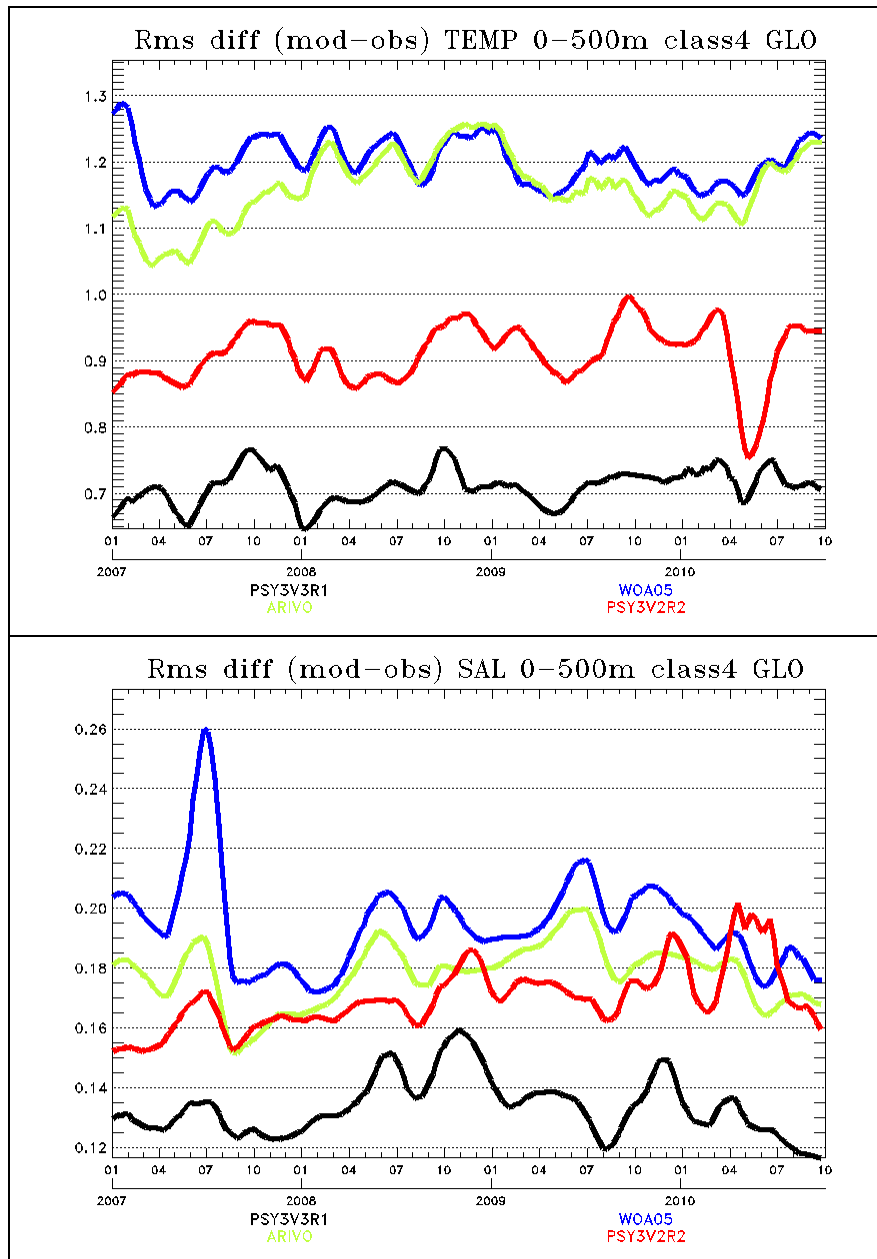


Figure 19: stability of the temperature (upper panel) and salinity (lower panel) RMS errors over the 2007-2010 period for PSY3V2R2 (red line), PSY3V3R1 (black line), Levitus WOA05 climatology (blue line) and Ifremer ARIVO climatology (green line).

Figure 19 illustrate the stability in time of the new system PSY3V3, as well as the improvement of in situ profile data assimilation. A gain of 0.2°C and 0.02 psu RMS error can be observed on average in the new system.

In April 2010 the PSY3V2 system is very close to temperature observations, and symmetrically drifts away from salinity observations, giving poor performance on average (the climatology is closer to the observations). This phenomenon is not observed in PSY3V3. Note that in PSY3V3, pseudo observations of salinity are used near estuaries and under sea ice (where error covariances are not trusted) in order to avoid error compensation phenomena.

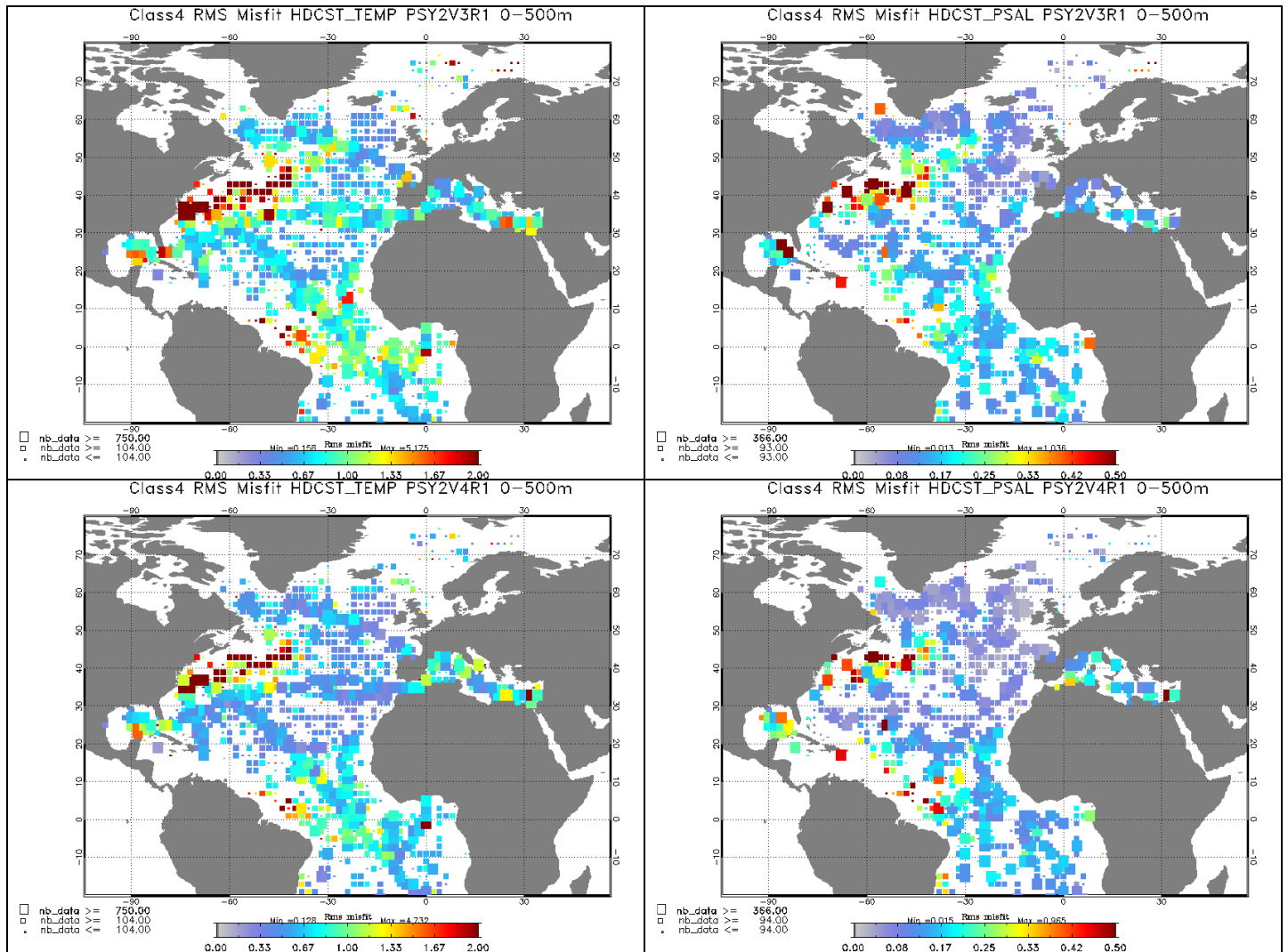
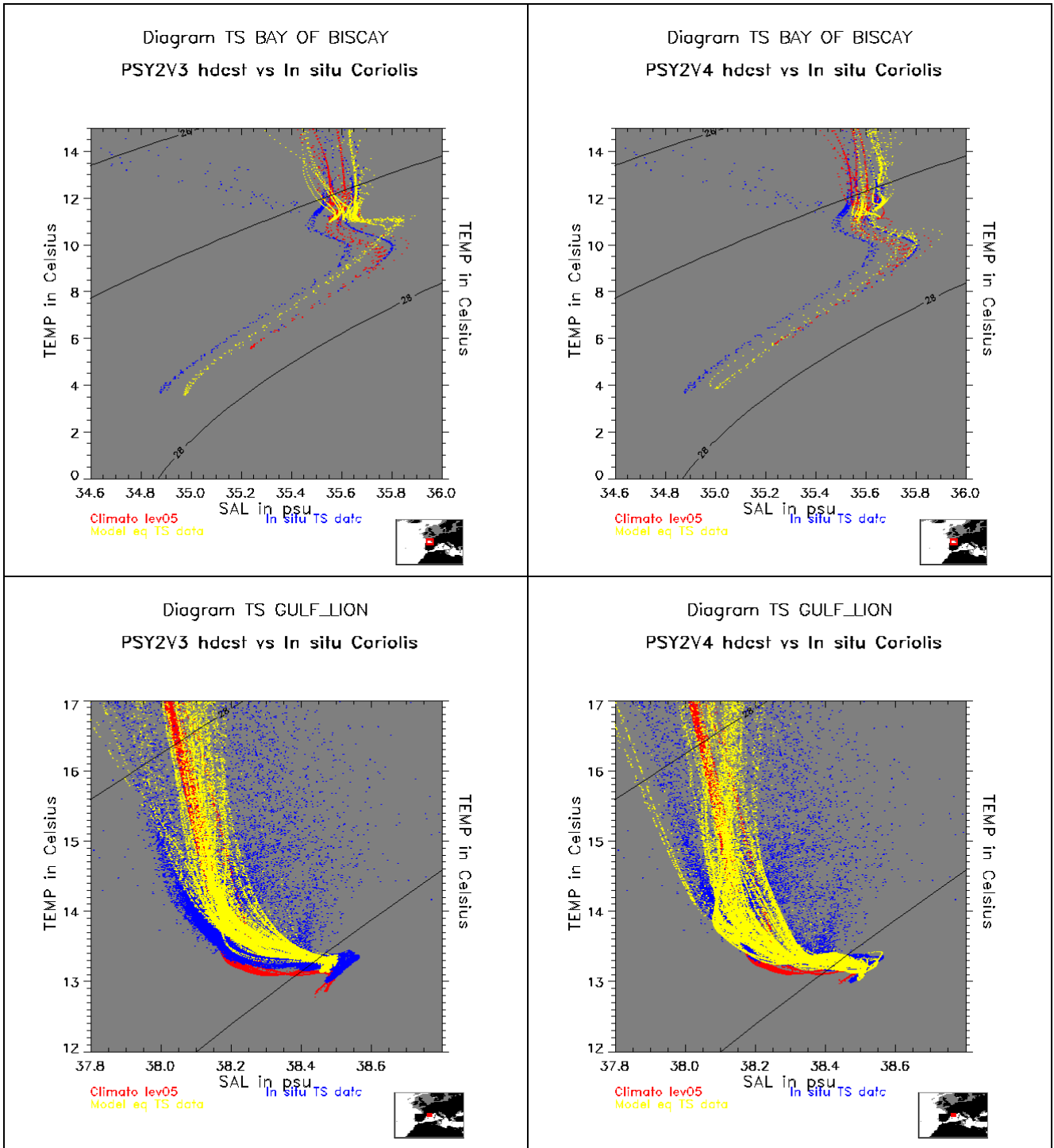


Figure 20: Upper panel: RMS temperature (left column) and salinity (right column) difference (model-observation) between all available T/S observations from the Coriolis database and the daily average PSY2V3 products colocalised with the observations. Lower panel: same with PSY2V4.

PSY2V4 is closer to the in situ profiles than PSY2V3, mainly in the tropics and the subtropics (Figure 20). In the Mediterranean Sea on average, PSY2V3 is still closer to the observations than the new version PSY2V4.

#### IV.2.1.2. Water masses diagnostics

We use here the daily products (analyses) collocated with the T/S profiles to draw “theta, S” diagrams. PSY2V4 better represents water masses characteristics than PSY2V3, especially in the Bay of Biscay (Figure 21). An improvement is also visible in the Gulf of Lyon, despite the bad statistical results in the Mediterranean Sea. The Tropical Atlantic is at least as realistic as in PSY2V3. We note the possibly (fresh) biased observations in the tropical Atlantic (Figure 22).



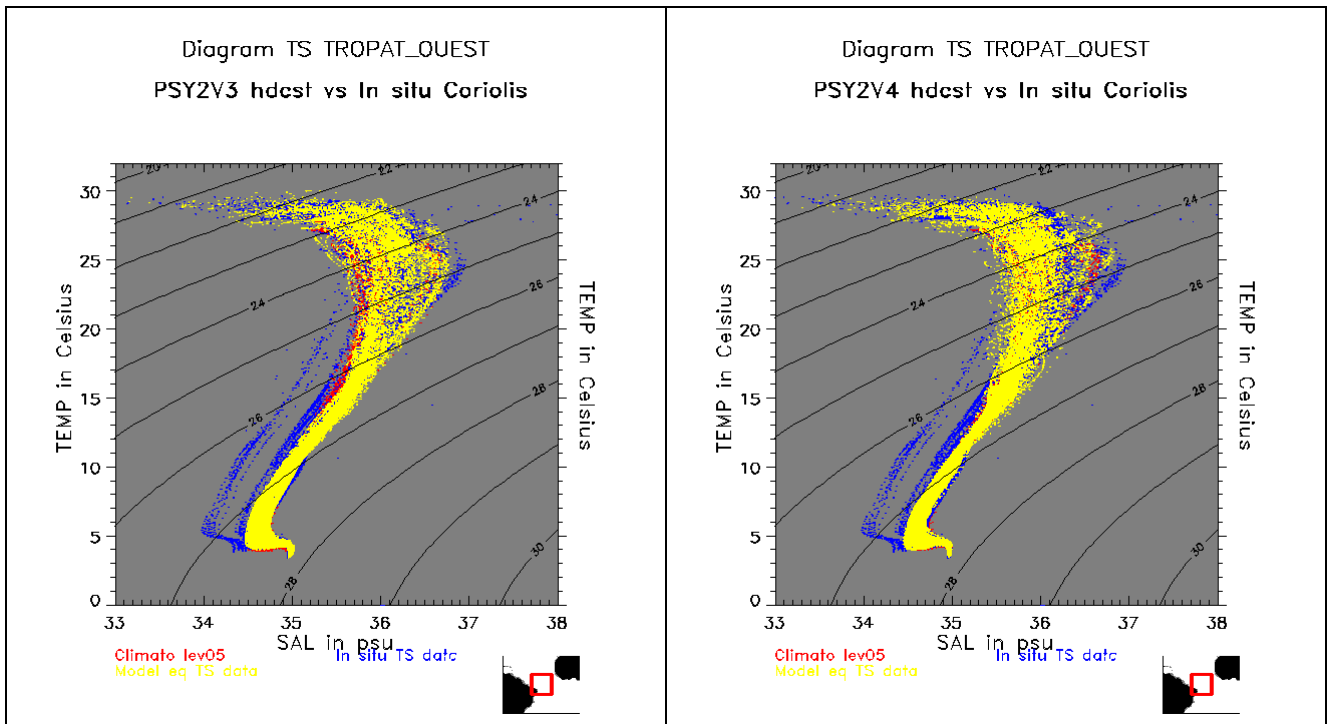
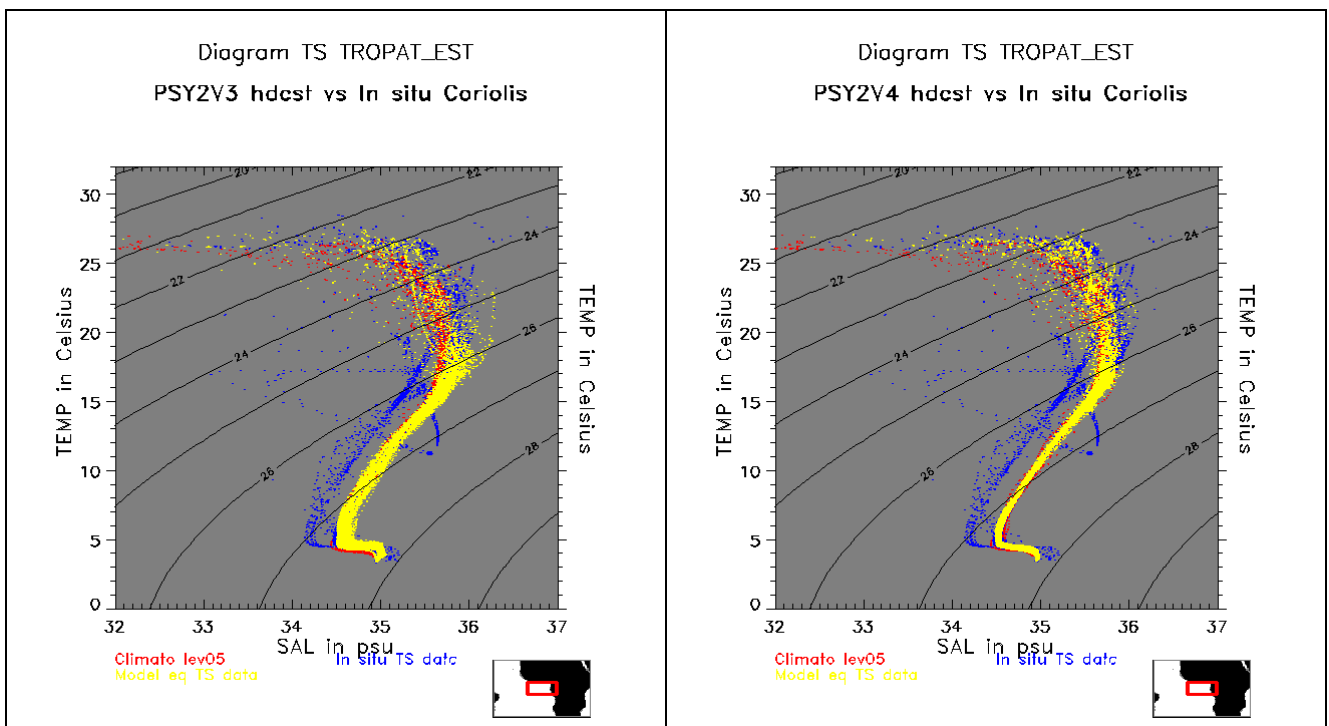


Figure 21: Water masses (Theta, S) diagrams in the Bay of Biscay (upper panel), Gulf of Lyon (middle panel) and Western Tropical Atlantic (lower panel), comparison between PSY2V3 (left column) and PSY2V4 (right column). PSY2 (yellow dots), Levitus WOA05 climatology (red dots), in situ observations (blue dots).

In the Eastern Tropical Atlantic, PSY3V3 and PSY2V4 have very similar behaviours, both displaying more realistic results than PSY3V2 and PSY2V3 (Figure 22). In the tropics the systems stick to the climatology.



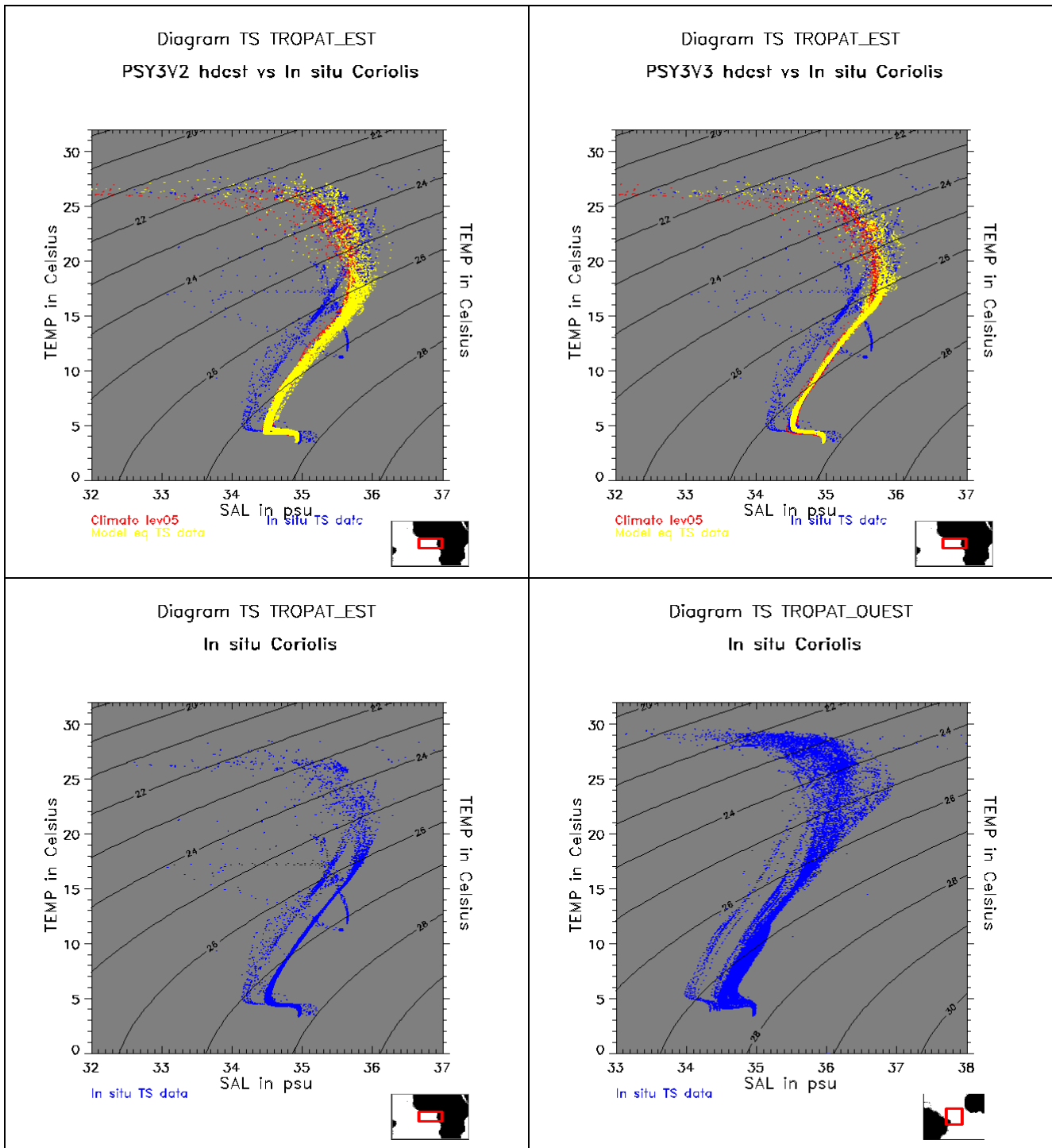


Figure 22 : Water masses (Theta, S) diagrams in the Eastern Tropical Pacific for PSY2V3 and PSY2V4 (upper panel), PSY3V2 and PSY3V3 (middle panel) and in situ observations (lower panel) only in the Western (right panel) and Eastern (left panel) tropical Atlantic. PSY2 (yellow dots), Levitus WOA05 climatology (red dots), in situ observations (blue dots).

In the Benguela current and Kuroshio current (Figure 23) PSY3V3 gives a more realistic description of water masses, with cold and fresh biases at depth disappearing with respect to PSY3V2.

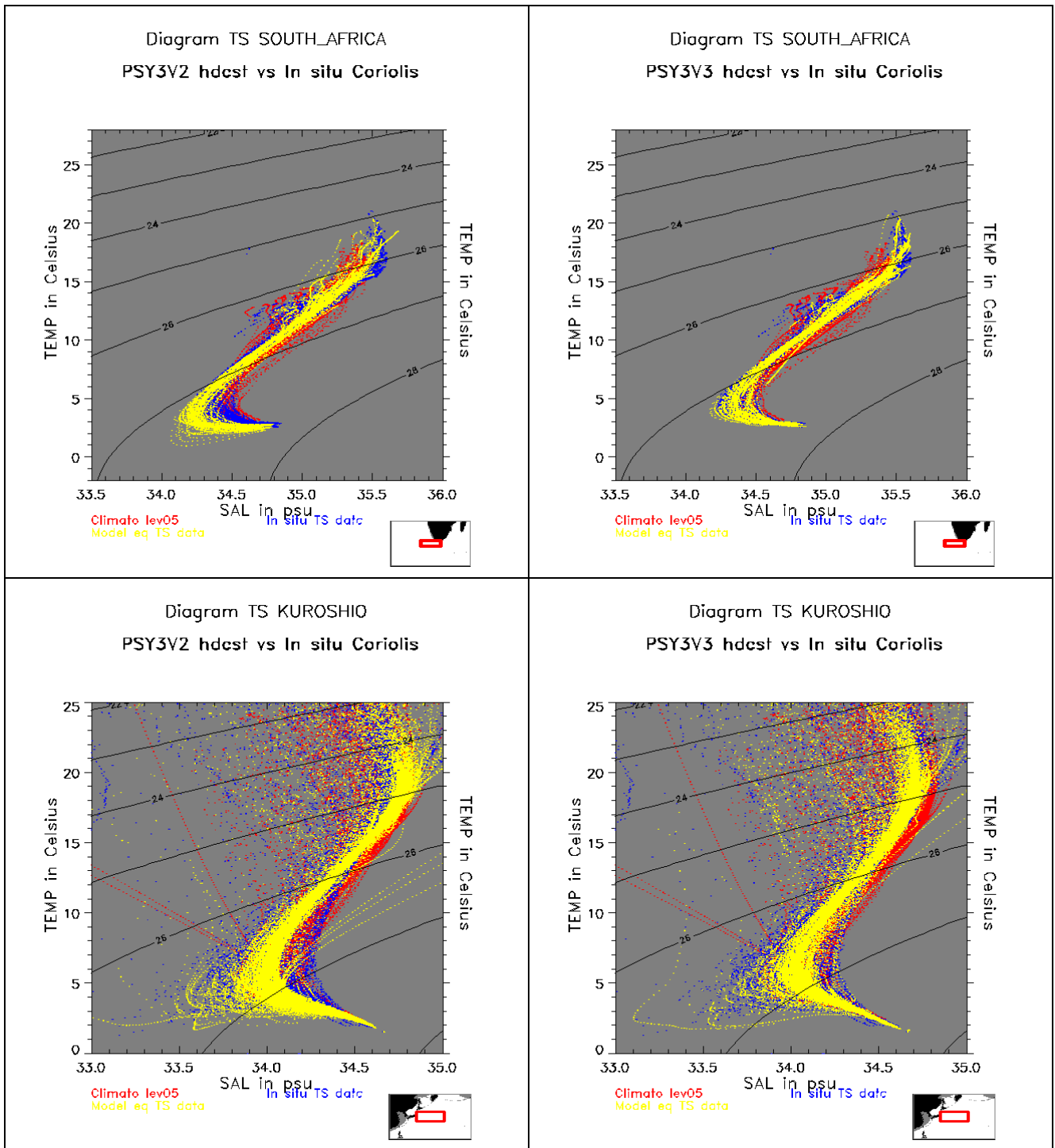


Figure 23: Water masses (Theta, S) diagrams in South Africa (upper panel) and Kuroshio (lower panel) in PSY3V2 and PSY3V3

#### IV.2.2. Drifting buoys velocity measurements

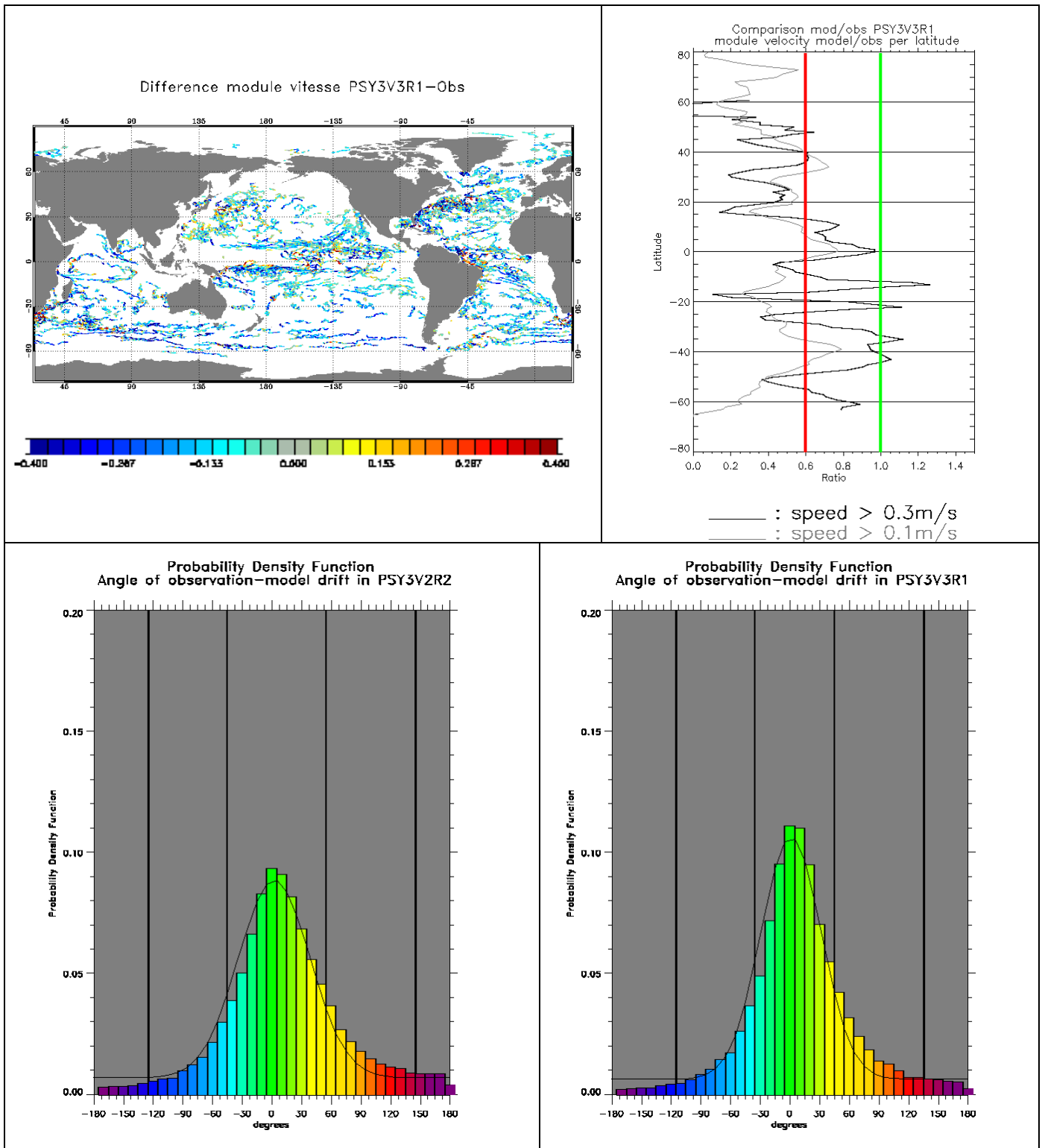


Figure 24: PSY3 analyses of velocity (m/s) collocated with drifting buoys velocity measurements. Upper left panel: difference model - observation of velocity module. Upper right panel: ratio model/observation per latitude. Lower panel: distribution of the velocity vector direction errors (degrees) for PSY3V2R2 (left panel) and PSY3V3R1 (right panel)

The surface velocity is globally underestimated by the new systems, as well as in the current PSY3V2 and PSY2V3, and as illustrated in Figure 24. Comparisons of surface drifter velocity

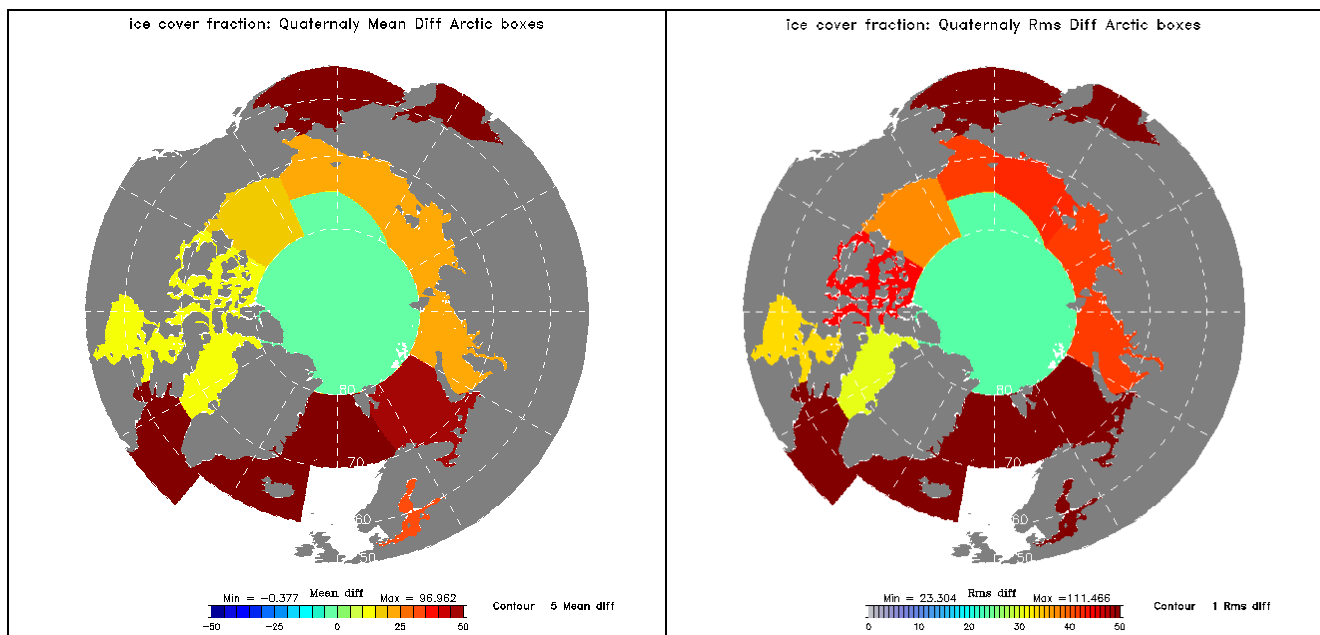
measurements with PSY3V3 velocities (comparisons done at 15m) show that the relative error is approximately 20 % and reaches locally more than 50 % (not shown). The zonal averaged ratio between modelled and observed velocities shows a latitudinal dependency of this bias which appears to be stronger north of 20°N. High velocities (> 30 cm/s) are better represented, which indicates that this bias is mainly due to small velocity values in the centre of gyres for instance. The large direction errors are localized and generally correspond to ill positioned mesoscale structures. The direction errors PDF is sharper in PSY3V3 than in PSY3V2 which indicates a larger number of small direction error and thus an improvement in PSY3V3. The IAU also improves the temporal coherence of the velocities and has an impact on reducing trajectory forecast errors (not shown).

### IV.2.3. Sea ice concentration

The melting of Sea Ice induces large differences between PSY3 and the observed sea ice cover fraction, especially in the Bering Sea, Barents Sea, Greenland Sea and Labrador Sea (Figure 25). These errors are not representative of the whole region (not significant) but only of local errors as there is very few sea ice in these regions in JAS (see Figure 26).

The sea ice doesn't melt enough in PSY3V2 (25 % ice cover average overestimation) while in PSY3V3 the sea ice fraction is underestimated (by 15%) in the "pack" in the centre of the Arctic, and still slightly overestimated (by 5 to 10%) in the marginal seas. The calibration on years 2007 to 2009 has shown that the system tends to melt too much ice during the summer, while the winter sea ice covers are much more realistic in PSY3V3 than in previous versions of PSY3 or even GLORYS reanalysis. See Figure 36 for monthly averages time series over the last 12 months.

The RMS error is reduced in PSY3V3 with a maximum of around 30% with respect to a maximum of around 50% in PSY3V2 in the Canadian Archipelago, where the model does not reproduce the variability of sea ice cover.



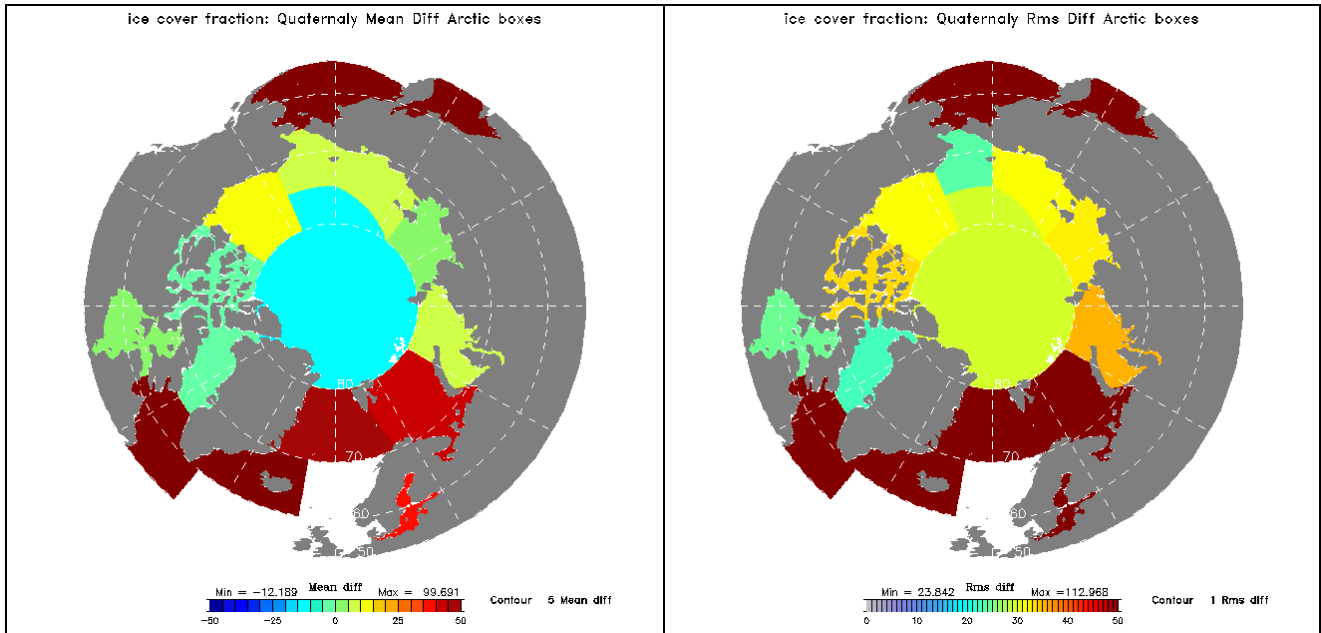


Figure 25: sea ice cover fraction (%) mean (left) and RMS (right) difference between CERSAT observations and PSY3V2 (upper panel) and PSY3V3 (lower panel) in regional boxes in the Arctic Ocean.

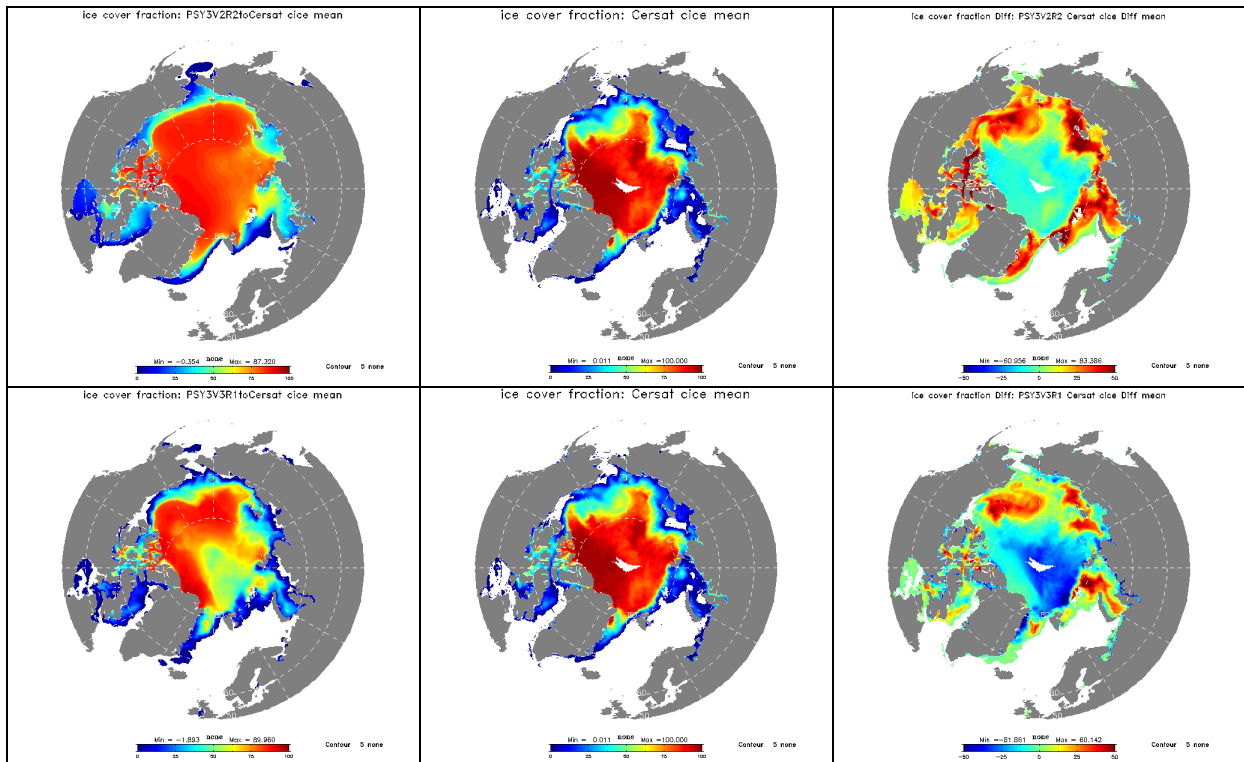


Figure 26: Comparison of the sea ice cover fraction mean for JAS 2010 between PSY3V2 (upper panel) and PSY3V3 (lower panel), for each panel the model is on the left the mean of Cersat dataset in the middle and the difference on the right.

## V Forecast error statistics

### V.1. Forecast accuracy: comparisons with observations when and where available

As can be seen in Figure 27 the PSY2V3 products have a better accuracy than the climatology in the North Atlantic region. The accuracy is lower this quarter in the near surface layer (0-50m) than in the 0-500m layer. The analysis is the best product, but the RMS error of the forecast is already approximately 3/4 of the climatologies in the 0-50m layer in July, and only slightly better in September. PSY2V3 products in general and especially the forecast have higher accuracy than the equivalent in PSY3V2 (not shown). PSY2V4 analysis is of higher accuracy than the equivalent in PSY2V3 in the North Atlantic (by 0.2°C), while PSY3V3 analyses can be of even better accuracy (not shown). The new systems forecast quality will be evaluated in the next QuO Va Dis.

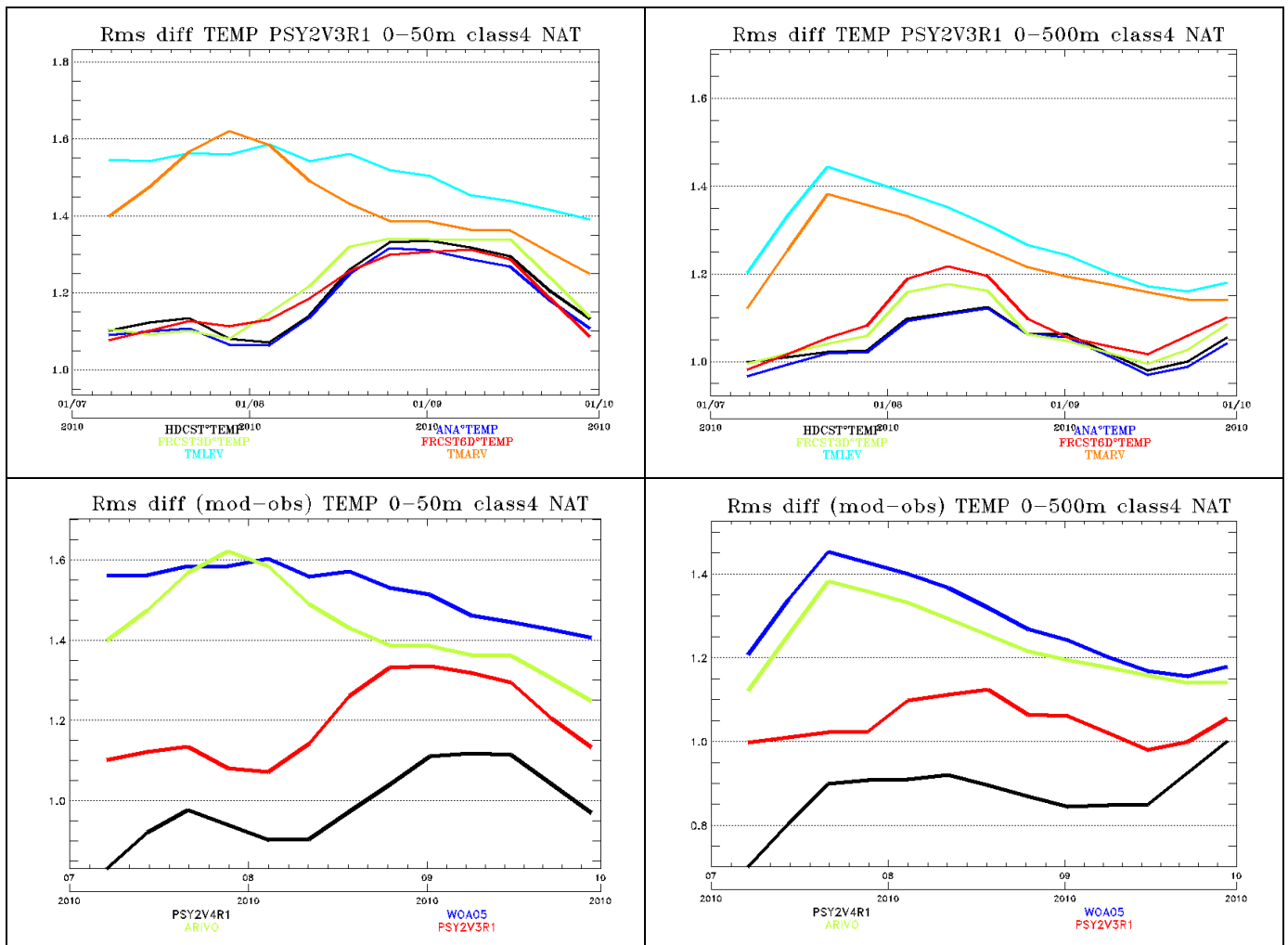


Figure 27: Upper panel: In the North Atlantic region for PSY2V3, time series of forecast (FRCST) accuracy at 3 (green line) and 6 (red line) days range, together with analysis (ANA in blue and HDCST in black), and climatology (TMLEV Levitus (2005) in cyan and in orange TMARV Arivo from Ifremer). Accuracy as measured by a RMS difference with respect to all available temperature (°C) observations from the CORIOLIS database. Lower panel: accuracy comparison of the analysis of PSY2V3 (red line) and PSY2V4 (black line) compared to WOA05 (blue line) and ARIVO (green line) climatologies. Left column: 0-50m layer, right column: 0-500m layer.

In the Mediterranean Sea (Figure 28), the PSY2V3 salinity forecast do not beat the climatology in August, while the temperature forecast are useful through the whole season. PSY2V4 analyses are less accurate than PSY2V3 analyses in the Mediterranean Sea in both temperature and salinity, consistently with data assimilation statistics. The accuracy of PSY2V4 seems to improve starting in August just after the recent scientific updates (as described in section I), which will have to be confirmed in the future. In addition a (locally strong) fresh bias has been diagnosed in the Mediterranean and the tropics and is under investigation.

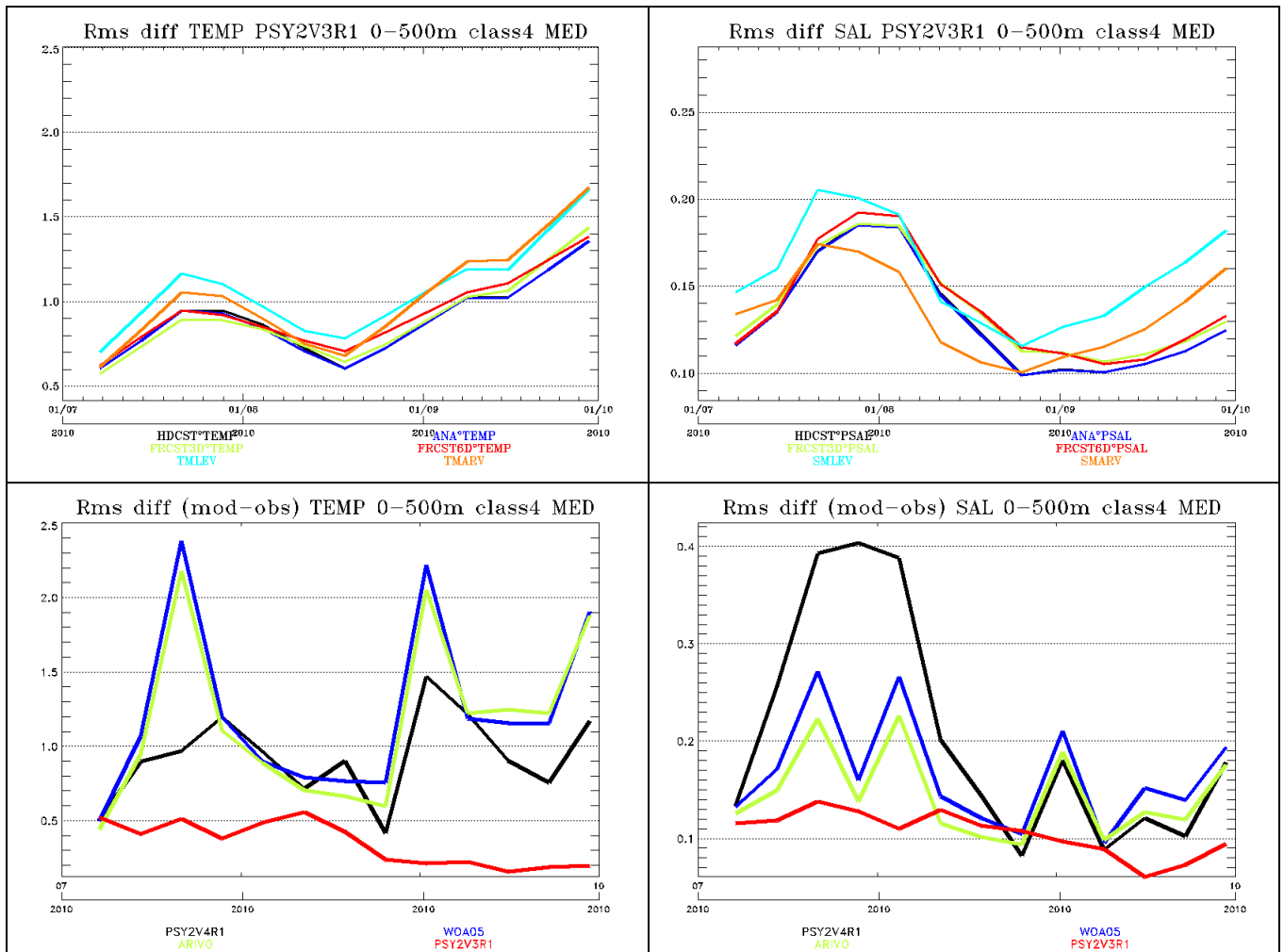


Figure 28: same as Figure 27 for the Mediterranean Sea in the PSY2V3 system (upper panel) and comparison with the new system PSY2V4 (lower panel), in the 0-500m layer. On the left temperature (°C) and on the right salinity (psu)

PSY3V2 statistics in the Atlantic, Pacific and Indian basin in the 0-500m layer (Figure 29) display a generally good accuracy and added value of the analyses and forecast with respect to climatology, especially in the Tropical Pacific. In this region the system is controlled by the TAO/TRITON array of T/S moorings. In July the accuracy of the forecast in the South Atlantic as well as the analysis in the Indian fall below the climatology probably due to biases data. (under investigation).

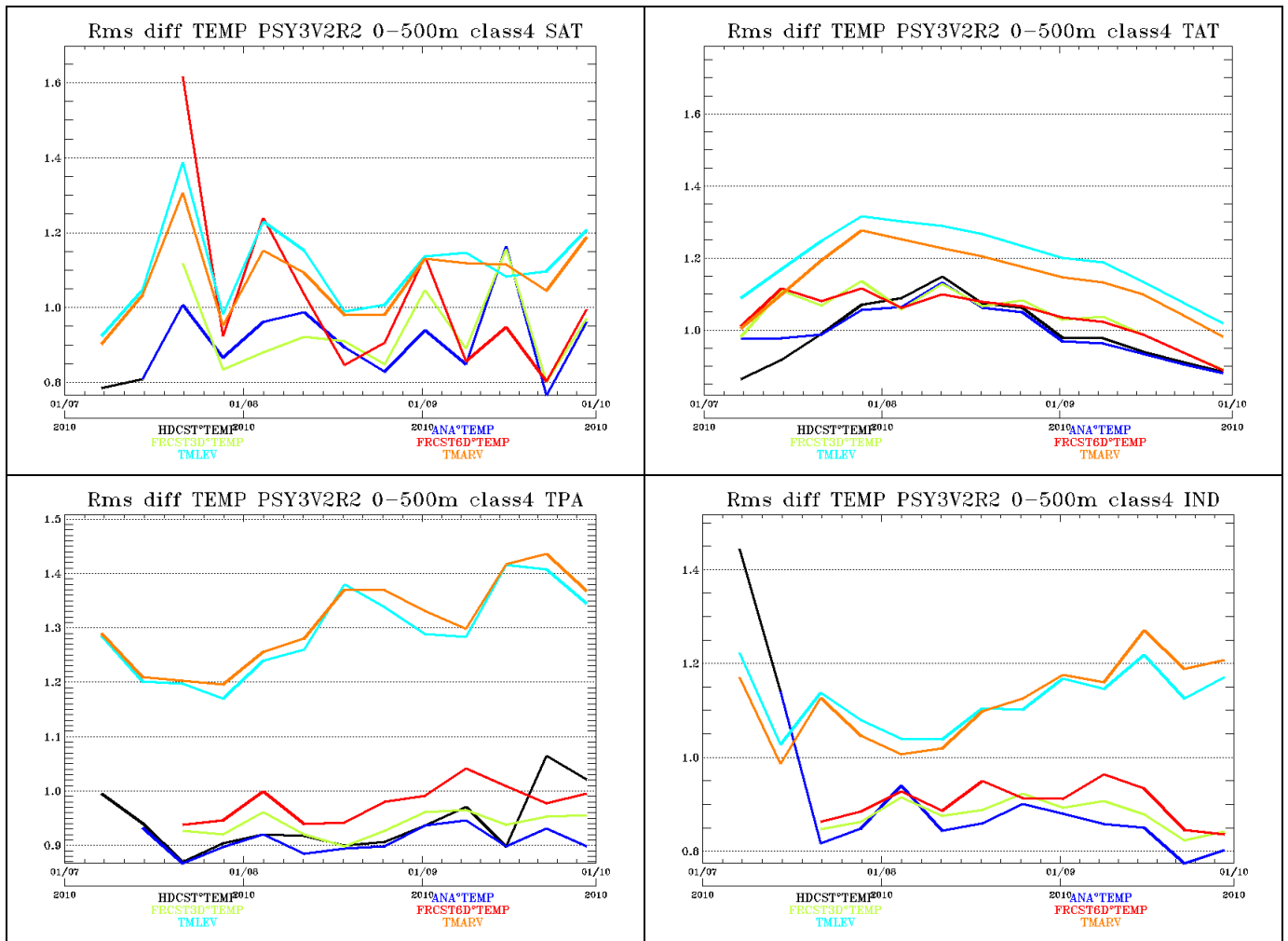


Figure 29: same as Figure 27 for temperature only in the 0-500m layer, the PSY3 system and the South Atlantic Ocean (upper left panel), the Tropical Atlantic (upper right panel), the Tropical Pacific (lower left panel) and the Indian Ocean (lower right panel).

## V.2. Forecast verification: comparison with analysis everywhere

The PSY3V2 “forecast errors” illustrated by the sea surface height RMS difference between the forecast and the hindcast for all given dates of the season JAS 2010 are displayed in Figure 30. The values on most of the global domain do not exceed 2 to 4 cm. In regions of high variability like the western boundary currents, Agulhas current and Zapiola eddy the errors reach around 20 cm, consistent with SLA innovation statistics.

High errors of more than 50 cm occur in the southern ocean (especially after two weeks), consistent with the drift of PSY3V2 SLA assimilation statistics in this region.

The results on the North Atlantic domain are very similar in PSY3V2 and PSY2V3 (Figure 31) ( $\sigma(2\text{ cm})$ ), reaching the same order of maximum values in the regions of highest variability ( $\sigma(20\text{ cm})$ ). PSY2V3 still seems to have better accuracy in the North Brazil Current.

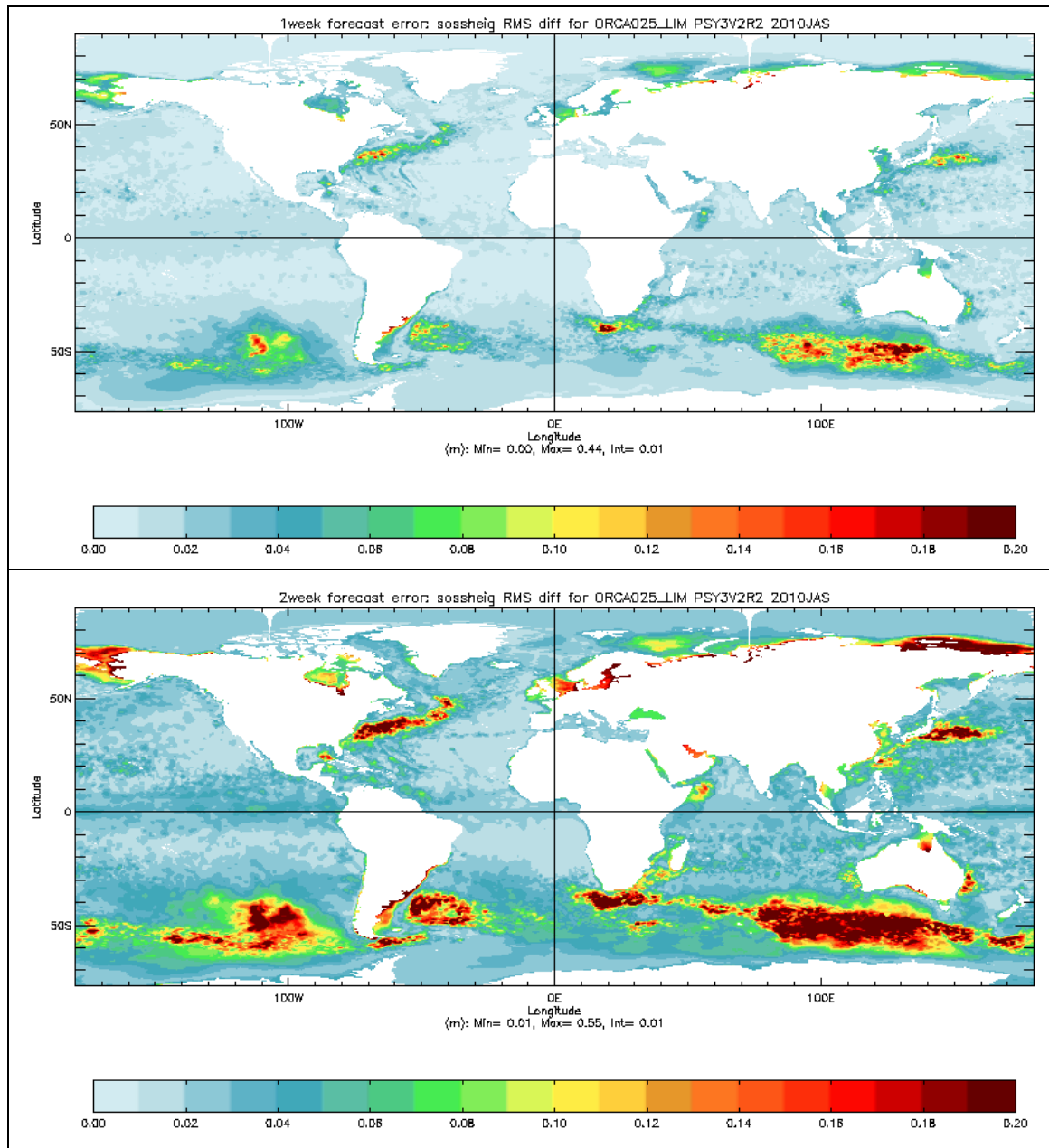


Figure 30: comparison of the sea surface height (m) forecast – hindcast RMS differences for the 1 week (upper panels) and 2 weeks (lower panels) ranges for the PSY3V2R2 system

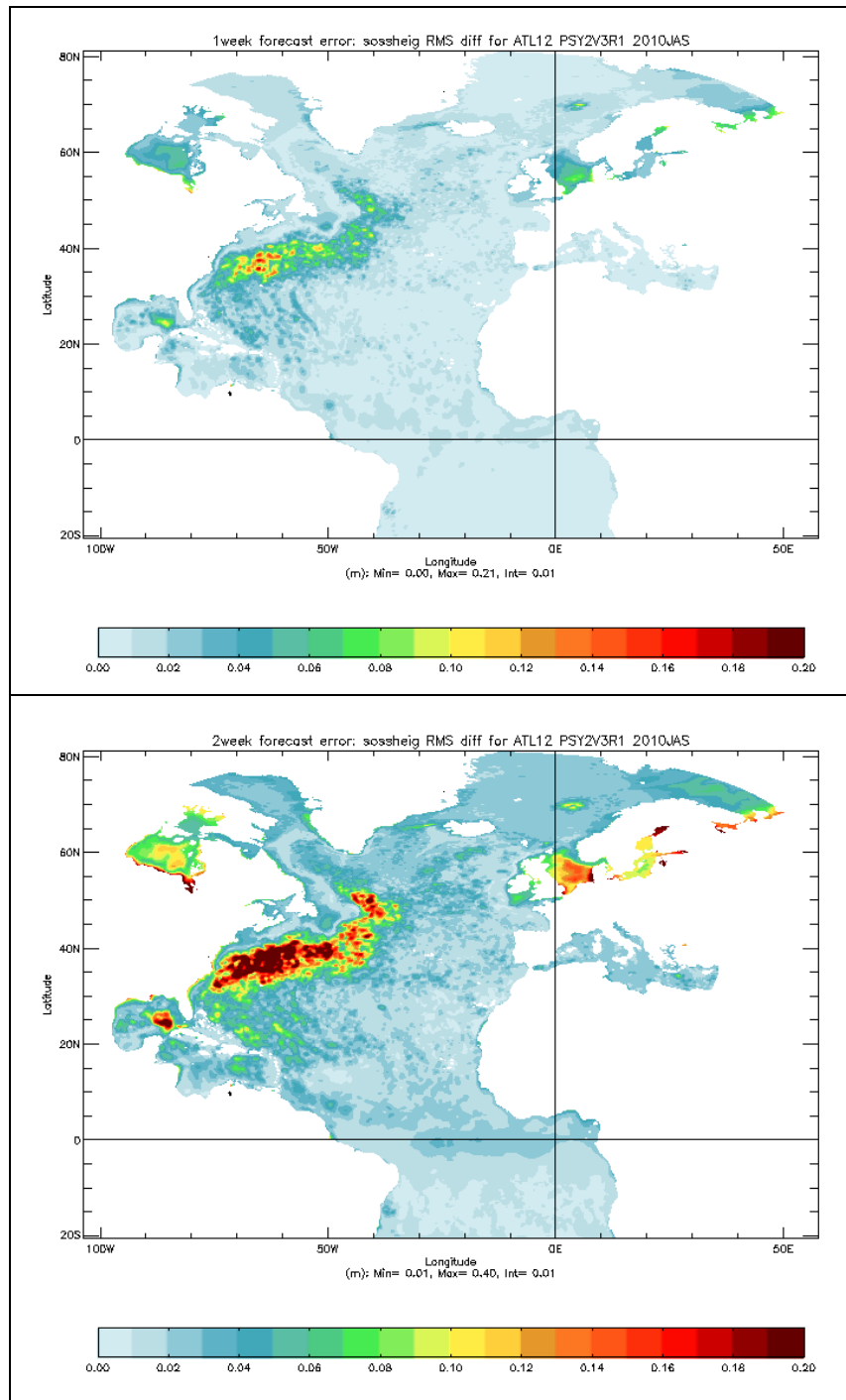


Figure 31: comparison of the sea surface height (m) forecast – hindcast RMS differences for the 1 week (upper panels) and 2 weeks (lower panels) ranges, for the PSY2V3R1 system.

Temperature forecast errors at all vertical levels show that the error is concentrated in the main thermocline in the tropical regions and in the mesoscale variability regions like the Gulf Stream (Figure 32).

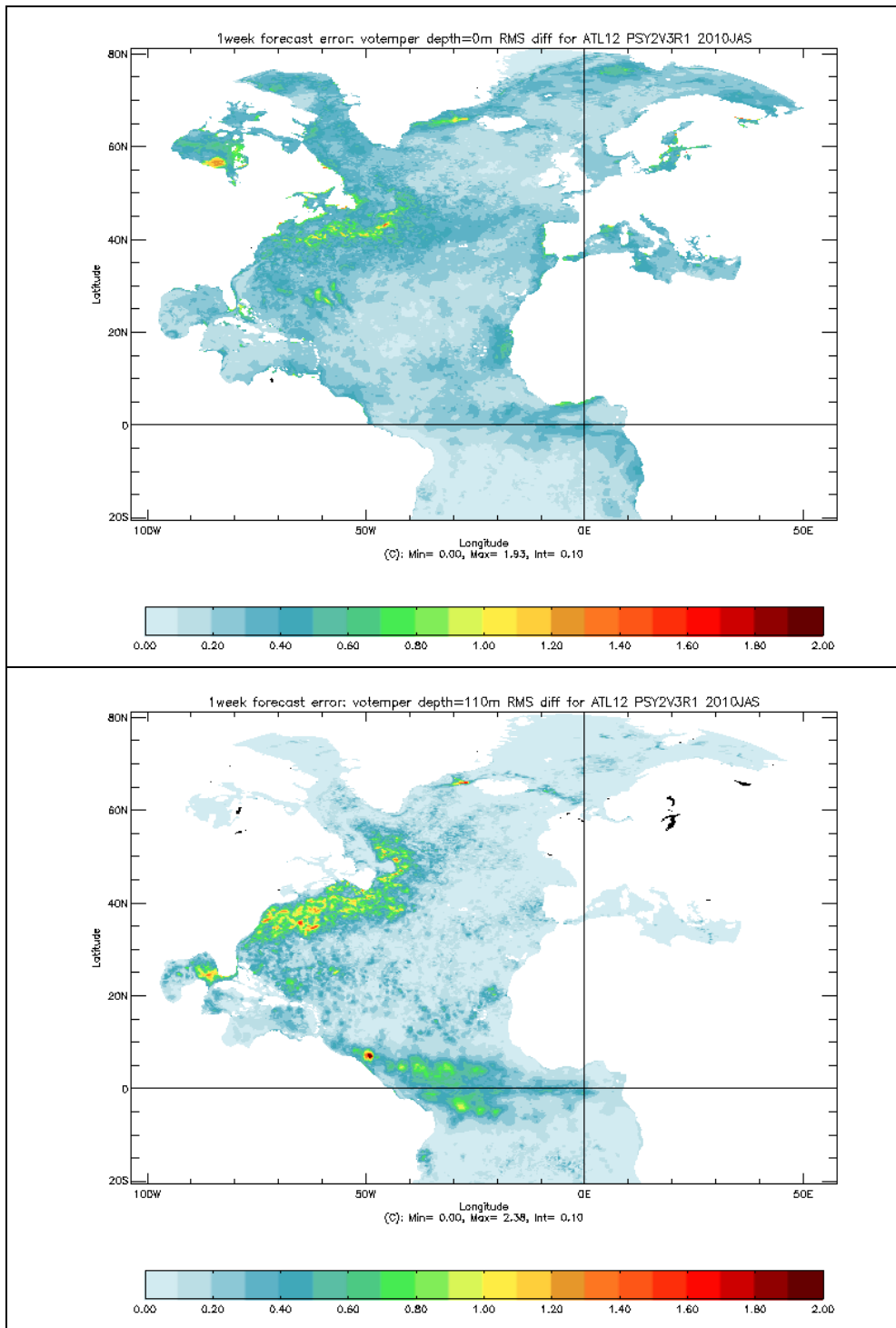


Figure 32: comparison of the temperature (°C) forecast – hindcast RMS differences for the 1<sup>st</sup> week at surface (upper panels) and 110 m (lower panels), for the PSY2V3R1 system

## VI Monitoring of ocean and sea ice physics

### VI.1. Global mean SST and SSS

A global mean cold bias can be diagnosed in PSY3V2 with respect to RTG-SST observations. At each analysis cycle, PSY3V2 tends to cool down after each analysis, as can be seen in Figure 33 (upper panel). Data assimilation shocks are also visible in the SSS time series. These shocks disappear in the new system PSY3V3, as shown in Figure 33 (lower panel), thanks to the IAU correction. A cold bias is still visible in PSY3V3, especially in summer, consistent with previous comparisons with observations.

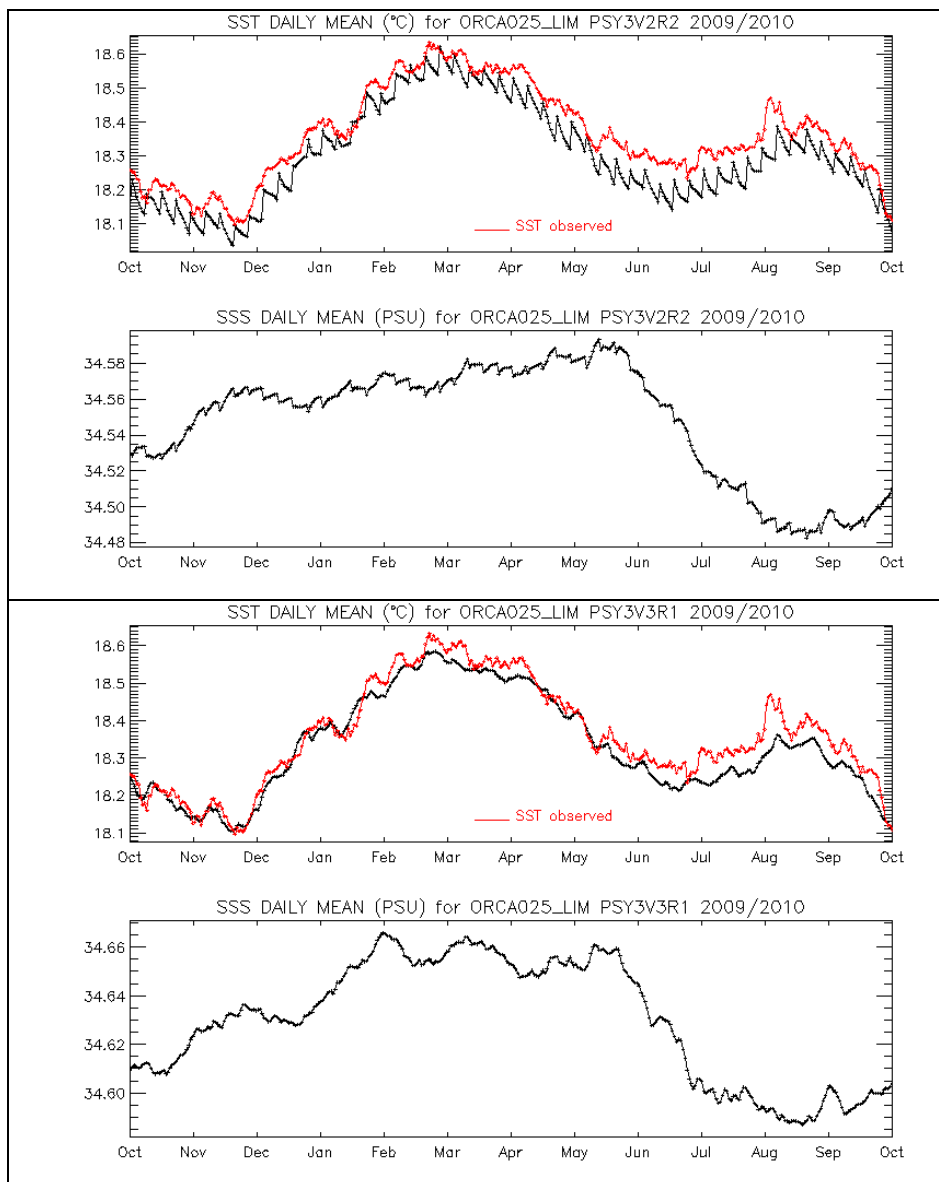


Figure 33: daily SST (°C) and salinity (psu) global mean for a one year period ending in JAS 2010, for PSY3 (in black) and RTG-SST observations (in red). Upper panel: PSY3V2R2, lower panel: PSY3V3R1.

## VI.2. Mediterranean outflow

As can be seen in Figure 34 the Mediterranean outflow in the Atlantic occurs at a realistic depth in PSY2V4, which was not the case in any of the previous systems. The Mediterranean outflow is also better represented in PSY3V3 than in PSY3V2 (not shown) but the improvement is not as important as in PSY2V4, which may take advantage from its high resolution (in addition to the bias correction implemented in both new systems).

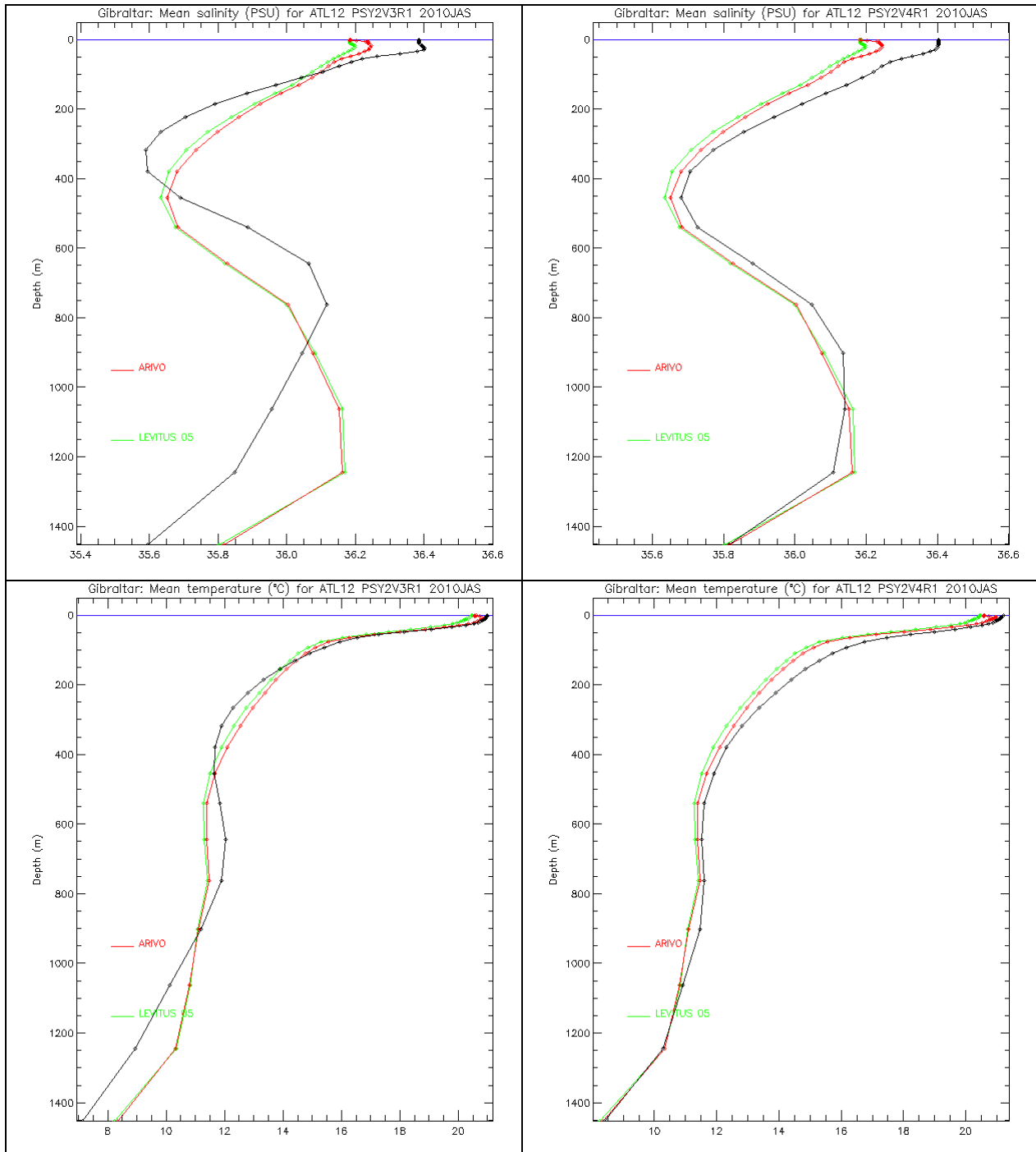


Figure 34: Comparisons between mean salinity (upper panel) and temperature (lower panel) profiles in PSY2V3 (left), PSY2V4 (right) and in the Levitus WOA05 and ARIVO climatologies.

### VI.3. Surface EKE

Regions of high mesoscale activity are diagnosed in Figure 35: Kuroshio, Gulf Stream, Nino 3 box in the Equatorial pacific, Indian Equatorial current, Zapiola eddy, Agulhas current, East Australian current, Madagascar channel etc... The signature of the SLA drift in PSY3V2 is also visible in the circumpolar current in the RMS of SSH (Pacific and Indian quadrant). In the new systems PSY2V4 and PSY3V3, the EKE is slightly lower than in the current systems.

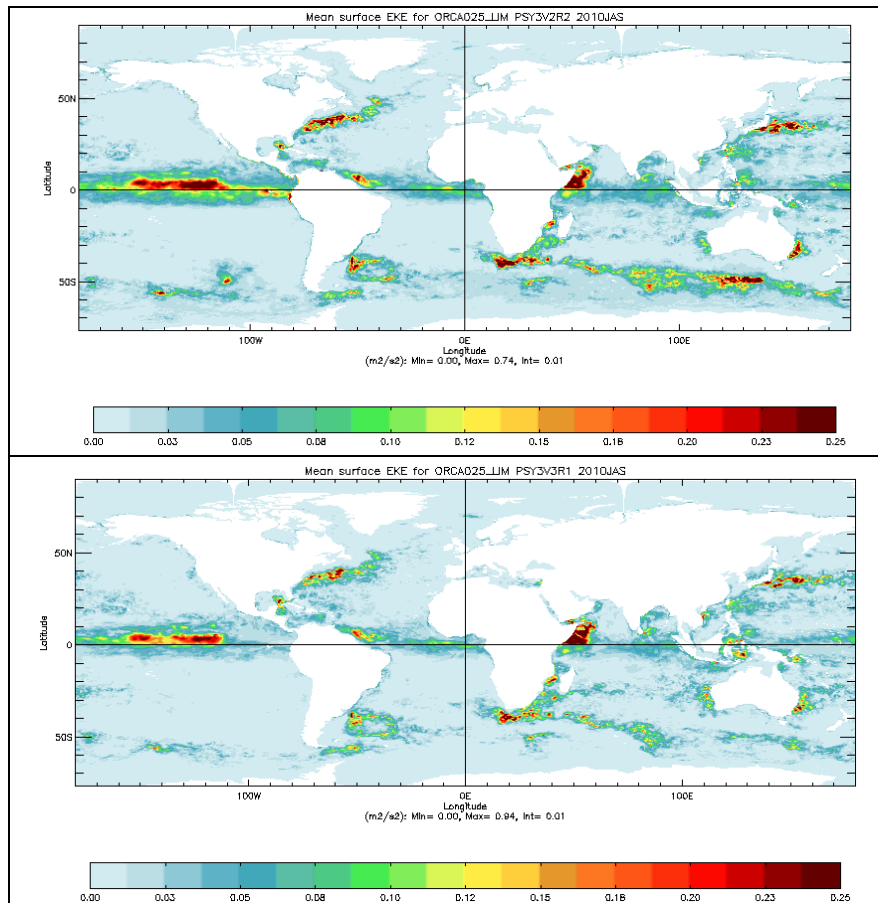


Figure 35: surface eddy kinetic energy EKE ( $\text{m}^2/\text{s}^2$ ) for PSY3V2R2 (left panel) and PSY3V3R1 (right panel) for JAS 2010.

### VI.4. Sea Ice extent and area

The time series of monthly means of ice area and ice extent (area of ocean with at least 15% sea ice) are displayed in Figure 36 and compared to SSM/I microwave observations. Both ice extent and area include the area near the pole not imaged by the sensor. NSIDC web site specifies that it is assumed to be entirely ice covered with at least 15% concentration. This area is 0.31 million square kilometres for SSM/I.

These time series indicate that during winter, both PSY3V2R2 and PSY3V3R1 perform very well, with respect to observations. During summer, PSY3V3 reproduces the melting season better than PSY3V2 in the Arctic; in the Antarctic, PSY3V2 shows a better area but PSY3V3's extent is closer to observations (see Figure 26 for details on distribution).

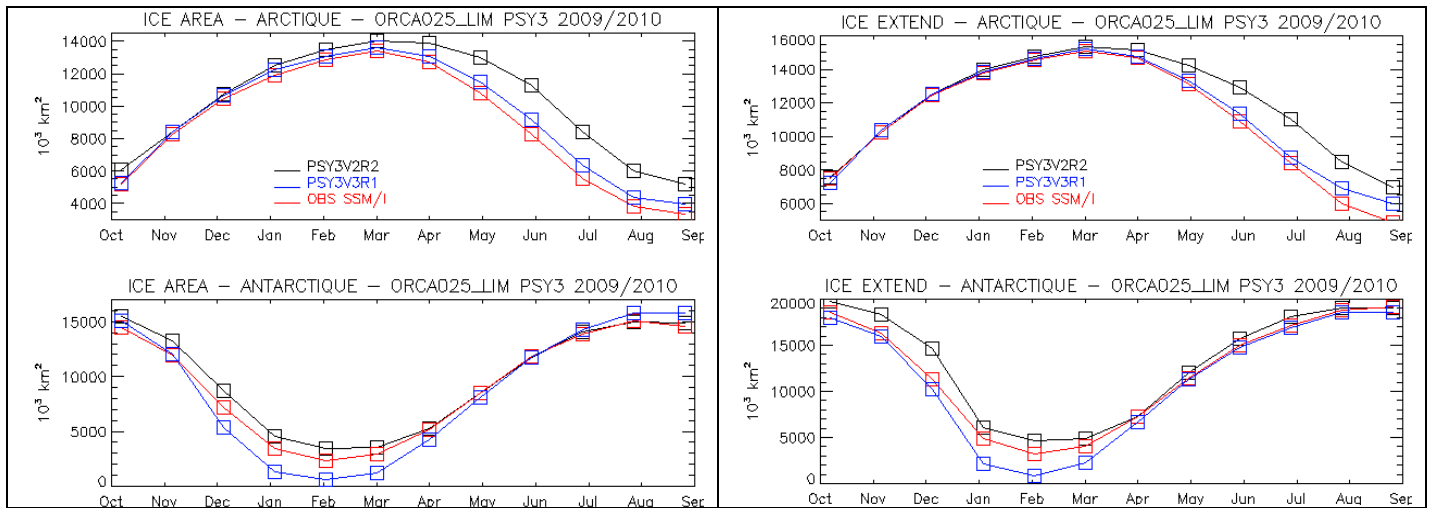


Figure 36: Sea ice area (left panel,  $10^3 \text{ km}^2$ ) and extent (right panel,  $10^3 \text{ km}^2$ ) in PSY3V2 (black line), PSY3V3 (blue line) and SSM/I observations (red line) for a one year period ending in JAS 2010, in the Arctic (upper panel) and Antarctic (lower panel).

### VI.5. High frequency behaviour at moorings

The behaviour at moorings is quite different in the new systems as illustrated with PSY2 in the following. As can be seen in Figure 37 PSY2V4 exhibits a strong wave response to a wind burst happening at BATS around September 10<sup>th</sup>. This wave is a lot weaker in PSY2V3, with less propagation at depth. Data assimilation shocks that were often diagnosed in PSY2V3 (mainly in SSH, T(z) and S(z)) disappear in PSY2V4, and more generally the time series of all variables are very different in this region of the Sargasso Sea (not shown).

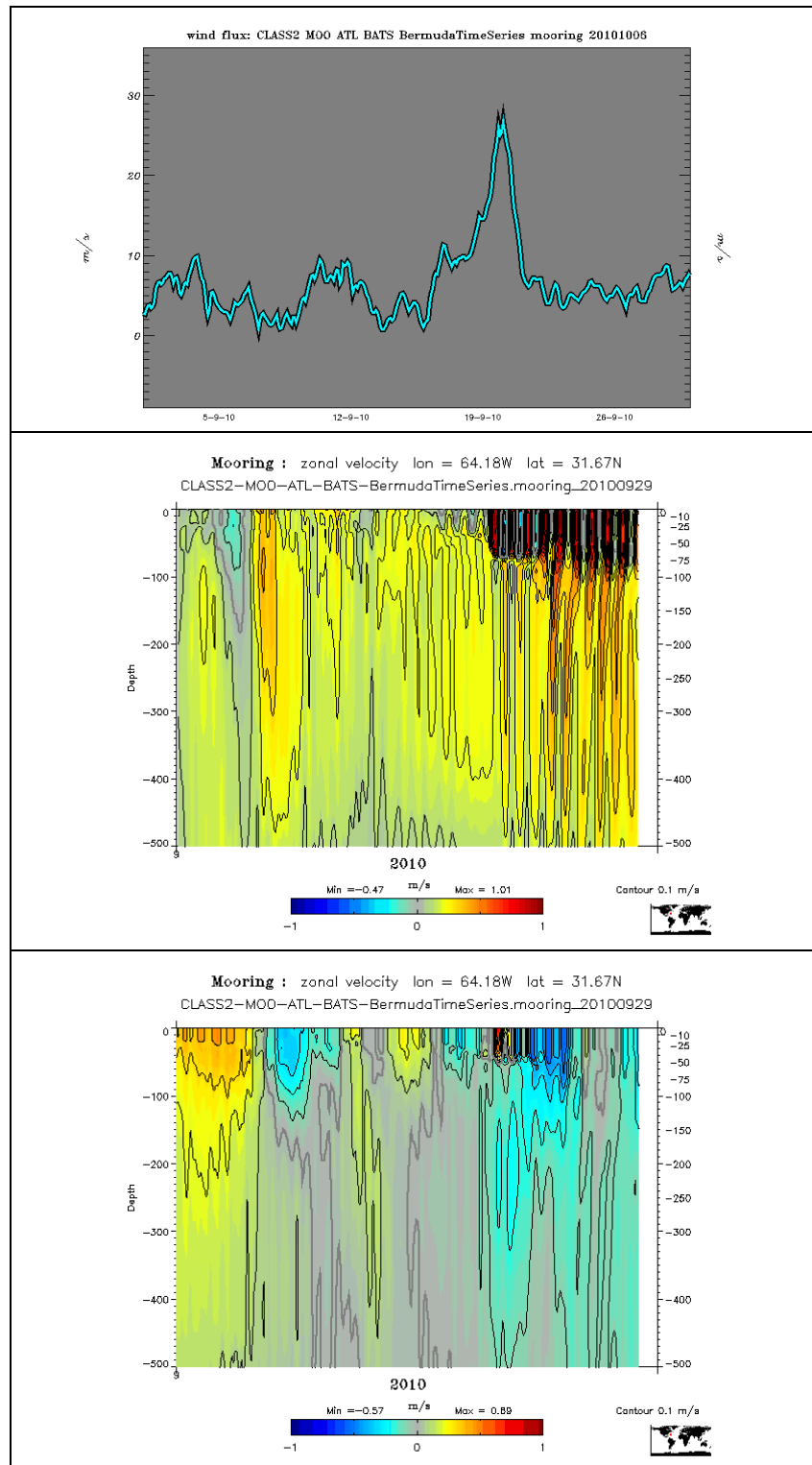


Figure 37: 2m wind velocity (upper panel, m/s), and 0-500 zonal velocity (in m/s, middle panel PSY2V4 and lower panel PSY2V3) 2-hourly time series at BATS near 64.18°W and 31.67°N in September 2010.

The physical consistency of the time series is improved in the new systems as illustrated by the PIRATA moorings at 23°W (Figure 38 and Figure 39). The data assimilation shocks

disappear, and the time evolution of  $T(z)$  and  $S(z)$  seems more in phase with the observations in the new PSY2 system. Nevertheless a fresh bias can be diagnosed near  $4^{\circ}\text{N}$  which is consistent with fresh biases that were diagnosed with respect to observations and climatologies in the Tropics (and in the Mediterranean Sea).

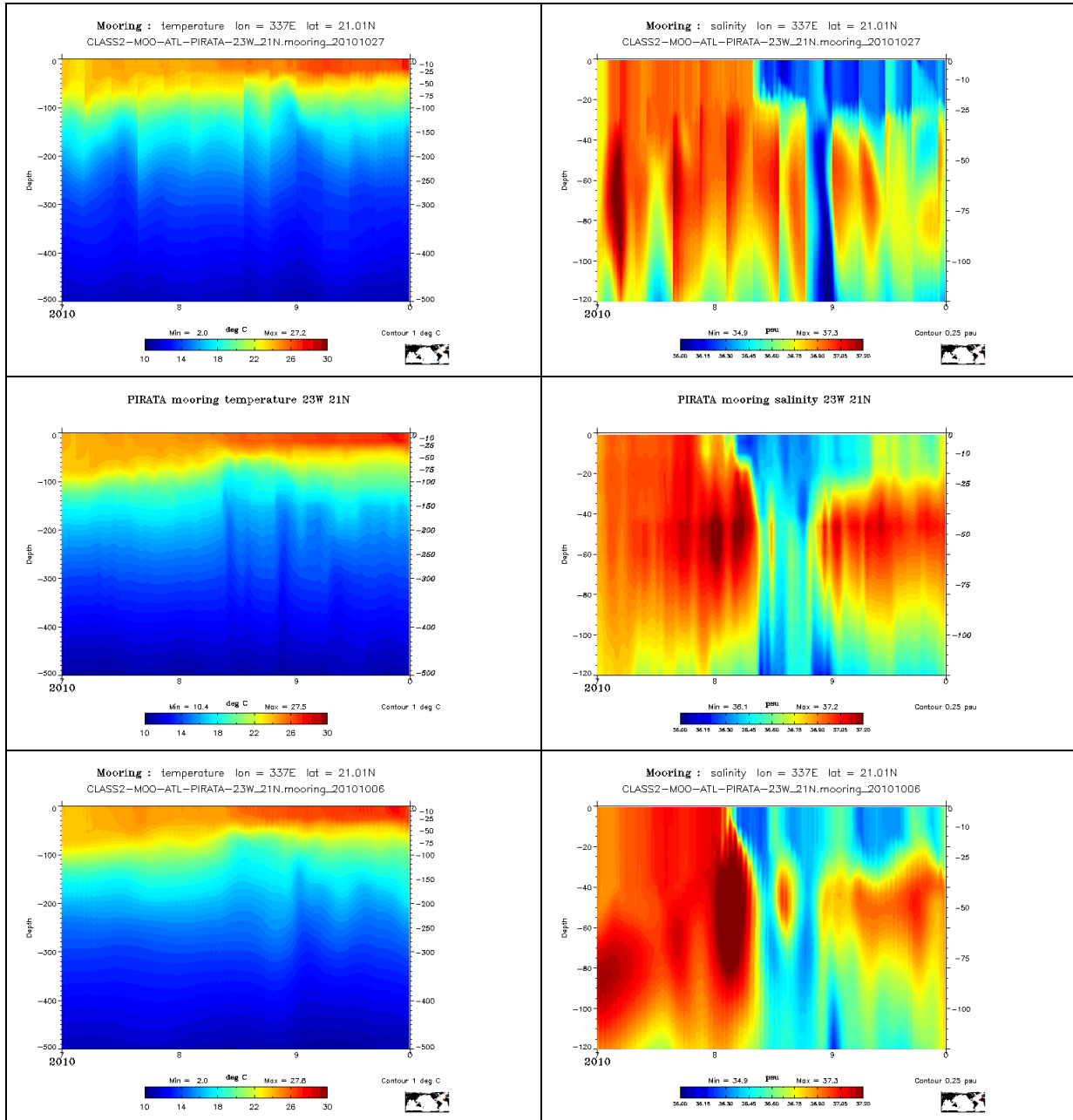


Figure 38: 0-500m temperature ( $^{\circ}\text{C}$ , left column) and salinity (psu, right column) time series for the JAS 2010 period at  $23^{\circ}\text{W}$  and  $21^{\circ}\text{N}$  for PSY2V3 (upper panel), at the PIRATA mooring (middle panel) and in PSY2V4 (lower panel) in July, August and September 2010.

Quo Va Dis ? Quarterly Ocean Validation Display #2, JAS 2010

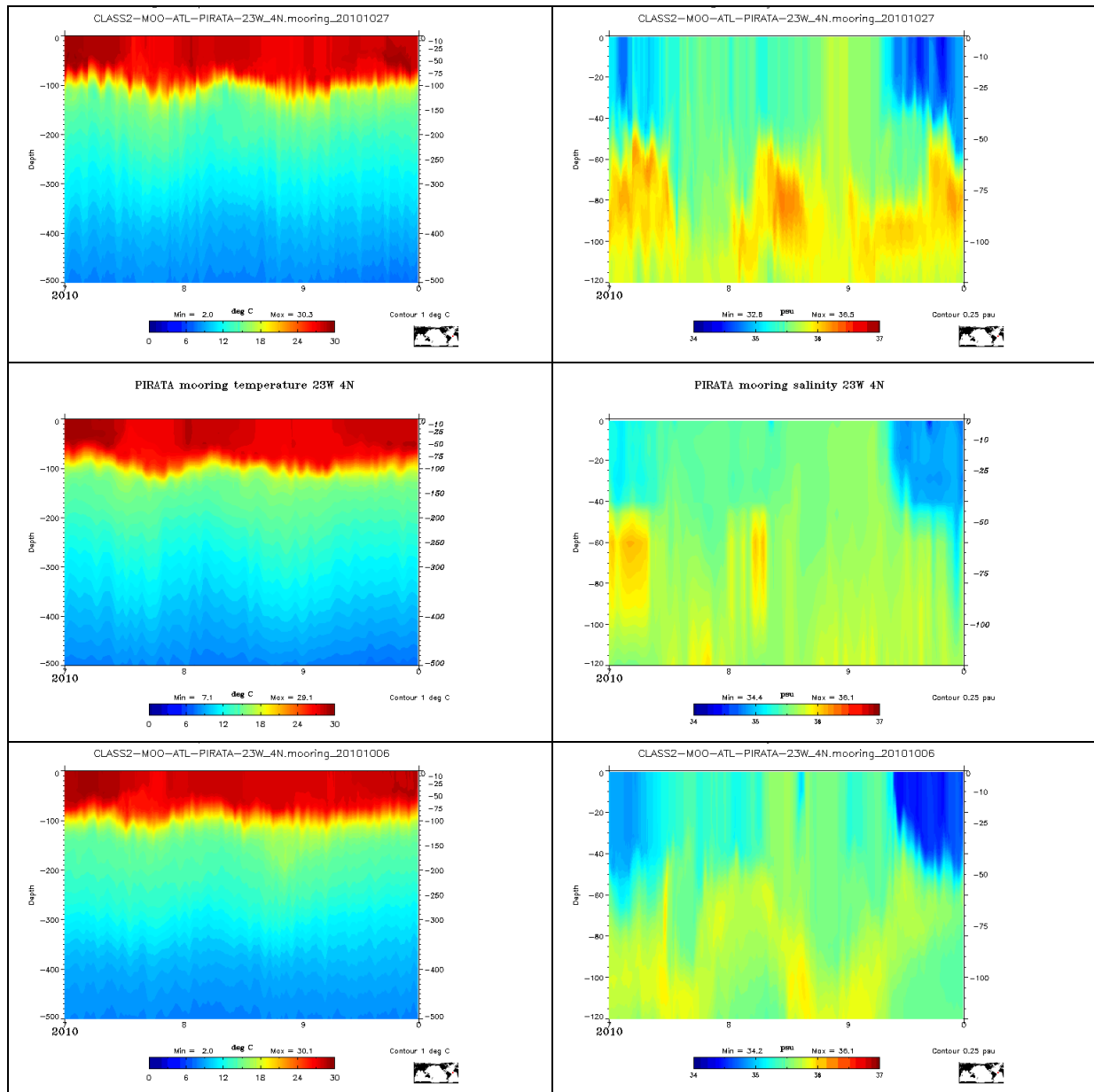


Figure 39: 0-500m temperature (°C, left column) and salinity (psu, right column) time series for the JAS 2010 period at 23°W and 3°N for PSY2V3 (upper panel), at the nearest PIRATA mooring (at 4°N, middle panel) and in PSY2V4 (lower panel) in July, August and September 2010.

## VII Process study: A warm coastal current in the Bay of Biscay

In august 2008 a warm northward coastal current was observed along the Landes shelf in the Bay of Biscay (P. Lazure, 2009, EPIGRAM meeting). This current was observed both in satellite SST with a thin tongue of warm water along the coast, and in ADCP measurements located at the Cap Ferret latitude on the 60 m isobath. The ADCP showed a sudden increase of the current velocity, oriented northward and associated with an increase of the bottom temperature. Satellite SST images suggest that this event not yet well understood could occur at other dates. This is the case of the SST image of September 15<sup>th</sup> 2010 (Figure 40): a warm tongue can be clearly seen along the Landes coast extending from 43.5°N to 45°N.

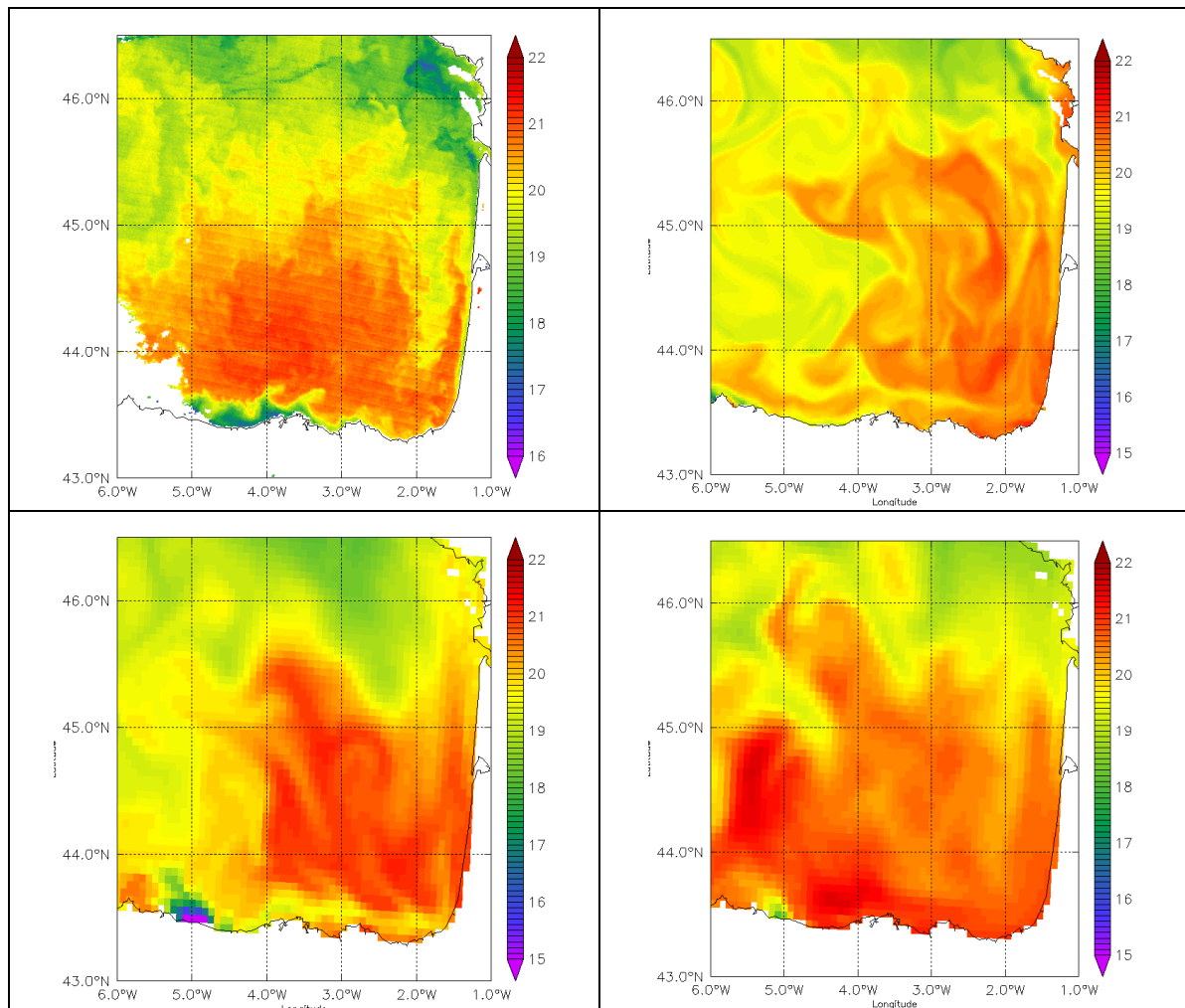


Figure 40: Sea Surface Temperature (°C) from MODIS on 15<sup>th</sup> September (upper left panel), IBI (upper right, hourly average of 2010/15/09 at 00h), PSY2V3 (lower left, daily average of 2010/14/09) and PSY2V4 (right panel, daily average of 2010/14/09).

This event seems to be represented by all the MERCATOR systems but the warm tongue is too wide and extends too far to the north. Time series (Figure 41) of model current velocity at the Cap Ferret latitude above the 60 m isobath (approximately near the location of the

ADCP measurements made in 2008) show an increase of the velocity associated with an increase of the bottom temperature (Figure 42).

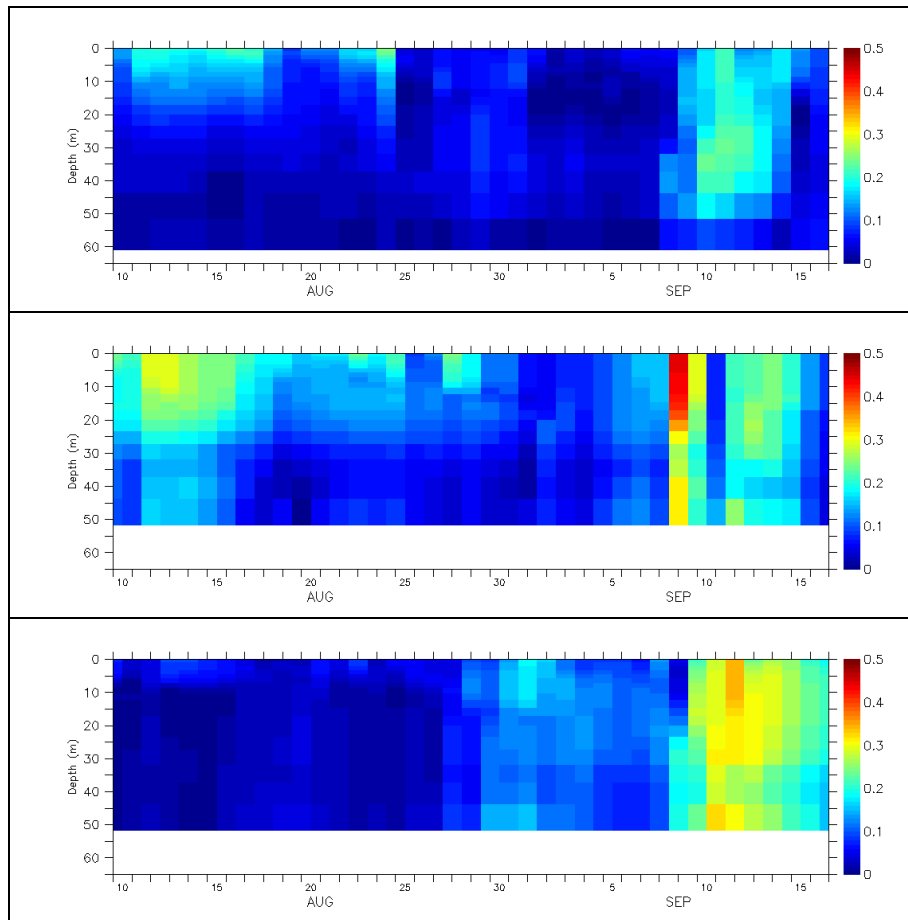


Figure 41: Current velocity (m/s, daily average) near 1.5°W, 44.6°N from 2010/10/08 to 2010/16/09 for IBI (upper panel), PSY2V3 (middle) and PSY2V4 (lower panel).

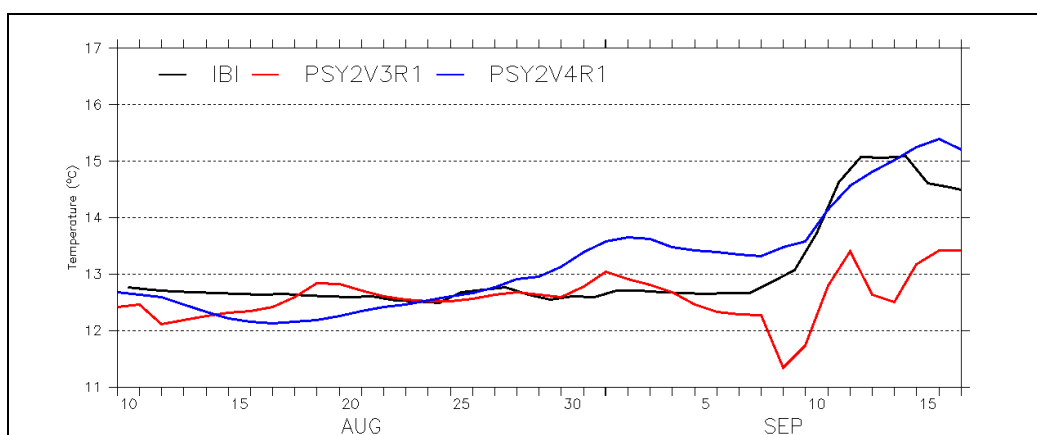
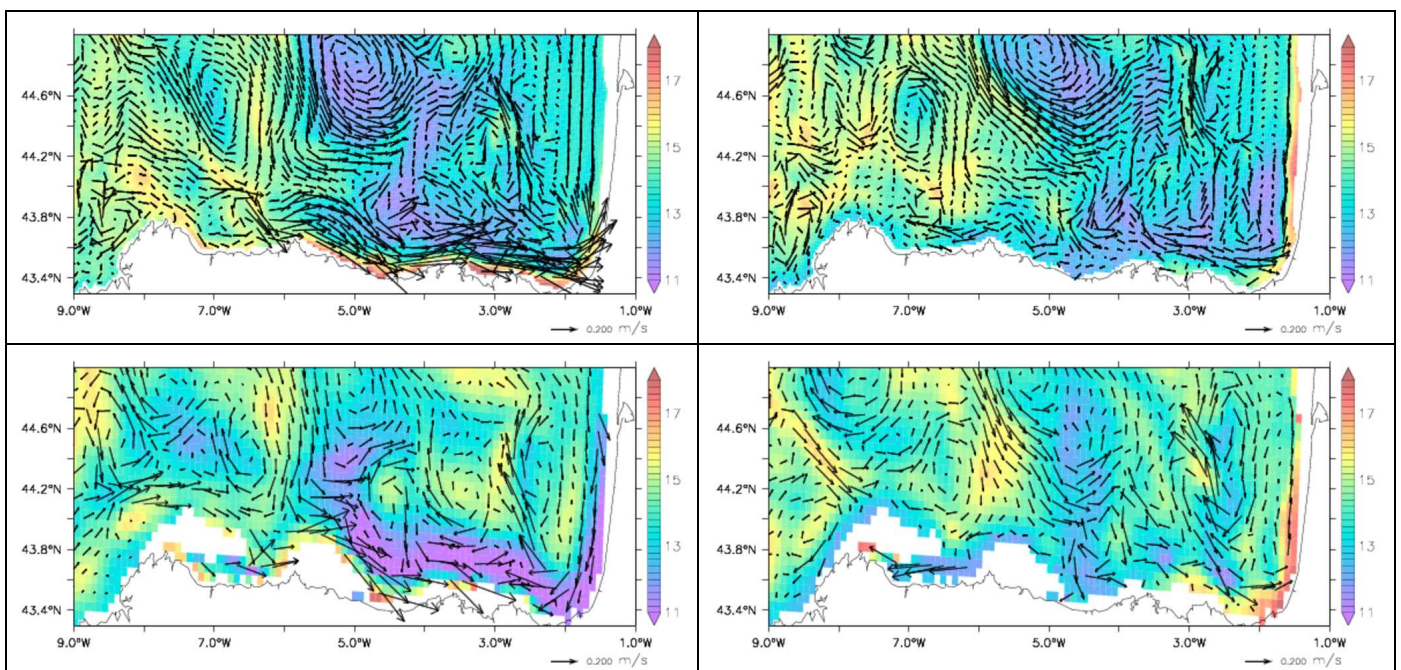


Figure 42: Bottom temperature (°C, daily average) near 1.5°W, 44.6°N from 2010/10/08 to 2010/16/09 for IBI (black curve), PSY2V3 (red) and PSY2V4 (blue).

Both systems show an increase of the current from the surface to the bottom around September 11<sup>th</sup>: the magnitude of the current differs from one system to another (between 25 and 35 cm/s). The bottom temperature increases from 12.6°C to 15°C in IBI, and from

12.1°C to 15.4°C in PSY2V4R1; on the other hand PSY2V3R1 does not show a significant increase. The increase of temperature in IBI seems to be more realistic compared to the measurement made in 2008: the temperature is constant during weeks and suddenly increases in some days. In PSY2V4R1 the temperature increases from the 16<sup>th</sup> August to the 15<sup>th</sup> September, with acceleration on the 10<sup>th</sup> September. The situation in PSY2V3R1 is unclear with a decrease of the temperature at the beginning of August, followed by an increase between the 9 and 12 September and then another decrease.

Maps of temperature and currents at 47 m depth (Figure 43) show that the northward current of the Landes coast is the extension of a coastal current developed along the north coast of Spain. On September 8<sup>th</sup> an eastward current is present along the Spanish shelf, associated with warm water close to the coast; this is clear in IBI and PSY2V4R1 and less clear in PSY2V3R1. One can notice the difference in the temperature field between PSY2V4R1 and the two other systems; comparisons with in situ profiles (not shown) indicate that the PSY2V4R1 temperature field is more realistic. IBI and PSY2V3R1 have close temperature fields because IBI has for initial conditions the PSY2V3R1 fields. On September 14<sup>th</sup>, all the systems show that the warm current has reached the Landes coast. The origin of this event can be partly explained by the wind forcing: on September 8<sup>th</sup> the wind is oriented eastward and its curl has a strong negative value close to the coast (not shown), favourable to downwelling. Sections of temperature (not shown) perpendicular to the coast clearly show a deepening of the isotherms along the slope so that the temperature along the coast is warmer than the temperature offshore at the same depth.



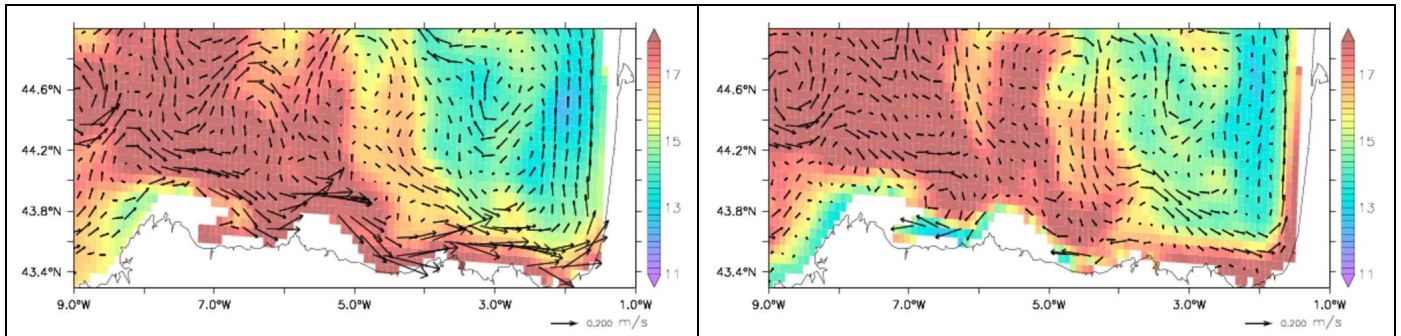


**Figure 43: temperature (°C) and current at 47 m depth for IBI (upper panel), PSY2V3 (middle) and PSY2V4 (lower) for 2010/08/09 (left column) and 2010/04/09 (right column).**

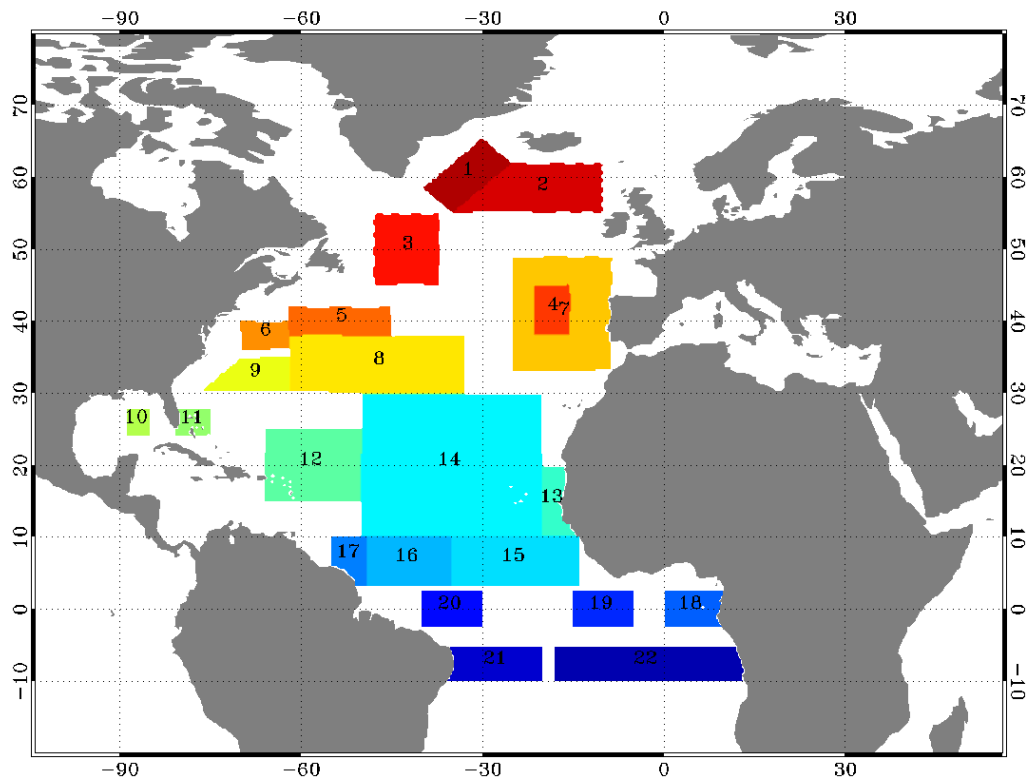
In conclusion, the MERCATOR systems show in September 2010 a coastal event in the Bay of Biscay characterized by a warm current developed along the northern Spanish coast after downwelling favourable winds, and extending along the Landes coast. This event shows likeness with the one observed in august 2008 in the same area. Available in situ measurements are too few in this period to validate the systems; we hope some will be soon available.

## VIII Annex A

### VIII.1. Maps of regions for data assimilation statistics

#### VIII.1.1. Tropical and North Atlantic

Mask for regional data assimilation statistics

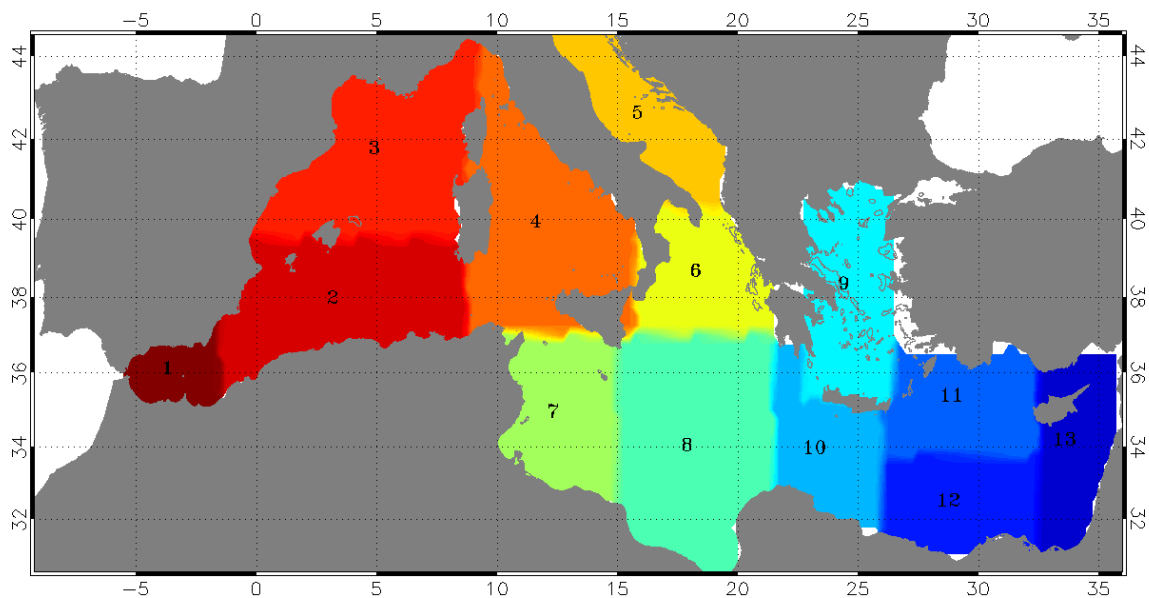


1	Irminger Sea
2	Iceland Basin
3	Newfoundland-Iceland
4	Yoyo Pomme
5	Gulf Stream2
6	Gulf Stream1 XBT
7	North Madeira XBT
8	Charleston tide
9	Bermuda tide
10	Gulf of Mexico
11	Florida Straits XBT
12	Puerto Rico XBT
13	Dakar
14	Cape Verde XBT
15	Rio-La Coruna Woce

16	Belem XBT
17	Cayenne tide
18	Sao Tome tide
19	XBT - central SEC
20	Pirata
21	Rio-La Coruna
22	Ascension tide

### VIII.1.2. Mediterranean Sea

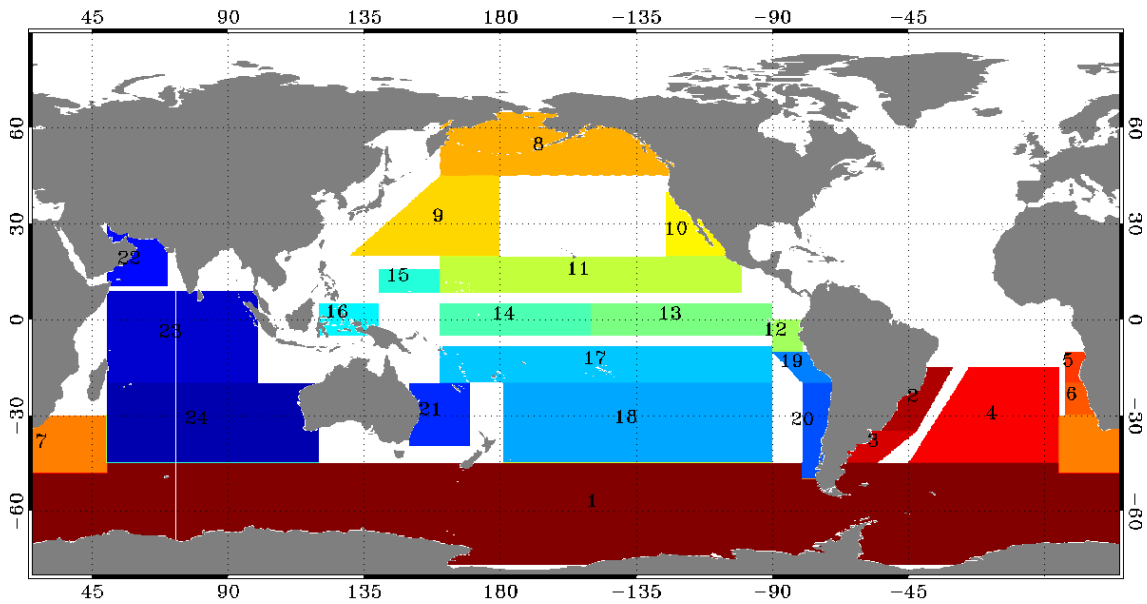
Mask for regional data assimilation statistics



1	Alboran
2	Algerian
3	Lyon
4	Thyrrhenian
5	Adriatic
6	Otranto
7	Sicily
8	Ionian
9	Egee
10	Ierepetra
11	Rhodes
12	Mersa Matruh
13	Asia Minor

VIII.1.3. Global ocean

Mask for regional data assimilation statistics



1	Antarctic Circumpolar Current
2	South Atlantic
3	Falkland current
4	South Atl. gyre
5	Angola
6	Benguela current
7	Aghulas region
8	Pacific Region
9	North Pacific gyre
10	California current
11	North Tropical Pacific
12	Nino1+2
13	Nino3
14	Nino4
15	Nino6
16	Nino5
17	South tropical Pacific
18	South Pacific Gyre
19	Peru coast
20	Chile coast
21	Eastern Australia
22	Indian Ocean
23	Tropical Indian Ocean
24	South Indian Ocean